

LABORATORY AND FIELD INVESTIGATIONS FOR
CAUSES OF UNWANTED DEFORMATIONS IN
EXISTING STEEL GIRDER BRIDGES
REHABILITATED WITH CONCRETE DECKS

By

KENDALL KE'VONN BELCHER

Bachelor of Science in Civil Engineering

Louisiana Tech University

Ruston, LA

2013

Submitted to the Faculty of the
Graduate College of the
Oklahoma State University
in partial fulfillment of
the requirements for
the Degree of
MASTER OF SCIENCE
July, 2017

LABORATORY AND FIELD INVESTIGATIONS FOR
CAUSES OF UNWANTED DEFORMATIONS IN
EXISTING STEEL GIRDER BRIDGES
REHABILITATED WITH CONCRETE DECKS

Thesis Approved:

Br. Bruce Russell

Thesis Adviser

Dr. Tyler Ley

Dr. Robert Emerson

ACKNOWLEDGEMENTS

Thanks to Dr. Bruce Russell for allowing me to work under him as GTA and GRA. This would not have been possible without his support and encouragement.

Thanks to my committee members, Dr. Tyler Ley and Dr. Robert Emerson for taking time out to help me complete my master's degree.

Thanks to the Oklahoma Department of Transportation for funding this project and providing me with an opportunity to conduct research in structural and materials engineering.

Thanks to Oklahoma State University and the Civil & Environmental Engineering Department for allowing me to attend this prestigious institution.

Thanks to my family, friends, and mentors who helped me, supported me, and believed in me.

Acknowledgments reflect the views of the author and are not endorsed by committee members or Oklahoma State University.

Name: KENDALL KE'VONN BELCHER

Date of Degree: MAY 2017

Title of Study: LABORATORY AND FIELD INVESTIGATIONS FOR CAUSES OF
UNWANTED DEFORMATIONS IN EXISTING STEEL GIRDER
BRIDGES REHABILITATED WITH CONCRETE DECKS

Major Field: CIVIL ENGINEERING

Many older steel girder bridges are rehabilitated by placing a new concrete deck upon the existing steel superstructure. In recent years, the Oklahoma Department of Transportation has reported issues of ride performance on some newly rehabilitated concrete and steel composite bridges. Shrinkage, creep, temperature, and other sources of time-dependent volume change can affect the ride quality, deck cracking, deflection, and long-term performance of steel girder bridges made composite with concrete decks. These time-dependent effects are sometimes considered minimal and ignored. After the initial set, concrete will experience volumetric changes caused primarily by shrinkage. Other time dependent changes, specifically temperature and creep, will have some effects, but these are likely small compared to shrinkage. Some researchers recommend waiting for concrete to develop its strength and full composite action to counter the effects of shrinkage before applying load (Chaudhary et al. 2009). Time-dependent volume changes do not impact the load carrying capacity of a simply supported bridge, but instead affect the composite response to service loads and deflections in supporting steel beams and the whole system. Some research has theorized that volumetric changes in concrete are the cause of unpleasant driving surfaces and unexpected deflections. My research develops new knowledge on volumetric effects in rehabilitated composite bridges through: 1) experimental research and 2) forensic investigation.

Research included laboratory analysis and forensic investigation. Companion laboratory concrete specimens and prototype bridge specimens were built. Various concrete mixtures were batched and standard ASTM tests were performed to measure compressive strength, splitting cylinder tensile strength, elastic modulus, and shrinkage over time. On the prototype bridges, temperature, deflections, and strains were measured daily. Forensic investigations were performed on three bridges in Oklahoma to determine the causes of serviceability problems. Serviceability issues refer to unsatisfactory performance of a bridge under service loads for its intended purpose; i.e. excessive deflections and adverse riding surfaces. The laboratory data show that concrete shrinkage is one possible contributor to poor ride quality and unanticipated deflections in rehabilitated bridges. However, the field investigations provide evidence that construction errors are likely the main cause of poor elevation control of finished bridge deck surfaces.

TABLE OF CONTENTS

Chapter	Page
I. INTRODUCTION.....	1
II. LITERATURE REVIEW	4
Literature Summary	4
Csagoly, P. & Long, A.E. (1975). A Note on Shrinkage Stresses in Continuous Steel-Concrete Composite Bridges. <i>The Structural Engineer</i>	5
Chaudhary, S., Nagpal, A., & Pendharkar, U. (2009). Control of Creep and Shrinkage Effects in Steel Concrete Composite Bridges with Precast Decks. <i>Journal of Bridge Engineering</i>	6
Bradford, M. (1991). Deflections of Composite Steel-Concrete Beams Subject to Creep and Shrinkage. <i>ACI Structural Journal</i>	7
Jung, C., Kwak, H., & Seo, Y. (2000). Effects of the Slab Casting Sequences and the Drying Shrinkage of Concrete Slabs on the Short-Term and Long-Term Behavior of Composite Steel Box Girder Bridges Part 1. <i>Engineering Structures</i> 23(500).....	9
Holloway, R. (1972). Precast Composite Sections in Structures. <i>ACI Journal</i>	10
Bradford, M. (1997). Shrinkage Behavior of Steel-Concrete Composite Beams. <i>ACI Structural Journal</i>	12
Alexander, S. (2003). How Concrete Shrinkage Affects Composite Steel Beams. <i>New Steel Construction</i>	14
Al-deen, S., Ranzi, G., & Vrcelj, Z. (2011). Shrinkage Effects on the Flexural Stiffness of Composite Beams with Solid Concrete Slabs: An Experimental Study. <i>Engineering Structures</i>	16
Section.....	11
III. METHODOLOGY	19
Prototype Composite Beams.....	19
Hardened Concrete Properties for the Prototype Beams	28
Computational Analysis on Prototype Beams	39
Forensic Investigation on Three Bridges in Oklahoma	43
Hardened Concrete Properties of SH 86.....	48
Computational Analysis of SH 86 Bridge	51
IV. RESULTS AND DISCUSSION.....	58
Results.....	58
Midspan Deflections from Prototype Beams 1 and 2	59
Temperatures of the Concrete and Steel	65
Strain Measurements for Prototype Beams 1 and 2.....	70

Unrestrained Shrinkage Strains from Shrinkage Prisms.....	98
Forensic Investigation	102
SH 86	102
SH 14	114
US 281	125
Discussion.....	130
V. CONCLUSIONS AND RECOMMENDATIONS	134
Conclusions	134
Recommendations.....	137
REFERENCES	140
APPENDICES	142

LIST OF TABLES

Table	Page
Table 1 Comparison of Stresses.....	8
Table 2 Comparison of Designs for Noncomposite and Composite Section	10
Table 3 ODOT AA Batch Weight/Volume and Saturated Surface Dry (SSD) Weights	26
Table 4 Concrete Fresh Properties of the ODOT AA Mixtures Used to Make the Two Prototype Beams	27
Table 5 Prototype Beam 1 Hardened Concrete Properties	31
Table 6 Prototype Beam 2 Hardened Concrete Properties	32
Table 7 Prototype Beams Concrete Slab Properties	39
Table 8 W8x15 Steel Beam Properties	40
Table 9 Prototype Beams Composite (Concrete to Steel) Properties	41
Table 10 Mix Design and Proportioning	48
Table 11 Fresh Concrete Properties for Both Prototypes Beams	48
Table 12 ODOT Fresh Concrete Tests for SH 86.....	49
Table 13 Hardened Concrete Properties at 28 Days for Prototype Beams	50
Table 14 ODOT 28 Day Compressive Strength Tests for SH 86.....	50
Table 15 SH 86 Slab Properties for 1 and 7 Girders	53
Table 16 W33x141 Steel Beam Properties	54
Table 17 SH 86 Composite (Concrete to Steel) Properties for 1 and 7 Girders	55
Table 18 Midspan Deflection for 1st Week.....	59
Table 19 Midspan Deflection for Year	61
Table 20 Early Age Concrete and Steel Temperatures Vs. Time for Week	66
Table 21 Concrete and Steel Temperatures for Year.....	69
Table 22 Prototype Beam 1 Shrinkage Strain on Concrete Slab for 1st Week.....	70
Table 23 Prototype Beam 2 Shrinkage Strain on Concrete Slab for 1st Week.....	72
Table 24 Prototype Beam 1 Shrinkage Strain on Concrete Slab for Year.....	75
Table 25 Prototype Beam 2 Shrinkage Strain on Concrete Slab for Year.....	77
Table 26 Average Shrinkage Strain on Concrete Slab for 1st Week.....	78
Table 27 Average Shrinkage Strain on Concrete Slab for Year	80
Table 28 Prototype Beam 1 Strain on Steel Beam for 1st Week.....	84
Table 29 Prototype Beam 2 Strain on Steel Beam for Week.....	86
Table 30 Prototype Beam 1 Strain on Steel Beam for Year	88
Table 31 Prototype Beam 2 Strain on Steel Beam for Year	91
Table 32 Average Strain in Steel Beam for 1st Week	92

Table 33 Average Strain in Steel Beam for Year	94
Table 34 Unrestrained Shrinkage Strains for 1st Week.....	99
Table 35 Unrestrained Shrinkage Strains for Year	101
Table 36 Roadway elevations (ft.) above the north abutment for SH 86.	104
Table 37 Roadway elevation profile for the SH 86 bridge	108
Table 38 Imputed changes in roadway elevations due to localized variance in the formwork.....	109
Table 39 Concrete slab thickness (ft.) on the north span of SH 86 bridge.	111
Table 40 Concrete slab thickness (in.) on the north span of SH 86 bridge.....	112
Table 41 Roadway elevations for SH 14.	116
Table 42 Elevations at the bottom of the concrete deck of SH 14.....	118
Table 43 Computed slab thicknesses (ft.) for SH 14	120
Table 44 Computed slab thicknesses (in.) for SH 14.....	122
Table 45 Roadway elevation taken on US 281	126
Table 46 Slab Thicknesses (ft.) for the US 281 Bridge	128

LIST OF FIGURES

Figure	Page
Figure 1 Cross Section Used in Analysis and Design.....	10
Figure 2 Midspan Deflection After 250 Days.....	13
Figure 3 Testing Frame and Setup	17
Figure 4 Formwork for concrete decks that were cast-in-place atop W8x15 steel girders	20
Figure 5 Prototype Beam 1 (to the right) and Prototype Beam 2 (to the left)	21
Figure 6 Welded pin support on the prototype beams)	22
Figure 7 Roller support on the prototype beams.....	22
Figure 8 DEMEC points to measure strains and thermocouples and thermometer to measure temperature variance.....	24
Figure 9 DEMEC points location on concrete slab for Prototype Beam 2.....	24
Figure 10 DEMEC points location on the web of the steel girder for Porotype Beam 1...	25
Figure 11 DEMEC points location on the web of the steel girder for Porotype Beam 2	25
Figure 12 Dial gauge used to measure midspans displacements of prototype beams.	26
Figure 13 Concrete cylinder exhibiting a crushing failure (ASTM C39)	29
Figure 14 Splitting cylinder tensile strength test setup (ASTM C496)	30
Figure 15 Measurement of the modulus of elasticity (ASTM C469)	31
Figure 16 Compressive Strength (C39) for Prototype Beams 1 and 2	34
Figure 17 Splitting cylinder tensile strength (C496) for Prototype Beams 1 and 2...35	35
Figure 18 Example of failure in the concrete paste instead of the aggregates)	35
Figure 19 Example of failure in the concrete aggregates instead of the paste.....	36
Figure 20 Tested (C469) and calculated (ACI 318) for Prototype Beams 1 and 2...37	37
Figure 21 Transverse view of unrestrained shrinkage prisms for Prototype Beam 1 and 2	38
Figure 22 Longitudinal view of unrestrained shrinkage prisms for Prototype Beam 1 and 2.....	38
Figure 23 Stresses in the composite section due to shrinkage for Prototype Beam 1.42	42
Figure 24 Stresses in the composite section due to shrinkage for Prototype Beam 2. 42	42
Figure 25 Stresses in the composite section due to temperature for Prototype Beam 1	43
Figure 26 Stresses in the composite section due to temperature for Prototype Beam 1	43
Figure 27 Ibrahim Sabri (Cairo University) from Cairo, Egypt and Kendall Belcher (Louisiana Tech University) from Shreveport, Louisiana)	45

Figure 28 Observing the superstructure and sub-structure of US 286 in Payne County	45
Figure 29 Identifying crack locations on SH 14 Eagle Chief Creek “A” in Woods County.....	46
Figure 30 Elevation surveying with optical surveying instruments of the SH 14 bridge	46
Figure 31 Elevation readings on the bottom of the steel girder at a pier for SH 14..	47
Figure 32 Slab elevations on the north approach of US 281	47
Figure 33 Stresses in the composite section due to shrinkage on one single interior girder line for SH 86	56
Figure 34 Stresses in the composite section due to shrinkage on all seven girder lines for SH 86.....	56
Figure 35 Stresses in the composite section due to temperature on one single interior girder line for SH 86	57
Figure 36 Stresses in the composite section due to temperature on all seven girder lines for SH 86.....	57
Figure 37 Midspan deflection for 1st Week	61
Figure 38 Midspan deflection for Year.....	65
Figure 39 Early age concrete and temperatures for 1st Week	68
Figure 40 Concrete and Steel Temperatures for Year	70
Figure 41 Prototype Beam 1 Shrinkage Strain on Concrete Slab for 1st Week	72
Figure 42 Prototype Beam 2 Shrinkage Strain on Concrete Slab for 1st Week	74
Figure 43 Prototype Beam 1 Shrinkage Strain on Concrete Slab for Year	76
Figure 44 Prototype Beam 2 Shrinkage Strain on Concrete Slab for Year	78
Figure 45 Average Shrinkage Strain on Concrete Slab 1st Week	79
Figure 46 Average Shrinkage Strain on Concrete Slab for Year.....	83
Figure 47 Prototype Beam 1 Strain on Steel Beam for 1st Week.....	86
Figure 48 Prototype Beam 2 Strain on Steel Beam for 1st Week.....	88
Figure 49 Prototype Beam 1 Strain on Steel Beam for Year.....	90
Figure 50 Prototype Beam 2 Strain on Steel Beam for Year.....	92
Figure 51 Average Strain in Steel Beam for 1st Week	94
Figure 52 Average Strain in Steel Beam for Year	98
Figure 53 Unrestrained Shrinkage Strains for 1st Week	100
Figure 54 Unrestrained Shrinkage Strains for 1st Year.....	102
Figure 55 SH 86 over Stillwater Creek in Paying County.....	103
Figure 56 Roadway elevation profile for the SH 86 bridge.....	106
Figure 57 Elevations taken at the bottom of north span of SH 86.....	109
Figure 58 Elevation profile of the cross section and slab for SH 86	113
Figure 59 Top and Bottom Elevations of Concrete Slab for SH 86	114
Figure 60 SH 14 bridge over Eagle Chief Creek in Woods County	116
Figure 61 SH 14 Roadway Elevations	118

Figure 62 Elevations at the bottom of the concrete deck of SH 14	120
Figure 63 A pre-existing core hole discovered in span 2 of SH 14	124
Figure 64 This pre-existing core hole discovered in span 4 of SH 14.....	125
Figure 65 US 281 over Mule Creek in Northern Woods County	126

CHAPTER I

INTRODUCTION

America is heavily dependent on its infrastructure to transport people, freight information, and energy. Our existing transportation infrastructure was built and maintained by numerous local, state, and federal agencies over the last century with a variety of design standards and construction practices. According to the Federal Highway Administration (FHWA), 27.5% (162,869) of our nation's 591,707 bridges are structurally deficient or functionally obsolete (LePatner 2012). As a result, government agencies are trying to develop long-term solutions in bridge design that lower maintenance and extend lifespan. According to the Oklahoma Department of Transportation (ODOT), Oklahoma's bridges ranked second worst in the nation with 372 structurally deficient and 544 functionally obsolete bridges (ODOT 2015). Over the next eight years, Oklahoma expects to invest \$500 million in safety and functionality improvements to its bridges (Neuwald 2010).

In Oklahoma, new bridges are principally built with concrete and featuring cast-in-place concrete decks made composite with the prestressed concrete girder. However, bridge rehabilitation is also an important component to improve and update our State's highway infrastructure. Many of these rehabilitated bridges were built originally with concrete decks on steel girders. As new concrete decks are cast, the new bridge deck is often made wider and thicker than the original deck. These changes challenge the original designs, and many rehabilitated bridges suffer from noticeable ride un-evenness and unwarranted

deformations.

Concrete bridge decks made composite with steel girders are one of the most common methods used for rehabilitating existing steel girder bridges. Composite construction has benefit over non-composite construction of improving strength, improving stiffness, reducing costs and improving efficiency. However, concrete –while hardening and curing – changes volume most notably by shrinking. As concrete shrinks, the associated volume changes are resisted by the steel girders made composite at the time of casting. It has been theorized by some engineers that the volume change in concrete has been the source of adverse ride quality in many rehabilitated bridges with newly cast concrete decks that were made composite with existing steel girders.

Our research had two primary components: (1) laboratory investigations on prototype bridge beams and smaller laboratory specimens, and (2) forensic investigations of newly rehabilitated concrete and steel composite bridges. The forensic investigations were conducted on three bridges in northwestern and northcentral Oklahoma. The laboratory prototype beams, concrete cylinders, and shrinkage prisms were built and tested at Oklahoma State University in Stillwater, Oklahoma. The forensic investigations resulted in elevation readings and inspection for cracks and other abnormalities. The laboratory experiments revealed insight into the nature of concrete shrinkage and its effect on deflections. The methodology and findings will be discussed in the coming chapter.

Our laboratory experiments measured fresh and hardened properties of concrete. The concrete batched was comparable to mixtures used in construction of bridge decks in Oklahoma. The concrete was used to construct two prototype concrete and steel composite

beams, and laboratory companion specimens consisting of eighty-eight cylinders and eight shrinkage prisms. After batching the concrete, fresh concrete properties measured were slump, temperature, air content, and unit weight. On the specimens, the hardened concrete properties measured were compressive strength, tensile strength, and modulus of elasticity on the cylinders and unrestrained shrinkage strain on the shrinkage prisms. On the two prototype scale model beams, concrete and steel strains and temperatures were measured for an extended period of time. Our laboratory experimentation indicates that concrete shrinkage may impact the ride quality of newly rehabilitated concrete bridges. However, the forensic investigation on three bridges in Oklahoma provided evidence that ride quality issues are most likely caused by construction issues and the inability of proper deck formwork and bracing to support the dead weight of the fresh concrete and construction loads. The phenomena results in permanent deflections in newly constructed bridges that affect ride quality immediately upon service.

CHAPTER II

LITERATURE REVIEW

Literature Summary

The chapter serves as a summary of the literature review. Shrinkage, creep, and other time-dependent volume changes effects are considered minimal. Currently, there is only a handful of articles available on the effects of time-dependent volume changes on rehabilitated concrete slab and steel girder composite bridges. Most theoretical research has been conducted using Age-Adjusted Effective Modulus Method (AEMM), Effective Modulus (EM), Mean Stress (MS), and Image Analysis. Some of the research has shown that time-dependent volume changes do not impact the load carrying capacity of a structural member, but instead affect the response to service loads and deflections. Some researchers recommend waiting for the concrete to develop its strength and necessary resisting moments to counter the effects of shrinkage and creep before applying loads to the structure (Chaudhary et al. 2009). Most of the research conducted for time-dependent volume changes are in regards to prestressed concrete and reinforced concrete not concrete and steel composites (Bradford 1991 and Jung et al. 2000).

Composite sections provide an increase in strength, but one downside is how the shrinkage in the concrete slab affects the steel beams. This is important because these new shrinkage stresses have a direct effect on bridge performance and durability. One possible consensus of the articles in the literature review is that shrinkage, creep, and other time-dependent

volume changes need to be considered in the design as they can cause adverse effects to sustainability.

The passages below comprise the literature review and each article has its own section:

Csagoly, P. & Long, A.E. (1975). A Note on Shrinkage Stresses in Continuous Steel-Concrete Composite Bridges. *The Structural Engineer*.

In this passage, the author recommends that the designer estimates stresses in the concrete slab caused by live loads, temperature, and shrinkage. Further stating how live loads can be determined with reasonable accuracy, but how little information exist on estimating the level of stresses caused by temperature and shrinkage effects. For their study, the authors performed shrinkage test on a two-span continuous steel and concrete composite beam and compared the data with analytical predictions.

For the laboratory shrinkage test, a two-span continuous composite beams consisting of a 254 mm x 104 mm I-section connected by shear stud connectors to a 760 mm x 76 mm slab was prepared in the Civil Engineering Department, Queen's University, Kingston, Canada (Csagoly et al. 1975). In addition, two 305 mm x 305 mm x 76 mm thick concrete slab control specimens were cast to provide unrestrained shrinkage data. All specimens had the same curing conditions applied. Once the control specimens had achieved 150 microstrains of unrestrained shrinkage, strain readings were taken on the top and bottom flanges of the steel girder of the composite beam at 4 discrete points with an electrical resistance strain gauge.

For the analytical approach, a computer program based on the stiffness method was utilized for the calculation of stresses on a continuous composite beam. Two assumptions made for simplification were: 1) the slab concrete remained uncracked as cracks induced by excessive tensile stresses will cause redistribution of stresses, and 2) full composite action in regions with or

without shear connectors (Casgoly et al. 1975). The authors stated that it would be beneficial to compare the data obtained with strain measurements from an actual bridge. Further stating that in the field, there is difficulty isolating the shrinkage strains with any degree of confidence from the temperature-induced strains.

The data from the laboratory and analytical approach revealed there is great correlation between the strains of the two methods measured on the two outer supports and not with the interior supports. But on the center support, there was greater variance. The authors believed this was a result of cracking being neglected in analysis and that cracking was likely to occur near the central support. Further stating that a more complicated analysis was not necessary at this time. Their conclusions were that: 1) analytical methods provide reasonable estimates for shrinkage stresses and strains, and 2) that continuous beams develop shrinkages stresses and strains twice the order of those induced in a simply supported beam (Casgoly et al. 1975).

Chaudhary, S., Nagpal, A., & Pendharkar, U. (2009). Control of Creep and Shrinkage Effects in Steel Concrete Composite Bridges with Precast Decks. *Journal of Bridge Engineering*.

Creep and shrinkage in the concrete deck of steel-concrete composite bridges can result in significant redistribution and consequent increase in bending moments at continuity (interior) supports and also increase deflection (Chaudhary et al. 2009). The author states that shrinkage, while considered minimal in impact, can have a significant impact. Creep is affected by the age of concrete at loading. Generally, there exists a small time span between the composite bond forming between steel and concrete, and the load being applied to the structure. This could affect the concrete developing its strength and necessary resisting moments to counter the effects of shrinkage and creep. The time-dependent nature of creep and shrinkage can lead to moment redistribution and progressive cracking.

Few studies have been conducted on the effect of the age of the concrete at the time of installing the precast panels on steel girders. However, no studies are available for the effect of the age of concrete at the time of loading or the formation of composite action on the creep and shrinkage behaviors of composite bridges consisting of steel girder and precast concrete decks incorporating all the three aspects: progressive cracking, creep and shrinkage (Chaudhary et al. 2009). The authors proposed a hybrid procedure for analyzing the effects of creep, shrinkage, and progressive cracking in concrete decks with different thicknesses and grades for single span, three span and five span bridges. Also, shored and unshored construction was taken into account. This paper came to several conclusions, one of them being the fact that volume changes due to the effects of creep and shrinkage in steel-concrete composite sections can be controlled solely by delaying the mobilization of composite action without any alterations to changes in design parameters.

Bradford, M. (1991). Deflections of Composite Steel-Concrete Beams Subject to Creep and Shrinkage. *ACI Structural Journal*.

Under service loading on a composite beam, the time-dependent factors of creep and shrinkage control the deflections of the concrete slab. Also under service loading, the deflections will increase with time under a sustained load. This is also true for reinforced and prestressed concrete members. Most of the studies of the response of structures to creep and shrinkage have been with reference to reinforced and prestressed concrete members only, and the application of the well-researched predictive models to composite steel-concrete members has received far less attention (Bradford 1991). This paper analyzes the time-dependent moment-curvature response of a steel and concrete composite beam with full composite action using a numerical method based on Age-Adjusted Effective Modulus Method (AEMM). This method was programmed into a microcomputer and utilized to acquire the time-dependent response of 65 T-beam composite

cross sections. The T-beams had variations in slab dimensions, slab reinforcement area ratio, steel dimensions, creep coefficient, and shrinkage strains.

Using the results, the aim is to create a proposed design method to calculate deflections of a composite T-beam under sustained service loads. The following assumptions were made in the approach: 1) full composite action, 2) short term stress-strain relation for concrete is linear, 3) no residual stresses in steel, 4) reinforcing steel in slab is elastic-perfectly plastic, 5) compressive stresses and deformations are positive, and 6) positive bending stresses cause tensile stresses in bottom fibers. The data obtained was compared to the data from another paper that used an analytical approach to measure stresses. The analytical approach was used on a composite beam in a real building. It was shown that after 493 days the stresses from the analytical and experimental approach were in good agreement. The table comparing the data is shown below in

Table 1:

Table 1: Comparison of Stresses

Comparison of Stresses		
Location	Stresses (Mpa)	
	Analytical	Numerical
Top of Concrete	-1.4	-2.9
Bottom of Concrete	-1.6	-2.3
Top of Steel	75.0	73.0
Bottom of Steel	-58.0	-52.0

Jung, C., Kwak, H., & Seo, Y. (2000). Effects of the Slab Casting Sequences and the Drying Shrinkage of Concrete Slabs on the Short-Term and Long-Term Behavior of Composite Steel Box Girder Bridges Part 1. *Engineering Structures* 23(500).

This paper takes on an analytical and experimental approach toward the time-dependent behavior of composite concrete and steel bridges. The authors used a first order algorithm in the analysis of creep based on the findings in previous studies. Furthermore, the authors used a layered sectional approach to get better results in relation to the time-dependent effects of creep and shrinkage on each layer. Accomplished with stress-strain relations in concrete, superposition, and total uniaxial concrete strain from the non-mechanical and mechanical strain. In addition, the authors performed field examinations on two continuous composite bridges in Korea and tested the bridges at the interior supports.

Variances in materials properties and age at loading between the steel girder and the cast-in-place concrete slab results in time-dependent differential strains and stress distributions along the span length. With a continuous composite member, cracking in the concrete slab leads to additional nonlinearity behavior at the interior supports. This nonlinearity behavior is not an issue in a simply supported beam. Referencing a paper by Csagoly et al. 1975, continuous composite beams develop shrinkage stresses in the slabs, which are of the order of twice those induced in simply supported beams with similar cross-sectional properties (Jung et al. 2000). This fact concludes that time-dependent effects are more significant on a continuous structure than a simply supported structure. The authors stated that relatively little research has been published on time-dependent behavior of continuous composite beams including the nonlinearity effects of cracks.

The authors concluded that the analytical results were in coherence with the experimental results and that to get results that are more realistic; one should consider using the aging coefficient. The

ultimate shrinkage strain recommended in the specifications can be significantly different from the actual rate of drying shrinkage (Jung et al. 2006). The Korea Highway Specifications recommends 150 to 200 microstrains for the ultimate shrinkage strain. From their study, the ultimate shrinkage strain varied from 400 to 800 microstrains, and 600 microstrains provided the best correlation for the analytical calculations to the measured results. These differences are attributed to field conditions such as concrete slump, ambient temperature, and relative humidity. Therefore, the effective quality control for the deck concrete is more important than the placing sequence of the concrete in order to prevent early transverse cracks (Jung et al. 2006). This leads to the premise that field conditions should be made as “ideal” as possible to get the best results.

Holloway, R. (1972). Precast Composite Sections in Structures. *ACI Journal*.

This paper analyzes the advantages and disadvantages of using composite construction and offers insight toward possible future development. The cross section shown below in Figure 1 has a 5” x 5’6” concrete slab atop of an 18” x 7.5” x 55 lb/ft. steel girder. Table 2 below shows the comparison between composite and non-composite sections for the cross section mentioned above and shown below.

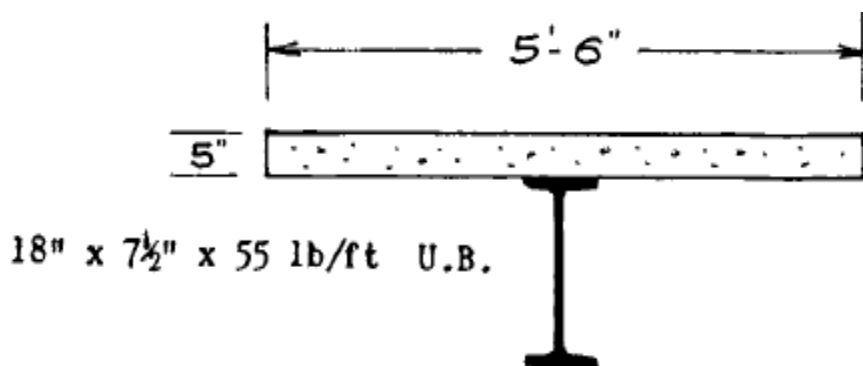


Figure 1: Cross Section Used in Analysis and Design

Table 2: Comparison of Designs for Noncomposite and Composite Section

Comparison of Designs for Noncomposite and Composite Section									
Concrete Quality 28-day Compressive Strength, psi		Steel Quality			Noncomposite Section	Composite Section			
						Elastic Design		Load Factor Design	
Cube	Cylinder	General Description	Fe Grading	Nearest ASTM Equivalent	Elastic Moment of Resistance, kip-in.	Elastic Moment of Resistance, kip-in.	Percent Increase	Ultimate Moment (1.75) kip-in.	Percent Increase
3000	2400	Mild Steel	43A	A36	2310	3250	41	3600	56
3000	2400	High Yield Steel	50B	A441	2970	4425	49	4800	62
4500	3600	Mild Steel	43A	A36	2310	3250	41	3950	71
4500	3600	High Yield Steel	50B	A441	2970	4500	52	5150	74

Fe grade number represents tensile strength in kg/mm³

From the Table 2 above, it is apparent the composite section can handle twice the load of a non-composite section, and has an increase in bending strength of approximately 50%. Composite sections are economic because of high strength steel, ultimate strength (load factor), and high quality concrete (Holloway 1972). Furthermore, it is apparent that an increase in concrete cylinder strength from 2,400 psi to 3,600 psi results in a considerable increase in bending strength from 3,250 psi to 4,500 psi for elastic design and 3,600 psi to 5,150 psi for load factor design.

Therefore, composite sections are helpful from a financial and durability standpoint. The author states that high strength steel allows shallow depth beams to be used, giving valuable savings in construction depth (Holloway 1972). High quality concrete used in a slab can increase the carrying capacity of the beam and can lead to a lighter section being used. Therefore, using high strength concrete can be beneficial especially in load factor design. The load factor design procedure was based on the British Code of Practice for composite beams in buildings since American specifications do not yet permit the use of load factor methods (Holloway 1972).

The author stated that one of the biggest disadvantages of composite construction is the necessity of being knowledgeable on steel and concrete to optimize the composite action between the two. Shoring is another downside because of the cost required along with shear connectors.

Furthermore, a concrete deck being added to the steel girders can strengthen existing bridges.

This allows structures to be modified, enlarged, or dismantled with ease (Holloway 1972).

Bradford, M. (1997). Shrinkage Behavior of Steel-Concrete Composite Beams. *ACI Structural Journal*.

The shrinkage of the concrete slab depends on the environment and constituents of the concrete, and may reach shrinkage strains up to 1000 microstrains (Bradford 1997). In this paper, the authors analyze shrinkage using the Age-Adjusted Effective Modulus Method (AEMM).

Through new uses for composite structures, this method has been used for decades to determine the effective modulus of elasticity of concrete based on shrinkage and creep. The author's aim is to develop a method of determining the shrinkage behavior of isolated steel-concrete composite tee-beams through theoretical modeling and experimental testing. In his analysis of shrinkage in unloaded simply supported composite tee-beams, it is assumed that shrinkage induces positive or sagging curvatures and that the beam is uncracked along the length. AEMM will follow the two fundamental approaches of lack of fit and relaxation; the results were shown to be identical. The

experimental test were performed on a composite beam with a steel profiled soffit with the ribs perpendicular to the beam's centerline. The beam was propped for ten days after casting and after the props were removed the beam was allowed to deform due to shrinkage for 250 days and the deformations were monitored. Furthermore, companion specimens were batched to monitor the elastic modulus, creep strain, and shrinkage strain. The deformations at midspan are compared to deformations predicted by the theory using the equation below. A parametric study was also conducted on the effects of age, joist depth, and slab width. The experimental data and theoretical models were shown to be in agreement as shown in Figure 2 below.

$$Deflection = \frac{Curvature \times Span^2}{8}$$

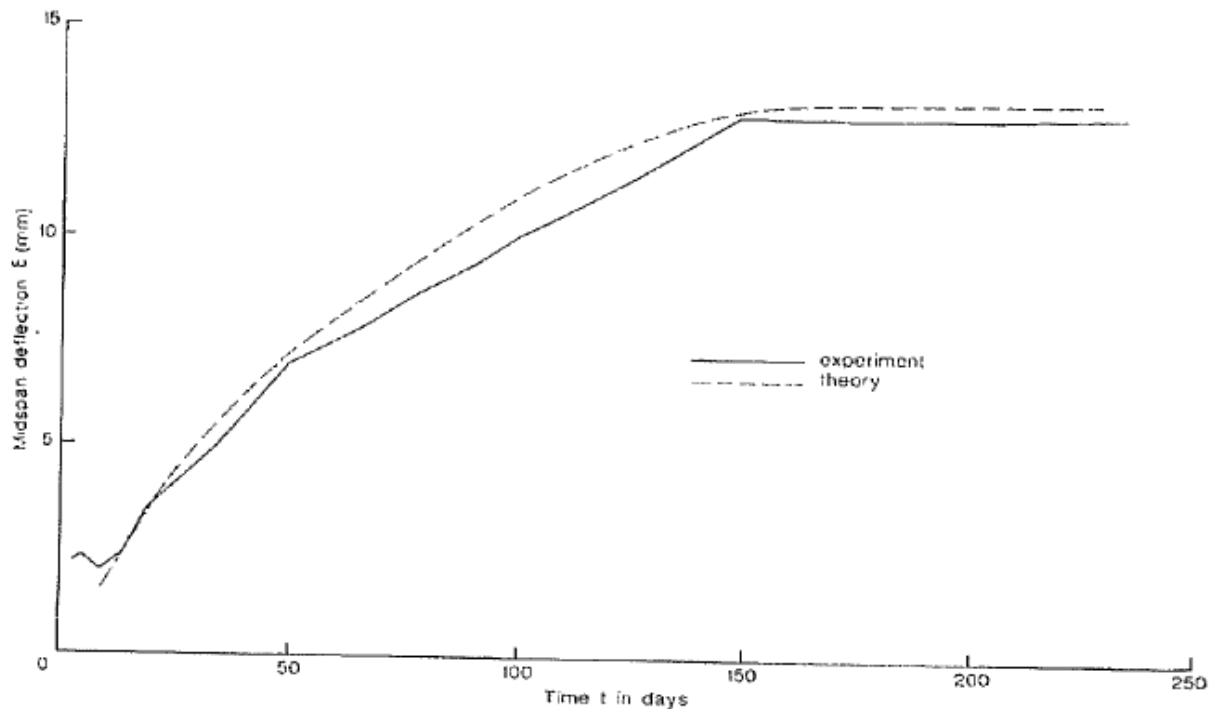


Figure 2: Midspan Deflection After 250 days

The author observed that the shrinkage induced curvatures may be high, up to 60% of the curvature to causes first yield of the steel joist, this effect is somewhat relived by providing reinforcement (Bradford 1997). Large reinforcement ratios for deflection control can cause cracking. In the absence of shear connectors and reinforcement, a concrete slab will contract due to shrinkage. The shear connectors and reinforcement serve as resistors to this contraction, and the forces in the connectors oppose those due to the gravity load so shrinkage is beneficial to the connectors (Bradford 1997). However, the contraction of concrete can offset this benefit because of the flexural stresses and deflections that arise. Furthermore, reinforcement in the concrete slab will increase the ductility of the composite beam, but the reinforcement can increase the tensile stresses in concrete due to shrinkage to the point of cracking. In conclusion, the author recommends that the structural designers are aware of the effects of concrete shrinkage in composite tee-beams when designing to meet serviceability limit states.

Alexander, S. (2003). How Concrete Shrinkage Affects Composite Steel Beams. *New Steel Construction*.

Shrinkage affects the serviceability of bridges through stress limitation and deflection. Concrete shrinks enough to warrant thinking about in the design and steel does not so in composite construction shrinkage of insitu concrete slabs induces stresses and deflections in the supporting steel beams (Alexander 2003). In this paper, the author explains the theory behind shrinkage and provides equations to calculate its effects. The author provided numerical examples and for simplicity, his research focused on shrinkage of simply supported beams in buildings in indoor conditions.

There are two potential sources of contraction, early thermal and shrinkage (Alexander 2003). When the chemical action of the heat of hydration heats the fresh concrete, early thermal contractions occur when the concrete hardens and cools. With the case of composite slabs, the

heat of hydration can possibly escape the top and bottom surfaces of a relatively thin composite member, resulting in early thermal contractions being small. Therefore, the author states that these early thermal contractions can be ignored. However, the effects of shrinkage, in particular drying shrinkage, is more important. Using the equation below, it is apparent that reinforcement is supposed to reduce contraction. ϵ_n is the net contraction, ϵ_{cs} is the estimated free shrinkage, m is the modular ratio, and ρ is the ratio of reinforcement area to concrete area.

$$\epsilon_n = \frac{\epsilon_{cs}}{1 + m\rho}$$

For stress limitations, the author concluded that overstressing the top flange is not important because the force could be transferred from steel to concrete slab with minimal deformation. Nevertheless, for the bottom flanges, the tensile stress is around 10% to 15% of the design stress and a designer should address the tensile stresses for service loading conditions. Further stating that since the service load is over estimated by the code and the design stress is below the onset of yield, it is reasonable to ignore the tensile stressed induced by shrinkage. Shrinkage deflection is clearly significant and should be included as part of the total long-term deflection (Alexander 2003). Therefore, addressing the effects of shrinkage in design could increase the quality of bridges and reduce cost. On shear connectors, shrinkage acts in the opposite direction of the applied loading and this lead to the consideration of using partial shear connectors to be “over-conservative.” Furthermore, it could be assumed that shrinkage deflection is equal to span/750 unless a more accurate calculation is provided.

Al-deen, S., Ranzi, G., & Vrcelj, Z. (2011). Shrinkage Effects on the Flexural Stiffness of Composite Beams with Solid Concrete Slabs: An Experimental Study. *Engineering Structures*.

Composite beams exhibit enhanced strength and stiffness when compared to the contribution of the slab and joist separately (Al-deen et al. 2011). This paper presents the results of a set of experiments targeted at evaluating how time-dependent responses of concrete influence the ultimate loading capacities of three full scale simply supported composite steel-concrete composite beams. Two of the beams were constructed un-propped and the other was propped. The three beams had a degree of shear connection of 0.5 with an 8 m length, concrete width of 2 m, and slab thickness of 125 mm. The parameters of the composite beams were based on a typical secondary beam used in composite flooring systems in Australia. The beams were loaded to failure 18 months after concrete casting by point load applied at midspan (Al-deen et al. 2011). During this period, monitoring of the specimens occurred to gather data on the time-dependent behavior and effect of concrete creep and concrete shrinkage. Afterwards, the ultimate tests were performed and the data collected was slip, strains, and deflection at quarter points.

When a beam is subjected to external loading, the deformability of the connectors lead to relative movement between the slab and the joist, denoted as interface slip. This behavior is referred to as partial shear interaction and its importance in predicting the composite response was originally pointed out in past findings (Al-deen et al. 2011). The slip of the interface was measured using LVDT sensors. This formulation is referred to as the Newmark model. Its main assumptions require that no vertical separation occurs between slab and joist, and plane sections remain plane except for the discontinuity at the connection interface. Other researchers have adjusted this model to account for time-dependent responses.

The test configuration consisted of a point load applied on a spreader beam at midspan of the simply supported beam shown in Figure 3 below. The load was applied with a servo-controlled hydraulic jack. The two un-propped beams were tested through a series of load cycles until 25 mm of deflection was achieved and the propped beam was tested until deflection reached 32 mm. The process was repeated three times before the beams were loaded to failure. All the beams failed at the shear connectors due to the partial shear connection design and the test were terminated once the first set of shear connectors failed. The ultimate load for the two unpropped beams was 210 kN and 207 kN and for the propped beam was 216 kN.



Figure 3: Testing Frame and Setup

The results obtained showed that time-dependent effects do not influence the load carrying capacity. Despite this, shrinkage effects had a detrimental influence on the flexural composite stiffness from service loads. This behavior happens because the composite beam is subjected to shrinkage and the beam slips in the opposite direction to the one it experiences under external loading. Therefore, with a beam subjected to shrinkage, the connector has to recover the slip previously induced by shrinkage before being able to reengage and to contribute to the load

carrying capacity of the member. This shrinkage was observed to cause the composite flexural stiffness to degenerate to the value calculated with no shear interaction for a certain range of loading (Al-deen et al. 2011). The authors concluded that further research is needed on the effects of shrinkage on the serviceability limit state.

CHAPTER III

METHODOLOGY

The methodology for this project involved three components:

1. Laboratory testing on two prototype concrete and steel composite beams
2. Laboratory testing on concrete cylinders and prisms from concrete batches used to make prototype beams
3. Forensic investigation on three bridges in Oklahoma

Prototype Composite Beams

Two prototype specimens were constructed. Each prototype was constructed from a W8x15 steel beam made composite with a concrete deck slab. The beams were designed to have an average tensile stress in the concrete slabs to mirror the average tensile stress in the concrete deck on the SH 86 Bridge over Stillwater Creek, Payne Co., Oklahoma. For the prototype beams, the concrete deck slabs were 14 in. wide and 12 ft. long. The steel girders were 12'-4" long, and the span for the composite beams was 12'-0". Prototype Beam 1 had a deck with a thickness of 3 in. while Prototype Beam 2 had a deck slab with a depth of 4.5 in.

Both beams were made composite with the shear stud connectors welded to the top flange of the steel beams. The shear studs were 2 in. tall with a diameter of 0.25 in. and a spacing of 6 in. The prototype beams are depicted in Figures 4 and 5 shown below.

Figure 4 shows the shear studs, transverse and longitudinal steel, and the placement of the thermocouples before casting. Figure 5 shows Prototype Beam 1 after the deck had cured and the formwork was removed and Prototype Beam 2 shortly after casting the slab. Prototype beam 1 was cast on August 28th, 2014 at 12:00 PM and prototype beam was cast on September 4th, 2014 at 12:00 PM.



Figure 4: Formwork for concrete decks that were cast-in-place atop W8x15 steel girders.

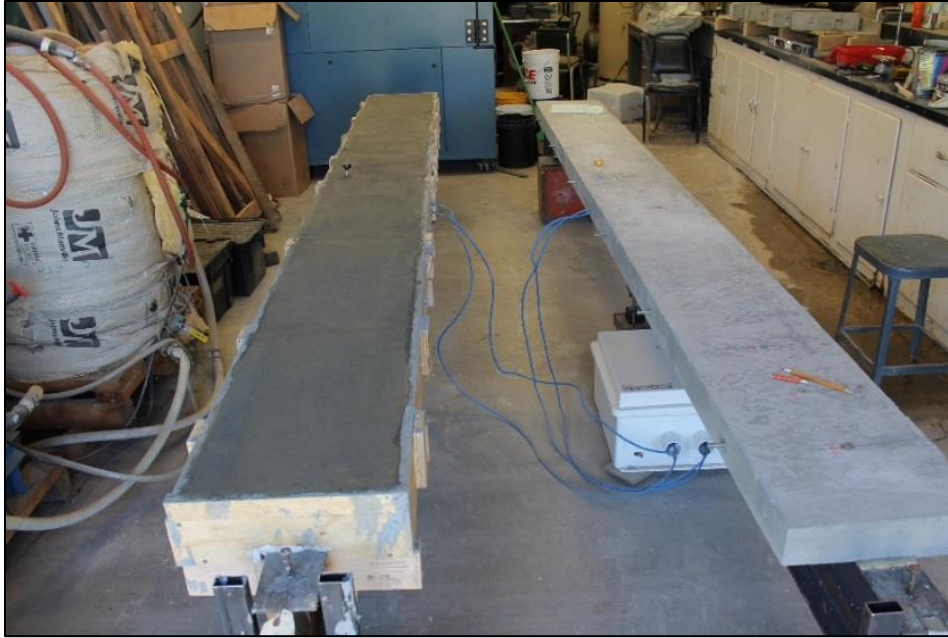


Figure 5: Prototype Beam 1 (to the right) and Prototype Beam 2 (to the left)

The prototype beams were cast-in-place to simulate a re-decking project typically done to aging steel girder bridges by ODOT. A welded pin and a roller supported each prototype beam as shown in Figures 6 and 7 respectively. Once the formwork had been installed, #3 reinforcing steel was added in the longitudinal and transverse direction. The transverse steel twelve bars was spaced at 12 in. The longitudinal steel was two bars spaced at 10 in.



Figure 6: Welded pin support on the prototype beams



Figure 7: Roller support on the prototype beams

For Prototype Beams 1 and 2, the following properties were measured, recorded, and observed periodically:

- Midspan deflections using dial gauges

- Concrete temperature of the deck slabs using embedded thermocouples and thermometers
- Steel temperature through a thermometer placed on the flange
- Ambient room temperature through a thermometer in the lab
- Concrete strains in the deck slab using demountable mechanical (DEMEC) strain gauges
- Strains in the web of the steel girders using DEMEC strain gauges
- Unrestrained concrete shrinkage in plain concrete prisms with DEMEC strain gauges
- Crack propagation on the surface of the concrete slab

At midspan, thermocouples were embedded on the side of the slab before pouring the concrete and thermometers were embedded on top of the slab after the concrete was poured. The thermocouples and thermometers were utilized to monitor the temperature variations of the concrete. After the initial set, DEMEC points were glued to the surface of the concrete deck. These points are used to measure strains resulting from temperature variance, shrinkage, and other volumetric changes. The DEMEC points were placed on several locations throughout the surface of the concrete slabs and the web of the steel beams to provide an adequate representation of the cross section. The DEMEC points, thermometer, and thermocouples are shown below in Figure 8.



Figure 8: DEMEC points to measure strains and thermocouples and thermometer to measure temperature variance.

Figure 9 shows the location and pattern of the DEMEC points on the concrete slab for Prototype Beam 2. The DEMEC points on the slab of Prototype Beam 1 were similar in location to Prototype Beam 2. Figures 10 and 11 show the location and pattern of the DEMEC points on web of the steel girder for Prototype Beam 1 and 2 respectively. Also, Figure 11 shows the thermocouple.



Figure 9: DEMEC points location on concrete slab for Prototype Beam 2



Figure 10: DEMEC points location on the web of the steel girder for Porotype Beam 1

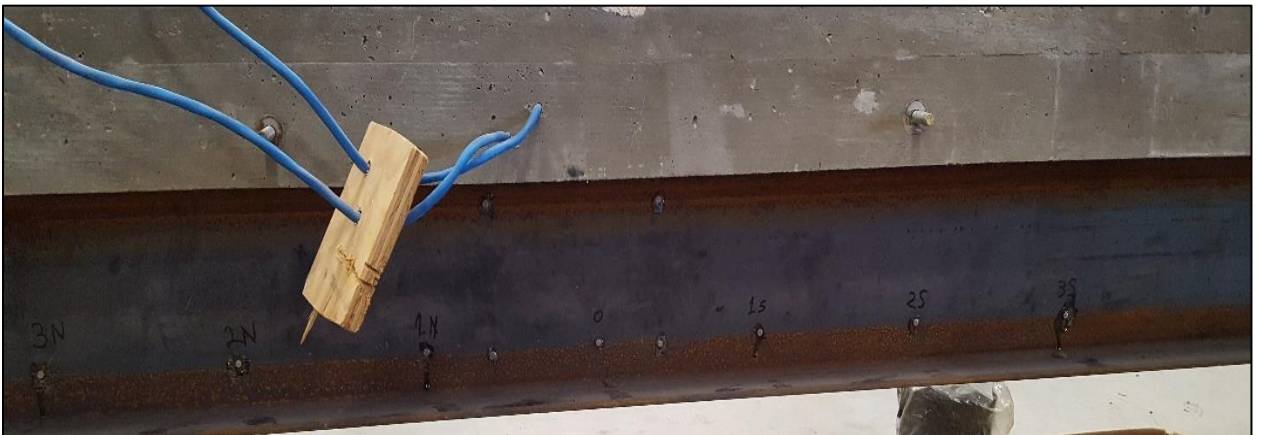


Figure 11: DEMEC points location on the web of the steel girder for Porotype Beam 2

Using dials gauges placed at midspan of each prototype beam, deflections were reported immediately before and immediately after slab pouring. The dial gauges are accurate to 0.001 in. The dial gauge at midspan is shown below in Figure 12. Also, Figure 12 shows the DEMEC points.



Figure 12: Dial gauge used to measure midspans displacements of prototype beams

Initially, readings for deflections, temperature, and strains were taking every hour for 48 hours. After 48 hours, measurements were transitioned to twice daily and then daily. The data provides insight into the shrinkage and deflection of the beams over a three month period to determine the causes of cracking, sagging, and durability issues. Furthermore, the strains can be used to determine the restrained shrinkage and curvature of the composite beam. The beams were batched with ODOT AA concrete mixtures and the proportions are provided below in Table 3.

Table 3: ODOT AA Batch Weight/Volume and Saturated Surface Dry (SSD) Weights

ODOT AA Batch Weight/Volume and SSD Weights		
Water to Cement Ratio	0.44	
	Weight (lb/cy)	Volume (ft³)
Cement (LaFarge Type I)	611.00	3.110

Fly Ash	0.0000	0.0000
Coarse (Richard Spur 57)	1900.0	11.28
Fine (Dover)	1217.0	7.360
Water	268.84	4.310
Air		0.940
Total		27.00

Fresh concrete properties measured were concrete temperature, slump, air content, and unit weight. The ambient temperature was also recorded. The two mixtures were ODOT AA batches and the tests were done in accordance with ASTM specifications. These measurements are reported below in Table 4.

Table 4: Concrete Fresh Properties of the ODOT AA Mixtures Used to Make the Two Prototype Beams

Fresh Concrete Properties for Both Prototypes Beams		
	Prototype Beam 1	Prototype Beam 2
Ambient Temperature (°F)	98.00	98.30
Concrete Temperature (°F)	94.60	96.60
Slump (in.)	4.50	9.00
Air Content (%)	2.70	4.00

Unit Weight (lb/ft ³)	154.64	152.00
Notes:		
<ol style="list-style-type: none"> 1. Prototype Beam 1 cast on 8.28.2014 12:00 PM 2. Prototype Beam 2 cast on 9.4.2014 12:00 PM 		

The concrete temperatures reported above were similar due to the relative hot ambient temperature on the separate day of batching of approximately 98 °F. The slump for Prototype Beams 1 and 2 were 4.5 in. and 9 in. respectively. For Prototype Beam 1, it is likely that the concrete vendor withheld water to ensure the ready mix concrete met specifications when arrived. This practice is common as the ready mix producer often anticipates that the contractor will add water at the jobsite. The mixture for Prototype Beam 1 was not very workable and made forming the cylinder and prisms rather difficult. Furthermore for Prototype Beam 2, we requested the vendor add an additional ten gallons, approximately eighty three pounds, of water to the specified amount in the mix design. The additional water improved workability.

Hardened Concrete Properties for the Prototype Beams

Eighty-eight cylinders and four shrinkage prisms were cast from each ODOT AA batch used to make the two prototype bridge beams. The cylinders were made using a standard 6”x12” cylinder mold and the shrinkage beams were made using a standard 4”x4”x12” prism mold. The cylinders and shrinkage prisms were molded following ASTM guidelines.

Following ASTM specifications, compressive strength (ASTM C39), splitting cylinder tensile strength (ASTM C496), and the modulus of elasticity (ASTM C469) were measured on the concrete cylinders. Tests for these material properties were performed at 12 hrs., 24 hrs., 36 hrs.,

48 hrs., 3 d., 4 d., 7 d., 14 d., 21 d., and 28 d. For each testing interval, 2 cylinders were used for ASTM C39 and one cylinder each for ASTM C496 and ASTM C469.

ASTM C39 test is used to determine the ultimate compressive failure load of a concrete specimen at a particular time interval. ASTM C496 test is used to determine the ultimate tensile failure load of a concrete specimen at a particular time interval. ASTM C469 test determines the modulus of elasticity of a concrete specimen at a particular time interval. ASTM C469 test must be performed after the compressive strength test as the failure load is required to get the loading rate. The data obtained can be used to calculate when the concrete will crack. Photographs of ASTM C39, ASTM C496, and ASTM C469 are shown below in Figures 13 through 15 respectively. The hardened concrete properties for Prototype Beams 1 and 2 are reported below in Tables 5 and 6.



Figure 13: Concrete cylinder exhibiting a crushing failure (ASTM C39)



Figure 14: Splitting cylinder tensile strength test setup (ASTM C496)



Figure 15: Measurement of the modulus of elasticity (ASTM C469)

Table 5: Prototype Beam 1 Hardened Concrete Properties

Prototype Beam 1 Hardened Concrete Properties			
Days	ASTM C39 (psi)	ASTM C496 (psi)	ASTM C469 (ksi)
0.5	2280	340	4600
1.0	3490	320	4800
2.0	4050	300	5300

4.0	4760	340	5400
5.0	5010	500	5800
7.0	5630	440	5900
14.0	5870	400	6000
21.0	6450	560	6700
28.0	6510	570	6500
Notes:			
<ol style="list-style-type: none"> 1. Date Cast: 8.28.2014 2. All data reported are the average of two specimens. 			

Table 6: Prototype Beam 2 Hardened Concrete Properties

Prototype Beam 2 Hardened Concrete Properties			
Days	ASTM C39 (psi)	ASTM C496 (psi)	ASTM C469 (ksi)
0.5	1270	220.0	3922
1.0	2200	280.0	4155
1.5	2600	200.0	4400
2.0	2600	200.0	4367
4.0	3380	360.0	4527

5.0	3480	300.0	4430
7.0	4190	360.0	4377
14	4670	420.0	4808
21	5160	440.0	5716
28	5340	380.0	5301
Notes:			
<ol style="list-style-type: none"> 1. Date Cast: 9.4.2014 2. All data reported are the average of two specimens. 			

Figures 16, 17, and 20 depicts the graphs of the compressive strength test (C39), splitting cylinder tensile strength test (C496), and modulus of elasticity test (C469) for both Prototype Beams respectively. The data reported on C39 is an average of two specimens. For Prototype Beam 1, the 24 hour compressive strength was 2,280 psi and 28 day compressive strength was 6,510 psi. For Prototype Beam 2, The 24 hr. compressive strength was 1,270 psi and 28 day compressive strength was 5,340 psi. Prototype beam 2 had one additional test done at 36 hours. It is worth noting how there was no compressive strength gain from 36 hours to 48 hours for prototype beam 2. This is most likely due to only the six hr. window for the concrete to further develop strength. The visual representation is shown below in Figure 16.

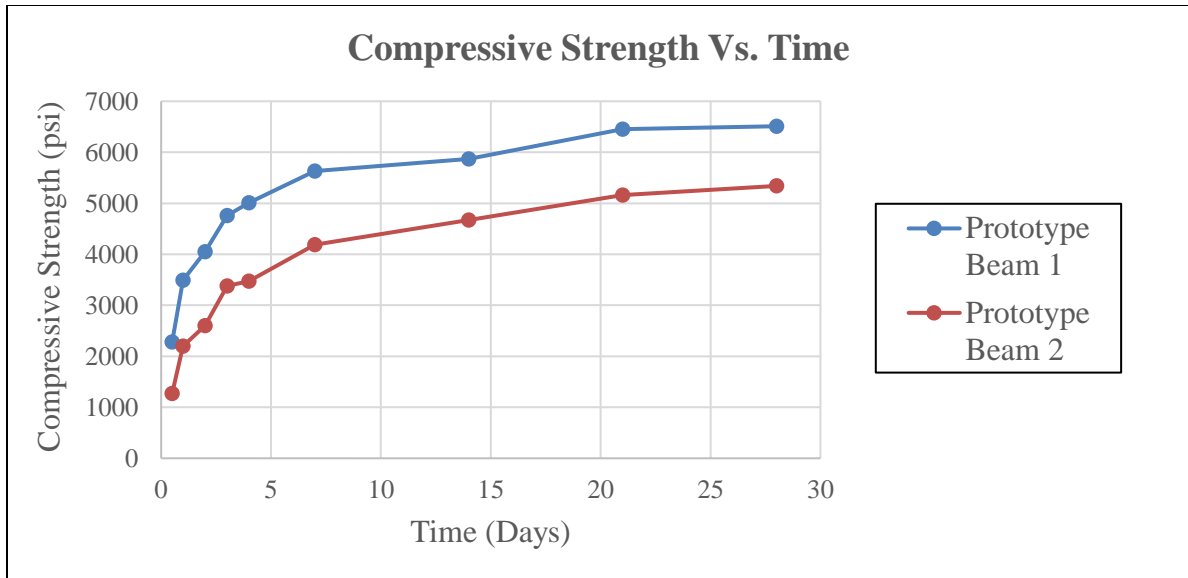


Figure 16: Compressive Strength (C39) for Prototype Beams 1 and 2

Figure 17 shows the graph of the splitting cylinder tensile strength test (C496) for both Prototype Beams. With the splitting cylinder tensile strength test, failure for early aged concrete occurs primarily in concrete paste. For more aged concrete the failures typically occur in the aggregates. Figure 18 provides an example of a splitting cylinder tensile strength test with failure in the concrete aggregates instead of the paste. Figure 19 provides an example of a splitting cylinder tensile strength test with failure in the concrete paste instead of the aggregates. For Prototype Beam 1, the 28 day splitting cylinder tensile strength of 570 psi was 8.8 % of the 28 day compressive strength of 6,510 psi. For Prototype Beam 2, the 28 d. tensile strength of 380 psi was 7.1 % of the 28 day compressive strength 5,301 psi. This relatively matches the general rule of thumb that the tensile strength of concrete is rough 10% of the compressive strength. In a sense, this validates the ASTM C39 and C496 tests.

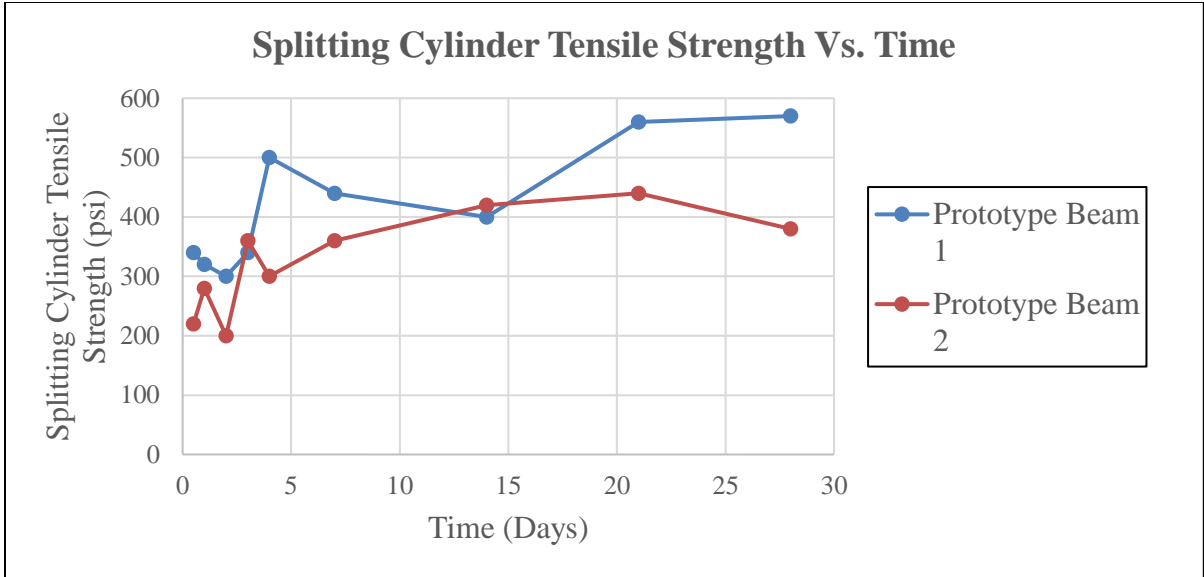


Figure 17: Splitting cylinder tensile strength (C496) for Prototype Beams 1 and 2



Figure 18: Example of failure in the concrete paste instead of the aggregates



Figure 19: Example of failure in the concrete aggregates instead of the paste

Figure 20 shows the graph of the modulus of elasticity test (C469) for both Prototype Beams.

Also included in Figure 20 is the graph of the calculated modulus of elasticity to compare with tested modulus of elasticity. The elastic modulus from the ASTM C469 tests are compared to the values calculated with the ACI 318 approximation formula shown below. Using these equations the calculated modulus of elasticity for Prototype Beam 1 and 2 would be 4,600 ksi and 4,165 ksi respectively. Compare this to the test values obtained by ASTM C469 and you obtain values of 6,500 ksi and 5,301 ksi for prototype beam 1 and 2 respectively. This shows that is a difference of about 30% for prototype beam 1 and about 21 % for prototype beam 2. E_c is the modulus of elasticity for concrete in psi, w is the unit weight of concrete in lb/ft^3 and f'_c is 28-day compressive strength in psi.

$$E_c = 33w^{1.5}\sqrt{f'_c}$$

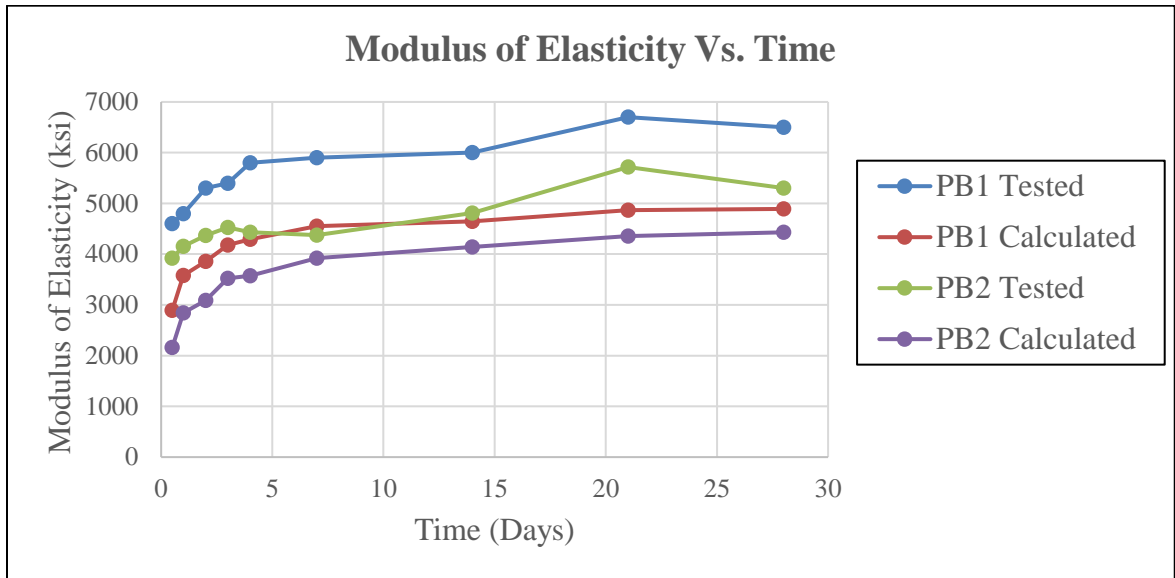


Figure 20: Tested (C469) and calculated (ACI 318) for Prototype Beams 1 and 2

The shrinkage prisms will provide unrestrained shrinkage strains that can be compared to the restrained shrinkage strains of the composite prototype beams. On the shrinkage prisms, strains were measured daily with DEMEC strain gauges. The shrinkage prisms are shown in Figures 21 and 22. Figure 21 shows the location of the DEMEC points on the prisms.



Figure 21: Transverse view of unrestrained shrinkage prisms for Prototype Beam 1 and 2



Figure 22: Longitudinal view of unrestrained shrinkage prisms for Prototype Beam 1 and 2

Computational Analysis on Prototype Beams

Table 7 shows the concrete slab properties for each prototype beam. Table 8 shows the properties of the W8x15 steel beam. Using Tables 7 and 8, the composite section properties for the prototype beams can be computed by converting the concrete to steel. The composite section properties are reported in Table 9. For the calculations the ultimate shrinkage strain was assumed to be 0.0005 strain and the creep coefficient was 2. In addition, the creep coefficient was used to determine the effective modulus. The effective modulus and modular ratio would be used to compute restraining forces and stresses, and composite section properties. The creep coefficient was used to give a better representation of the effects of shrinkage and the elastic modulus. The effective modulus of 1,207 ksi is a third less than the short term modulus of 3,605 ksi. The effective modulus results in lower stresses, restraining force, and deflections than the short term modulus. For Prototype Beam 1, calculations showed that the deflection from the slab and haunch would be 0.015 in. For Prototype Beam 2, calculations showed that the deflection from the slab and haunch would be 0.022 in. Figures 23 and 24 show the stresses and deflection that occur from shrinkage on Prototype Beams 1 and 2. The figures show that the final restrained shrinkage stress to the right is equal to the summation of the restrained concrete shrinkage stress, axial load on the composite section, and the bending moment on the composite section. Therefore, the actual stresses acting on the beam due to shrinkage restraint are the addition of the stresses: shrinkage restraint, axial load, and bending moment. The deflection from shrinkage alone was calculated to be 0.102 in. and 0.114 in. for Prototype Beams 1 and 2 respectively. This values show that shrinkage is a contributor to ride quality even if minimal. For Prototype Beam 1, the theoretical tension at the bottom of the slab is 313 psi, which is very nearly the same as the 287 psi for Prototype Beam 2.

Table 7: Prototype Beams Concrete Slab Properties

Prototype Beams Concrete Slab Properties
--

	Prototype Beam 1	Prototype Beam 2
γ (k/ft ³)	0.15	0.15
h_{slab} (in.)	3.0	4.5
b_{eff} (in.)	14.0	14.0
A_{slab} (in ²)	42.0	63.0
I_{slab} (in ⁴)	31.5	106.31
f'_c (ksi)	4.0	4.0
E_c (ksi)	3605	3605
h_{haunch} (in.)	0.0	0.0
A_{haunch} (in ²)	0.0	0.0
I_{haunch} (in ⁴)	0.0	0.0
$W_{\text{slab/haunch}}$ (klf)	0.044	0.065
$\Delta_{\text{slab/haunch}}$ (in. ↓)	0.015	0.022

Table 8: W8x15 Steel Beam Properties

W8x15 Steel Beam Properties		
A	4.44	in ²
I	48.0	in ⁴

d	8.11	in.
b _f	4.015	in.
E _s	29000	ksi

Table 9: Prototype Beams Composite (Concrete to Steel) Properties

Prototype Beams Composite (Concrete to Steel) Properties		
	Prototype Beam 1	Prototype Beam 2
n = E _c /E _s	0.12431	0.12431
L (ft.)	12.00	12.00
d (in.)	11.11	12.61
A (in. ²)	9.66	12.27
y _t (in.)	4.05	4.53
y' _b (in.)	7.06	8.08
I (in ⁴)	125.95	173.86
C (creep)	2	2
E _{eff} (ksi)	1201.67	1201.67
n _{eff}	0.04	0.04

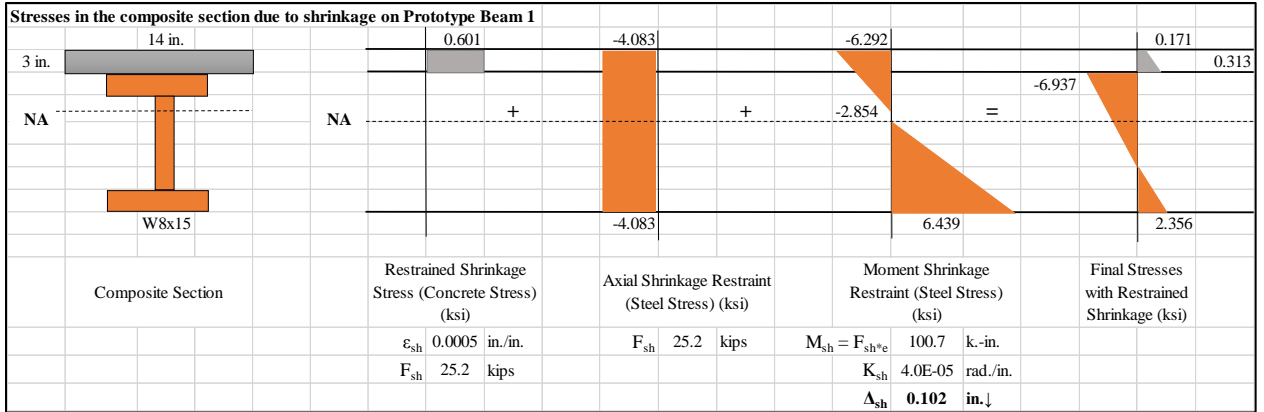


Figure 23: Stresses in the composite section due to shrinkage for Prototype Beam 1

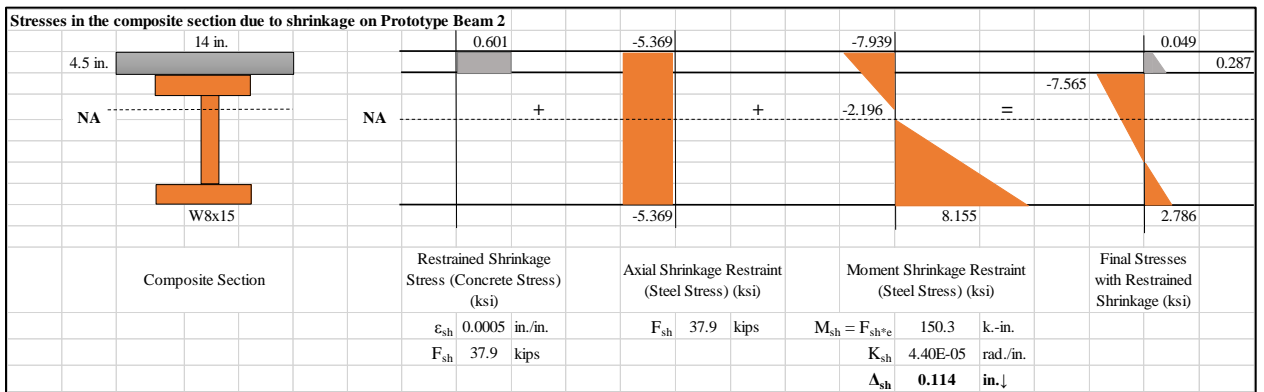


Figure 24: Stresses in the composite section due to shrinkage for Prototype Beam 2

Figures 25 and 26 shows the stresses that occurred as a result of a Zone 2 temperature gradient being imposed on Prototype Beams 1 and 2 respectively. Due to the temperature gradient, Prototype Beam 1 deflected upward 0.047 in. and Prototype Beam 2 deflected upward 0.041 in.

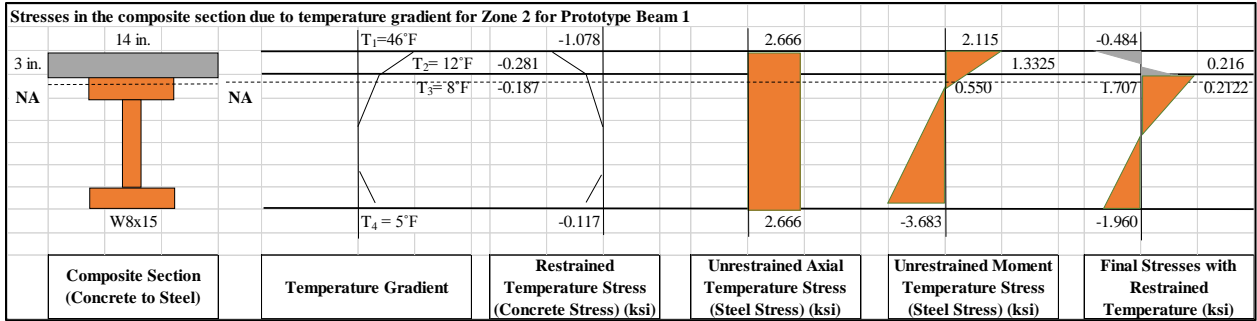


Figure 25: Stresses in the composite section due to temperature for Prototype Beam 1

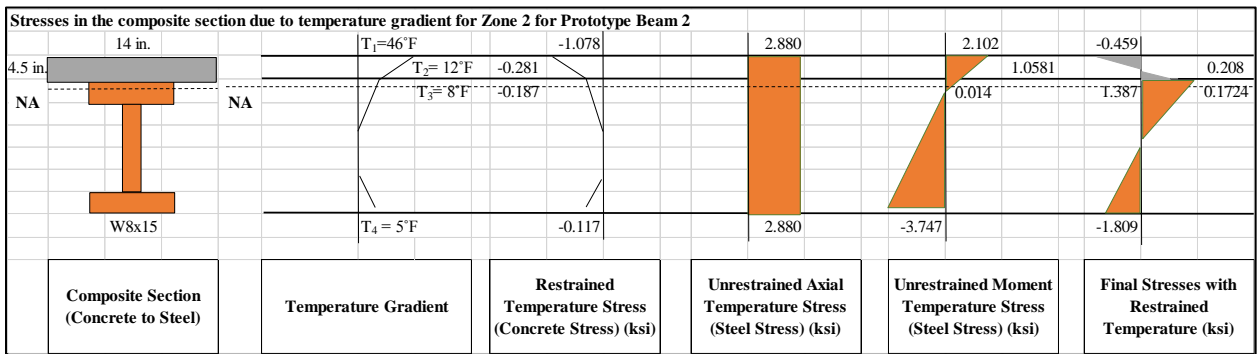


Figure 26: Stresses in the composite section due to temperature for Prototype Beam 1

Forensic Investigation on Three Bridges in Oklahoma

Forensic investigations were performed on three bridges located in Woods County and Payne County. The bridges were SH 86 Stillwater Creek in Payne Co., SH 14 over Eagle Chief Creek in Woods County, and US 281 over Mule Creek in Woods County. SH 86 was investigated first then SH 14, and lastly US 281. ODOT was contacted and they provided traffic control for our investigations. Using an optical engineering level, elevations readings at several locations of the abutments, surface of the concrete deck, underneath the concrete deck, along the steel girders, and the guardrails. In addition, the bridges were inspected for cracks, support conditions, observable deflections, diamond grinding, ride quality, and other detectable and visual observations. The investigations were conducted in September of 2014.

SH 86 is a three span bridge with each span approximately 60'-0 in length. Only the northernmost span was surveyed due to lack of access caused by Stillwater Creek in western Payne County on the westernmost fringes of Carl Blackwell. Ride ability issues were observed immediately after construction and this is made apparent by each span exhibiting a dip of 1.5 in. ODOT provided a concrete break summary report and fresh concrete tests and properties report for only SH 86. SH 14 is a four span bridge each span approximately 60'-0 in length, and we investigated this bridge. A new bridge was constructed in 2010 or 2011 and some rehabilitation or reconstruction of the abutments were also done.

Figure 27 shows a picture of my partner, Ibrahim Sabri, and I at US 281. Figure 28 is a side view of SH 86 over Lake Carl Blackwell. Figure 29 shows me identifying cracks on the concrete bridge deck of SH 14 to determine if there were any systematic patterns. One of the things we were looking for were to determine if there were any systematic patterns. Figure 30 shows readings being taken underneath the SH 14 bridge. Figure 31 shows elevations readings being taken with a leveling rod on the bottom of the steel girder against the pier on US 281. Figure 32 shows slab elevations being taken on the north approach for US 281.

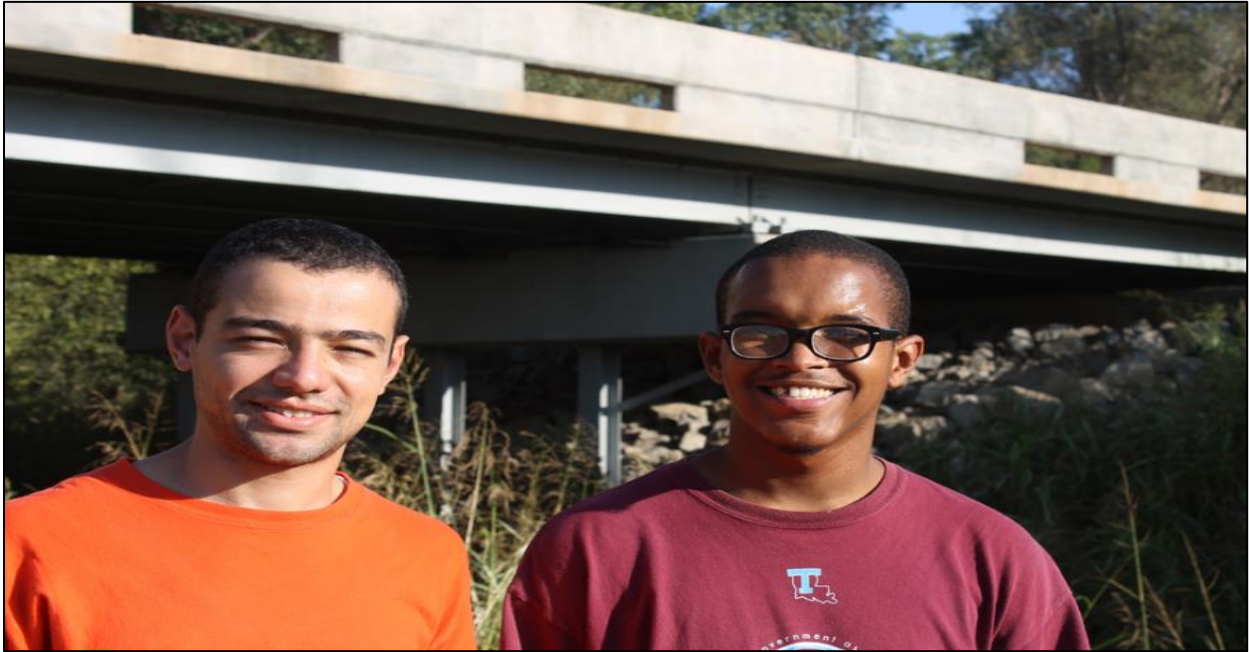


Figure 27: Ibrahim Sabri (Cairo University) from Cairo, Egypt and Kendall Belcher (Louisiana Tech University) from Shreveport, Louisiana



Figure 28: Observing the superstructure and sub-structure of US 286 in Payne County



Figure 29: Identifying crack locations on SH 14 Eagle Chief Creek “A” in Woods County



Figure 30: Elevation surveying with optical surveying instruments of the SH 14 bridge



Figure 31: Elevation readings on the bottom of the steel girder at a pier for SH 14



Figure 32: Slab elevations on the north approach of US 281

Hardened Concrete Properties of SH 86

ODOT has specifications on mix design and proportion for Class AA concrete and those requirements are listed below in Table 10. Class AA concrete should be used in superstructure items, such as bridge floors, approach slabs, reinforced concrete piles, drilled shaft foundations, parapet walls, concrete rail and handrails. The proportions provided by Dolese to batch the two Prototype Beams are listed below in Table 11.

Table 10: Mix Design and Proportioning

Mix Design and Proportioning					
Class of Concrete	Minimum Cement Content	Air Content	Maximum Water/Cement Ratio	Slump	Minimum 28-Day Compressive Strength
	lb/yd³ (kg/m³)	%	lb/lb (kg/kg)	in. (mm)	psi (kPa)
AA	611 (363)	6.5±1.5	0.44	2±1 (50±25)	4000 (27,580)

Table 11: Fresh Concrete Properties for Both Prototypes Beams

Fresh Concrete Properties for Both Prototypes Beams		
	Prototype Beam #1	Prototype Beam #2
Ambient Temperature (°F)	98.00	98.30

Concrete Temperature (°F)	94.60	96.60
Slump (in.)	4.50	9.00
Air Content (%)	2.70	4.00
Unit Weight (lb/ft ³)	154.64	152.00
Notes:		
<ol style="list-style-type: none"> 1. Prototype Beam 1 cast on 8.28.2014 12:00 PM 2. Prototype Beam 2 cast on 9.4.2014 12:00 PM 		

Neither mixtures achieved the desired air content and slump. The 3 in. slump limit specified by ODOT for an AA mixture was exceeded in Prototype Beam 2 by 6 in. due to the additional water. I believe that Doles withheld some water on site as is common practice and this would affect our w/cm ratio which in turn affects the slump and workability of the concrete. The fresh properties data from SH 86 performed by ODOT is provided below in Table 12.

Table 12: ODOT Fresh Concrete Tests for SH 86

ODOT Fresh Concrete Tests for SH 86			
	Test 1	Test 2	Test 3
Concrete Temperature (°F)	68.00	75.00	75.00
Slump (in.)	4.25	3.25	4.00
Air Content (%)	4.40	5.30	6.00

Tests performed on 10.15.2010

From comparing the data from our prototype beams and SH 86, Prototype Beam 1 had similar the slump and air content to the tests values provided by ODOT. Prototype Beam 2 possessed similar air content to the values provided by ODOT, but the slump was larger due to the additional 10 gallons of water. Concrete temperature for the Prototype Beams were higher than the SH 86 project because of the time of year. The Prototype Beams were cast in late August and early September, and the bridge deck for SH 86 was cast in mid-October.

In Table 13 below, the hardened concrete properties for the prototype beams at 28 days are shown. Table 24 shows the ODOT 28 day compressive strength test data for SH 86. ODOT did not provide data on the tensile strength and modulus of elasticity at 28 days.

Table 13: Hardened Concrete Properties at 28 Days for Prototype Beams

Hardened Concrete Properties at 28 Days for Prototype Beams			
	Prototype Beam 1	Prototype Beam 2	Average
Compressive Strength (psi)	6,510	5,340	5,925
Tensile Strength (psi)	570	380	475
Modulus of Elasticity (ksi)	6,500	5,301	5,901

Table 14: ODOT 28 Day Compressive Strength Tests for SH 86

ODOT 28 Day Compressive Strength Tests for SH 86

	Compressive Strength (psi)
Cylinder 1	5,980
Cylinder 2	5,900
Cylinder 3	4,880
Cylinder 4	5,550
Average	5,578

From the concrete used on the SH 86 Bridge, the 4,000 psi minimum threshold was achieved. The average compressive strength is similar to the compressive strength on prototype beam 2. Neither of their test values fall in range of the compressive strength of 6,510 psi for prototype beam 1.

Computational Analysis of SH 86 Bridge

SH 86 was the first bridge investigated to collect elevation data and to observe cracks and other abnormalities. This bridge had the worst ride quality of the three bridges, which is made apparent due to the 1.5 in. dip in each span. Therefore, the prototype beams were modeled off this bridge. To begin, an excel spreadsheet was created shows the stresses and deflections developing in the beam for the SH 86 bridge. SH 86 was analyzed as one single interior girder and with seven girders for the full bridge width. The steel girders are a W 33x141 rolled shape and an 8 in. concrete deck with a 1 in. haunch that varies from girder to girder as the slab has to account for the 2 % super elevation. The stresses computed were restrained shrinkage stresses, axial shrinkage restrained stresses, moment shrinkage restrained stresses, and final stresses with restrained shrinkage.

The calculation procedure followed matched that done for the prototype beams. An ultimate design shrinkage of 0.0005 strains was assumed as this is common practice in the field. Then, the restrained shrinkage strains can be converted to restraining shrinkage force by multiplying it by the concrete modulus of elasticity. The compressive strength of the concrete was assumed to be 4,000 psi based off the design specifications provided by ODOT. This 28 day compressive strength was used to determine the modulus of elasticity through the following equation $57,000\sqrt{f'_c}$ provided by the ACI 318. This equation gives units in psi and is designed for 28 day concrete compressive strength in psi. This equation gave a modulus of elasticity of 3,605 ksi. But for the calculations, a short term modulus was employed and was calculated using the creep coefficient. This modulus can be used to get the theoretical restraining force or a modulus of elasticity test (C469) can be performed to get the actual modulus. The tensile restraining force acting on the centroid of the cross section of the concrete slab will be compensated by a compressive force with a determinable eccentricity in the composite cross section. Stresses produced by the eccentric compressive force are axial stress (P/A) for the force alone and bending stress (My/I) resulting from the eccentricity of the force producing bending. These restrained shrinkage stresses contribute to the downward deflection of composite beams.

The calculated modulus of elasticity of concrete (1,201 ksi) was used with the modulus of elasticity of the steel of 29,000 ksi to get the modular ratio for the composite section of 0.04. The modular ratio was used to convert the concrete to steel for our analysis. Full composite action is assumed at the interface due to the shear studs although we know some slip had to occur. Once the stresses were determined, the prototype beams were designed to have similar stresses in the concrete deck and steel beam. This would aid determining the optimal design for our prototypes.

Figure 33 represents accounting for one single interior girder and Figure 34 accounting for all seven girder lines. This value is one of the contributors to 1.5 in. dip seen on all three spans.

When concrete cracks, the curvature would be significantly reduced and the downward deflection

calculations would be considered theoretical. If not properly accounted for in the design and construction, this deflection can create a rather unpleasant driving surface. It had been proposed that during the design process for the rehabilitation that the dead weight of the concrete was not accurately calculated. If so then it is likely one of the culprits of ride issues. From the drawings provided by ODOT, the contractor was required to account for a downward deflection of 0.65 in. at midspan. This value would have also included the weight of the guardrails leading to the conclusion that a poor estimate of downward deflection was likely not a cause of ride issues. The curvature was calculated for both cases, this value was used to get the deflection from shrinkage.

Table 15 shows the concrete slab properties for SH 86. Table 16 shows the properties of the W33x141 steel beam. Using Tables 15 and 16, the composite section properties for SH 86 can be computed by converting the concrete to steel. The composite section properties are reported in Table 17.

Table 15: SH 86 Slab Properties for 1 and 7 Girders

SH 86 Slab Properties for 1 and 7 Girders		
	1 Girder	7 Girders
γ (k/ft ³)	0.15	0.15
h_{slab} (in.)	8.0	8.0
b_{eff} (in.)	51.0	398.0
A_{slab} (in ²)	408.0	3184
I_{slab} (in ⁴)	2176.0	16981.0

f_c (ksi)	4.0	4.0
E_c (ksi)	3605.0	3605.0
h_{haunch} (in.)	1.0	1.0
A_{haunch} (in ²)	11.535	11.535
I_{haunch} (in ⁴)	0.96	0.96
$W_{\text{slab/haunch}}$ (klf)	0.437	3.328
$\Delta_{\text{slab/haunch}}$ (in. ↓)	0.551	0.600

Table 16: W33x141 Steel Beam Properties

W33x141 Steel Beam Properties		
A	41.6	in ²
I	7450	in ⁴
d	33.3	in.
b_f	11.535	in.
E_s	29000	ksi

Table 17: SH 86 Composite (Concrete to Steel) Properties for 1 and 7 Girders

SH 86 Composite (Concrete to Steel)		
Properties for 1 and 7 Girders		
	1 Girder	7 Girders
$n = E_c/E_s$	0.12431	0.12431
L (ft.)	59.0	59.0
d (in.)	42.3	42.3
A (in. ²)	93.75	688.4
y_t (in.)	13.68	13.17
y'_b (in.)	28.62	29.13
I (in ⁴)	18472.03	132929.60
C (creep)	2	2
E _{eff} (ksi)	1201.67	1201.67
n _{eff}	0.04	0.04

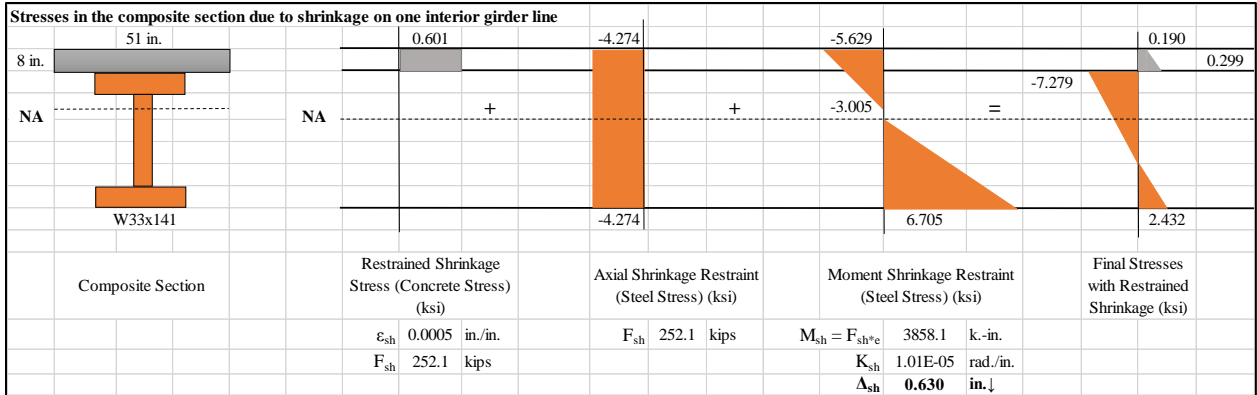


Figure 33: Stresses in the composite section due to shrinkage on one single interior girder line for SH 86

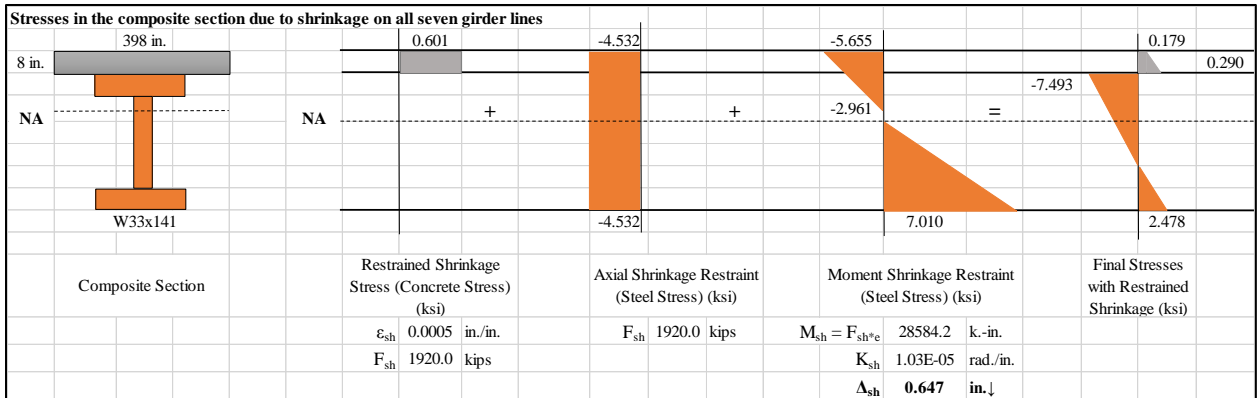


Figure 34: Stresses in the composite section due to shrinkage on all seven girder lines for SH 86

Figures 35 and 36 shows the stresses that occurred as a result of a Zone 2 temperature gradient being imposed on SH 86 respectively. Due to the temperature gradient, SH 86 with one girder deflected upward 0.242 in. and SH 86 with seven girders deflected upward 0.247 in.

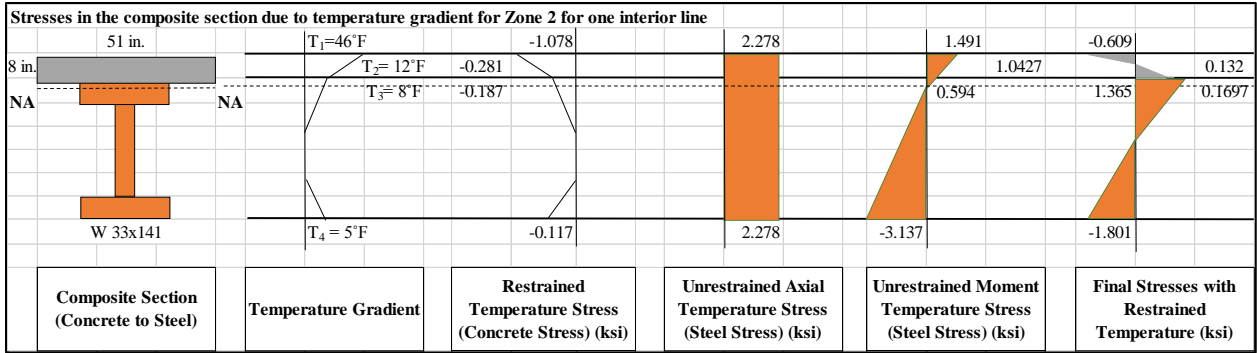


Figure 35: Stresses in the composite section due to temperature on one single interior girder line for SH 86

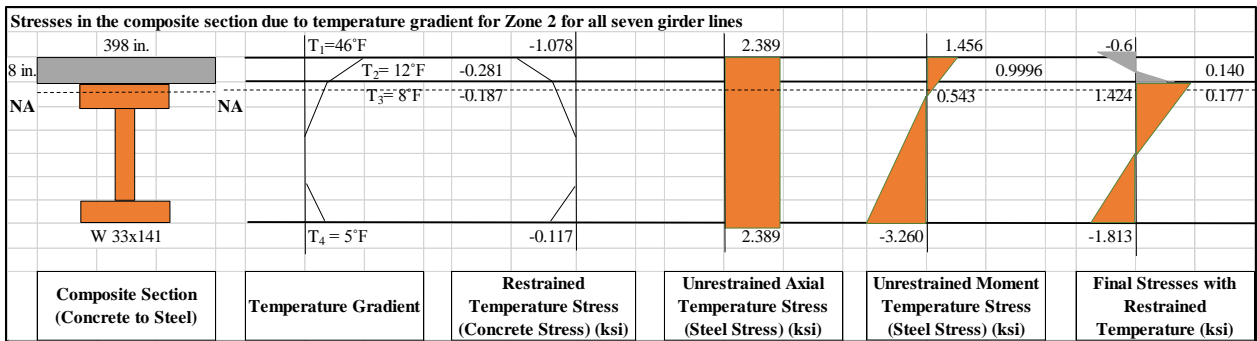


Figure 36: Stresses in the composite section due to temperature on all seven girder lines for SH

86

CHAPTER IV

RESULTS AND DISCUSSION

Results

This chapter reports the data collected from the prototype beams, the data from the concrete materials testing performed on the concrete batches from the prototype beams, and the data from the forensic investigation of the three bridges in the field.

The data that will be reported are the following:

1. Laboratory testing on two prototype concrete and steel composite beams
 - Midspan deflections over time;
 - Temperature of the concrete decks during casting and curing over an extended period of time;
 - Steel temperatures and ambient temperatures over time;
 - Strain measurements on surfaces of concrete slabs and on the webs of the steel girders.
2. Laboratory testing on concrete cylinders and shrinkage prisms
 - Hardened concrete properties (Compressive Strength C39, Splitting Cylinder Tensile Strength C496, and Modulus of Elasticity C469);

- Fresh concrete properties (unit weight C138, air content C138, slump C143, and concrete temperature);
 - Strain measurements on the longitudinal axis of the shrinkage prisms C878.
3. Forensic investigations of SH 86 over Stillwater Creek, Payne Co., SH 14 over Eagle Chief Creek “B”, Woods Co., and US 281 in Woods Co.
- Elevation readings, visual observations, and field data
 - Hardened concrete properties of SH 86
 - Computational analysis of SH 86

Midspan Deflections from Prototype Beams 1 and 2

Deflection readings were recorded from dial gauge measurements. The dial gauge was located at midspan of the composite beams. The midspan deflections vs. time for the first 168 hours (1 week) for Prototype Beams 1 and 2 are reported below in Table 18, and in Figure 37. Initial deflection readings are reported before the casting of the concrete deck. Immediately after the slab was cast, Prototype Beam 1 deflected 0.017 in. and Prototype Beam 2 deflected 0.038 in. This deflection is accounted for by the self-weight of the deck. The larger deflection of Prototype Beam 2 can be attributed to having a 4.5 in. thick concrete deck as opposed to a 3 in. thick concrete slab in Prototype Beam 1. Midspan deflection measurements were recorded for one year. The midspan deflections vs. time for the year for Prototype Beams 1 and 2 are reported below in Table 19, and in Figure 38.

Table 18: Midspan Deflection for 1st Week

Midspan Deflection for Week

Time (hours)	Midspan Deflection (in.)	
	Prototype Beam 1	Prototype Beam 2
0	0.000	0.000
1	-0.017	-0.036
2	-0.022	-0.037
3	-0.017	-0.038
4	-0.017	-0.038
5	-0.020	-0.038
6	-0.022	-0.039
9	-0.027	-0.038
12	-0.023	-0.040
15	-0.029	-0.042
18	-0.029	-0.044
21	-0.029	-0.046
24	-0.035	-0.051
48	-0.046	-0.048
72	-0.052	-0.051
96	-0.057	-0.053

120	-0.057	-0.059
144	-0.070	-0.066
168	-0.068	-0.062
<p>1. Time 0.00 = concrete casting</p> <p>2. Readings with “-” are downward</p>		

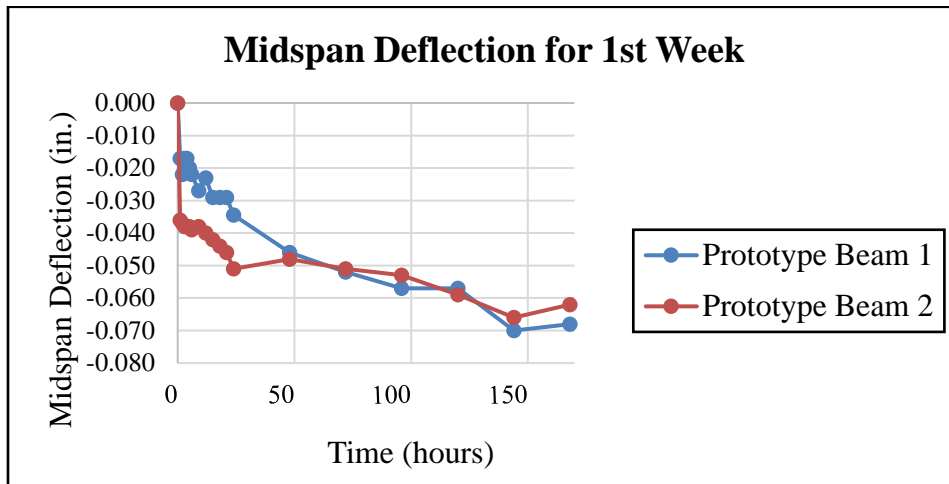


Figure 37: Midspan deflection for 1st Week

Table 19: Midspan Deflection for Year

Midspan Deflection for Year		
Time (days)	Midspan Deflection (in.)	
	Prototype Beam 1	Prototype Beam 2
0	0.000	0.000

7	-0.068	-0.062
14	-0.069	-0.098
21	-0.073	-0.107
28	-0.086	-0.113
35	-0.089	-0.119
42	-0.091	-0.120
49	-0.096	-0.123
56	-0.097	-0.126
63	-0.098	-0.130
70	-0.099	-0.128
77	-0.097	-0.127
84	-0.094	-0.129
91	-0.095	-0.132
98	-0.095	-0.130
105	-0.090	-0.126
112	-0.084	-0.122
119	-0.083	-0.125
126	-0.085	-0.121

133	-0.084	-0.119
140	-0.083	-0.116
147	-0.092	-0.113
154	-0.079	-0.110
161	-0.077	-0.114
168	-0.081	-0.111
175	-0.078	-0.113
182	-0.076	-0.115
189	-0.079	-0.117
196	-0.081	-0.118
203	-0.084	-0.119
210	-0.087	-0.118
217	-0.086	-0.121
224	-0.092	-0.125
231	-0.093	-0.127
238	-0.093	-0.129
245	-0.095	-0.131
252	-0.092	-0.128

259	-0.097	-0.134
266	-0.099	-0.136
273	-0.101	-0.135
280	-0.106	-0.133
287	-0.107	-0.132
294	-0.106	-0.131
301	-0.105	-0.130
308	-0.106	-0.127
315	-0.107	-0.129
322	-0.108	-0.134
329	-0.107	-0.132
336	-0.106	-0.131
343	-0.105	-0.129
350	-0.104	-0.134
357	-0.103	-0.132
364	-0.101	-0.131

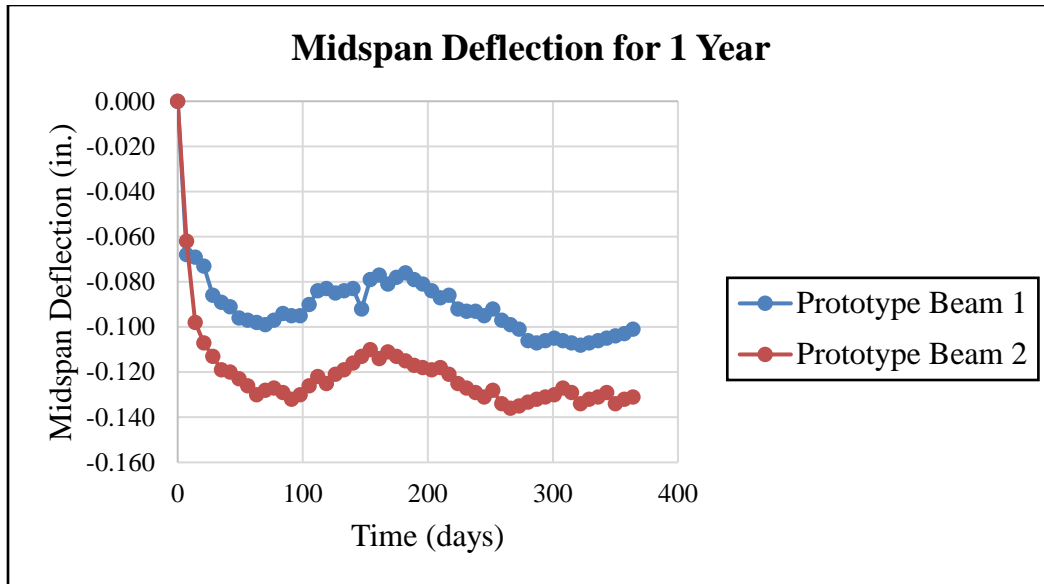


Figure 38: Midspan deflection for Year

Temperatures of the Concrete and Steel

Initially after casting concrete, the heat of hydration cause the concrete temperature to increase as it cures in the first 48 hour period. After this period, concrete cools to match the ambient temperature. From this point forward, both steel and concrete will exhibit nearly identical temperatures due to the similar coefficient of thermal expansions. Table 20 and Figure 39 show the changes in temperature over a week for concrete and steel for Prototype Beams 1 and 2. Table 20 depicts the changes in temperature for the first twenty-four hours after casting for prototype beam 2 in tabular form. For prototype beam 1, it was not initially planned to take steel temperature readings, which explain the lack of readings until 170 hours and absence of readings during a similar time duration. Table 21 and Figure 40 show the changes in temperature over a week for concrete and steel for Prototype Beams 1 and 2.

Table 20: Early Age Concrete and Steel Temperatures Vs. Time for Week

Early Age Concrete and Steel Temperatures Vs. Time for Week						
Time (hours)	Material Temperatures (°F)					
	Prototype Beam 1			Prototype Beam 2		
	Concrete PB 1	Steel PB 1	Ambient PB 1	Concrete PB 2	Steel PB 2	Ambient PB 2
0	100.2			100.8	92.0	96.6
1	100.4			100.9	93.0	97.1
2	100.1			98.9	91.2	97.0
3	100.2			97.8	91.1	97.2
4	100.8			97.7	90.8	97.0
5	100.0			95.4	87.0	96.5
6	98.8			93.4	86.4	95.3
9	93.4			90.7	84.8	92.3
12	84.5			85.1	82.1	86.1

15	79.6			81.7	80.7	82.7
18	75.1			82.4	83.2	83.0
21	75.5			83.4	86.5	83.3
24	76.0			86.4	91.3	84.1
48	81.0			68.2	68.7	70.1
72	85.7			70.1	70.3	70.8
96	85.3			69.2	69.5	70.2
120	80.0			70.3	70.1	69.9
144	89.8			69.5	70.0	69.7
168	92.2	89.8	91.3	71.2	71.1	71.1

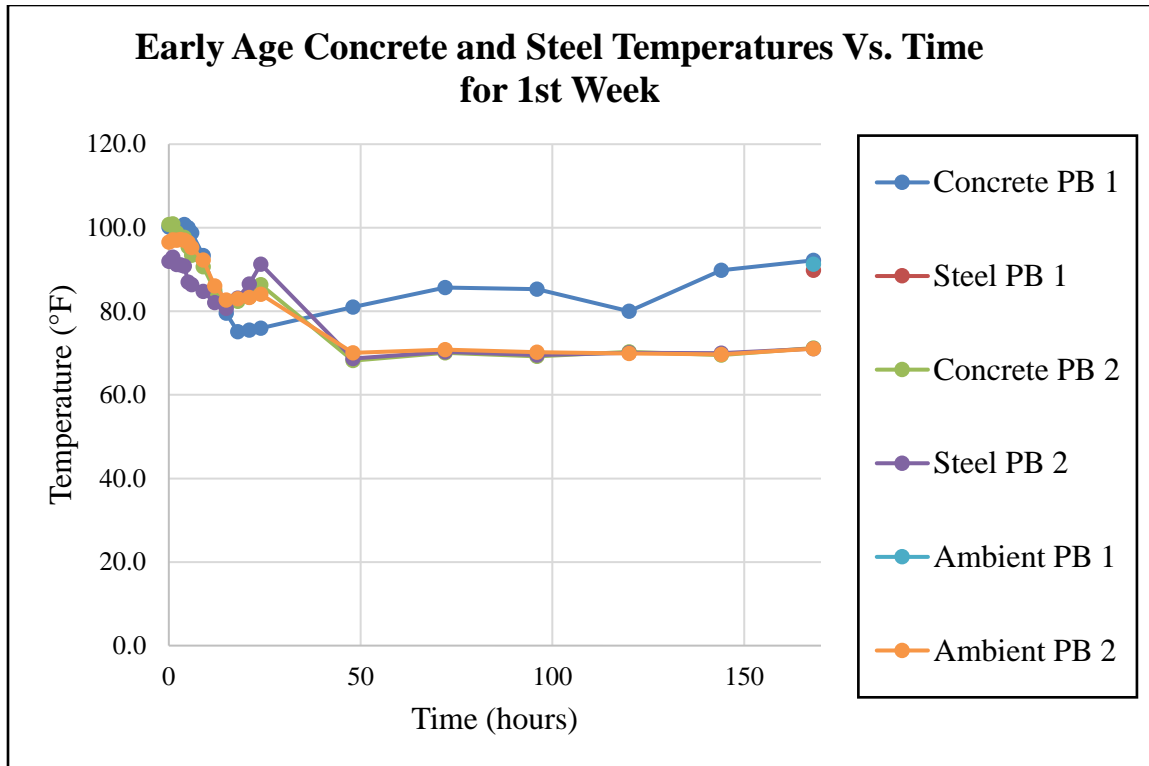


Figure 39: Early age concrete and temperatures for 1st Week

Table 21: Concrete and Steel Temperatures for Year

Concrete and Steel Temperatures Vs. Time for Year						
Time (Days)	Material Temperatures (°F)					
	Prototype Beam 1 - Concrete	Prototype Beam 1 - Steel	Prototype Beam 1 - Ambient	Prototype Beam 2 - Concrete	Prototype Beam 2 - Steel	Prototype Beam 2 - Ambient
0	100.2			100.8	92.0	96.6
7	92.2	89.8	91.3	68.0	66.2	67.1
14	76.9	72.8	74.4	76.6	76.7	76.9
21	76.7	76.5	76.6	72.1	72.6	72.4
28	71.0	71.4	71.3	72.7	73.1	73.9
35	72.8	72.7	72.9	74.1	74.1	74.1
42	73.9	73.8	74.0	63.4	62.0	62.7
49	73.0	73.1	73.0	64.6	65.2	65.0
56	70.2	70.1	70.0	63.9	64.1	64.0
63	67.2	67.1	67.4	64.8	64.8	64.8
70	64.7	64.8	64.7	63.6	63.7	63.4
77	63.1	63.4	63.3	60.4	57.7	59.2
84	60.2	57.7	59.0	59.9	59.8	59.7
91	59.8	59.6	59.7	57.2	57.4	57.9
98	58.9	57.6	58.2	52.4	52.1	52.2
105	52.1	51.9	52.0	49.4	49.8	50.1
112	49.7	49.8	49.7	45.4	45.3	45.4
119	45.4	45.3	45.9	40.6	40.8	40.7
126	40.2	39.4	40.6	38.5	37.9	38.3
133	38.3	37.9	38.1	37.5	37.0	37.3
140	37.6	37.0	37.3	40.0	40.8	40.4
147	40.1	40.9	40.5	48.6	47.4	48.0
154	48.8	48.1	48.5	47.1	47.0	48.1
161	46.8	46.8	46.8	49.1	49.6	49.6
168	48.9	49.2	49.1	51.0	51.1	51.0
175	51.4	51.2	51.3	54.4	54.3	54.8
182	54.6	54.5	54.6	55.6	55.6	55.6
189	55.6	55.6	55.6	53.4	54.5	54.1
196	53.3	53.6	53.1	57.9	58.3	58.1
203	57.4	57.9	57.7	60.4	59.8	61.0
210	60.2	59.7	60.0	59.3	59.4	59.7
217	58.7	58.8	59.4	62.6	62.8	62.7
224	62.2	62.5	62.0	63.5	63.5	64.0
231	63.7	63.7	64.2	66.6	66.6	67.2
238	66.6	66.6	67.4	69.5	69.7	70.5
245	68.9	68.5	68.7	70.0	70.2	69.9
252	70.1	70.3	70.2	70.6	70.4	70.5
259	69.7	69.5	70.2	70.9	71.2	71.4
266	71.6	71.7	71.9	74.9	75.2	75.5
273	74.9	75.6	75.3	79.0	79.3	79.9
280	78.9	79.2	79.0	82.1	82.6	83.1
287	82.5	82.0	82.3	80.0	79.4	79.7
294	79.8	80.8	80.4	73.5	73.6	73.8
301	72.8	73.3	74.5	77.5	77.7	77.6
308	78.4	78.9	78.7	77.9	78.1	78.4
315	79.9	80.1	80.0	80.2	80.6	80.9
322	80.2	80.3	80.1	81.6	81.7	81.9
329	81.4	81.3	81.2	80.4	80.5	80.3
336	80.6	80.8	80.7	82.1	82.5	82.4
343	82.3	82.4	82.5	82.7	82.8	83.1
350	82.6	82.7	82.4	82.0	81.9	81.8
357	81.7	81.6	81.8	80.7	80.8	80.8
364	80.5	80.4	80.6	81.1	80.9	80.0

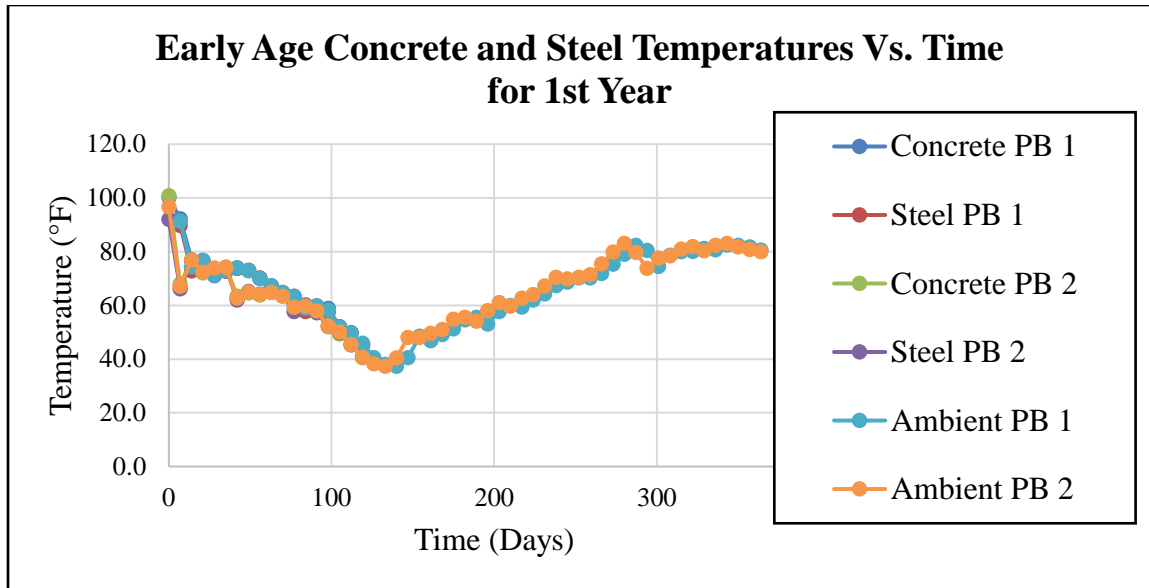


Figure 40: Concrete and Steel Temperatures for Year

Strain Measurements for Prototype Beams 1 and 2

The DEMEC points were added shortly after the slab was poured and then the initial readings were taken. For Prototype Beam 1, the strain readings from the 1st week for the concrete slab are depicted in Table 22 and Figure 41. The strains readings for Prototype Beam 2 for the 1st week for the concrete slab are depicted in Table 23 and Figure 42.

Table 22: Prototype Beam 1 Shrinkage Strain on Concrete Slab for 1st Week

Prototype Beam 1 Shrinkage Strain on Concrete Slab for Week											
Time (hours)	Shrinkage Strain (10^{-6} in.\in.)										
	1N-0	0-1S	0-2S	3N-0	0-3S	4N-0	5N-0	0-5S	6N-0	0-6S	Average
0	0	0	0	0	0	0	0	0	0	0	0
1	0	-20									-10

2	-25	-15									-25
3	-20	-35									-28
4	-30	-50									-40
5	-50	-55									-53
6	-55	-101									-78
9	-81	-101									-91
12	-96	-123									-110
15	-106	-161									-134
18	-126	-171									-151
21	-106	-197									-151
24	-121	-237									-179
48		-197	-20	-96	-35						-87
72		-197	-15	-76	-35						-81
96		-197	-20	-66	-35						-79
120		-222	-60	-111	-76						-52
144		-202	-10	-66	-35	66	50	40	66	45	-5
168		-166	-20	-71	-20	55	126	45	66	40	6

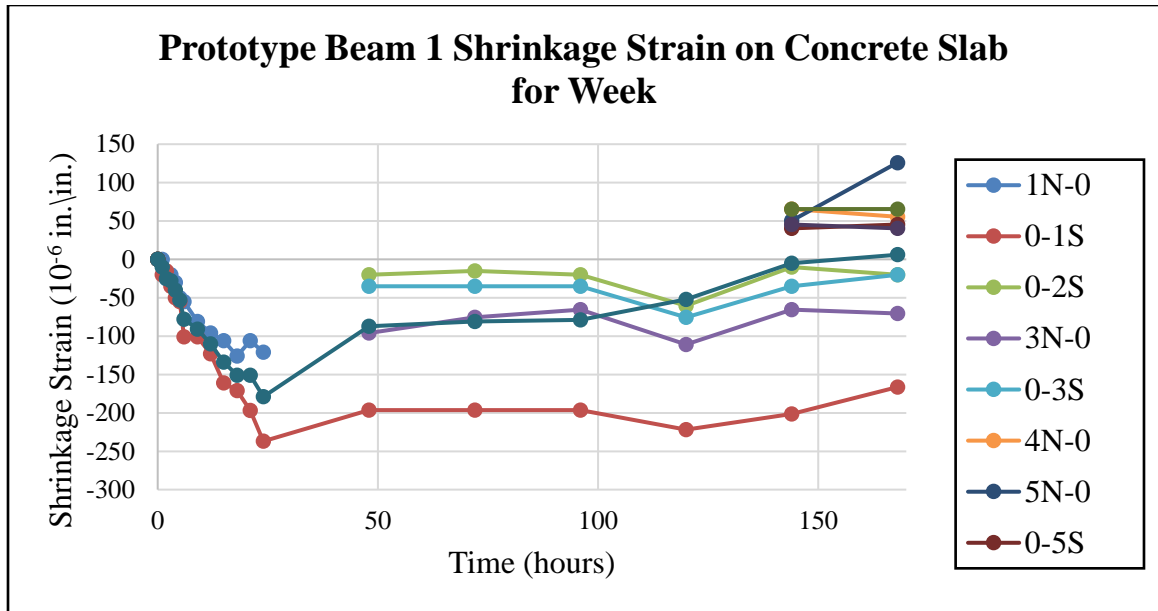


Figure 41: Prototype Beam 1 Shrinkage Strain on Concrete Slab for 1st Week

Table 23: Prototype Beam 2 Shrinkage Strain on Concrete Slab for 1st Week

Prototype Beam 2 Shrinkage Strain on Concrete Slab for Week							
Time (hours)	Shrinkage Strain (10^{-6} in./in.)						
	3N-2N	2N-1N	1N-0	0-1S	1S-2S	2S-3S	Average
0	0	0	0	0	0	0	0
1	-18	-22	-31	-15	-30	-10	-18
2	-32	-45	-46	-31	-58	-37	-41
3	-42	-50	-59	-48	-60	-39	-50
4	-50	-73	-48	-83	-91	-43	-66
5	-62	-100	-51	-111	-106	-55	-81

6	-75	-125	-81	-109	-123	-69	-97
9	-92	-151	-112	-117	-140	-99	-123
12	-111	-181	-153	-125	-173	-123	-144
15	-121	-186	-142	-37	-156	-117	-135
18	-138	-188	-134	-152	-140	-120	-129
21	-150	-148	-137	-177	-161	-97	-145
24	-145	-181	-150	-136	-202	-118	-155
48	-274	-289	-293	-315	-368	-223	-294
72	-322	-178	-318	-303	-411	-213	-291
96	-334	-226	-424	-247	-428	-261	-320
120	-307	-168	-346	-204	-456	-163	-274
144	-332	-327	-437	-255	-491	-223	-344
168	-357	-365	-487	-383	-469	-349	-402

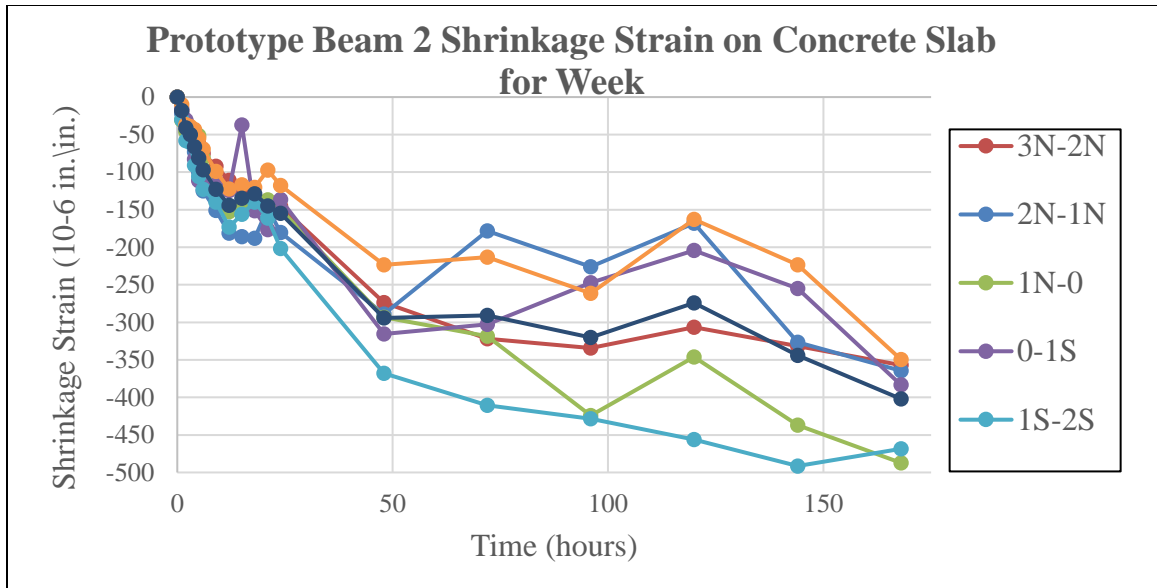


Figure 42: Prototype Beam 2 Shrinkage Strain on Concrete Slab for 1st Week

For Prototype Beam 1, the shrinkage strain in the concrete slab after a year are reported in Table 24 and Figure 43. For Prototype Beam 2, the shrinkage strain in the concrete slab after a year are reported in Table 25 and Figure 44.

Table 24: Prototype Beam 1 Shrinkage Strain on Concrete Slab for Year

Prototype Beam 1 Shrinkage Strain on Concrete Slab for Year										
Time (days)										Average
	0-1S	0-2S	3N-0	0-3S	4N-0	5N-0	0-5S	6N-0	0-6S	
0	0	0	0	0	0	0	0	0	0	0
7	-166	-20	-71	-20	55	126	45	66	40	6
14	-272	-139	-202	-126	-66	-18	-71	-60	-78	-115
21	-302	-141	-217	-151	-76	-35	-86	-81	-86	-130
28	-330	-222	-297	-229	-151	-101	-146	-146	-151	-197
35	-338	-242	-292	-242	-141	-101	-151	-156	-166	-203
42	-353	-242	-277	-242	-161	-126	-161	-166	-192	-213
49	-421	-320	-368	-328	-244	-202	-237	-260	-244	-291
56	-418	-322	-379	-330	-254	-201	-241	-254	-250	-294
63	-420	-329	-384	-315	-239	-207	-245	-247	-255	-293
70	-416	-328	-393	-323	-244	-204	-247	-242	-267	-296
77	-427	-343	-409	-331	-252	-217	-253	-253	-279	-307
84	-433	-355	-426	-343	-272	-229	-265	-267	-292	-320
91	-450	-360	-415	-329	-278	-235	-270	-265	-303	-323
98	-445	-371	-430	-337	-284	-220	-279	-257	-295	-324
105	-464	-372	-441	-335	-294	-198	-281	-252	-305	-327
112	-471	-372	-444	-330	-306	-170	-287	-260	-306	-327
119	-474	-381	-453	-322	-311	-132	-293	-264	-299	-325
126	-481	-383	-457	-333	-315	-105	-275	-259	-297	-323
133	-463	-372	-451	-318	-301	-99	-271	-254	-291	-313
140	-452	-370	-439	-321	-295	-75	-263	-247	-285	-305
147	-448	-355	-437	-317	-285	-78	-257	-239	-290	-301
154	-436	-344	-435	-310	-275	-55	-251	-235	-286	-292
161	-430	-339	-430	-304	-267	-23	-244	-228	-280	-283
168	-445	-328	-421	-301	-270	-3	-237	-227	-290	-280
175	-436	-332	-430	-304	-280	10	-242	-220	-300	-282
182	-420	-316	-437	-299	-297	27	-247	-238	-295	-280
189	-437	-305	-427	-305	-285	69	-239	-251	-291	-275
196	-441	-299	-420	-307	-292	94	-251	-264	-315	-277
203	-457	-284	-404	-310	-301	115	-248	-279	-323	-277
210	-471	-290	-399	-303	-297	147	-249	-289	-339	-277
217	-485	-275	-400	-299	-306	183	-256	-284	-351	-275
224	-496	-271	-388	-304	-311	201	-242	-297	-366	-275
231	-489	-259	-392	-306	-314	229	-252	-303	-360	-272
238	-502	-248	-384	-302	-317	256	-250	-315	-375	-271
245	-499	-235	-379	-300	-310	298	-241	-321	-381	-263
252	-507	-228	-374	-298	-327	327	-251	-334	-391	-265
259	-515	-220	-381	-299	-339	348	-261	-338	-395	-267
266	-525	-218	-386	-294	-352	371	-266	-341	-385	-266
273	-527	-226	-378	-298	-358	411	-269	-352	-382	-264
280	-520	-215	-374	-296	-361	445	-274	-358	-387	-260
287	-526	-209	-367	-297	-364	466	-275	-365	-390	-259
294	-530	-212	-370	-296	-370	498	-270	-360	-393	-256
301	-535	-212	-368	-295	-375	519	-277	-370	-402	-257
308	-540	-210	-359	-292	-374	521	-280	-375	-400	-257
315	-543	-206	-375	-288	-381	520	-279	-369	-398	-258
322	-547	-198	-381	-285	-370	518	-267	-365	-405	-256
329	-552	-191	-385	-296	-363	517	-269	-360	-410	-257
336	-542	-194	-379	-298	-369	521	-265	-371	-407	-256
343	-539	-198	-392	-301	-372	523	-262	-377	-403	-258
350	-540	-200	-393	-299	-369	525	-258	-384	-399	-257
357	-541	-205	-391	-296	-367	526	-264	-370	-404	-257
364	-545	-202	-388	-292	-365	524	-267	-380	-412	-259

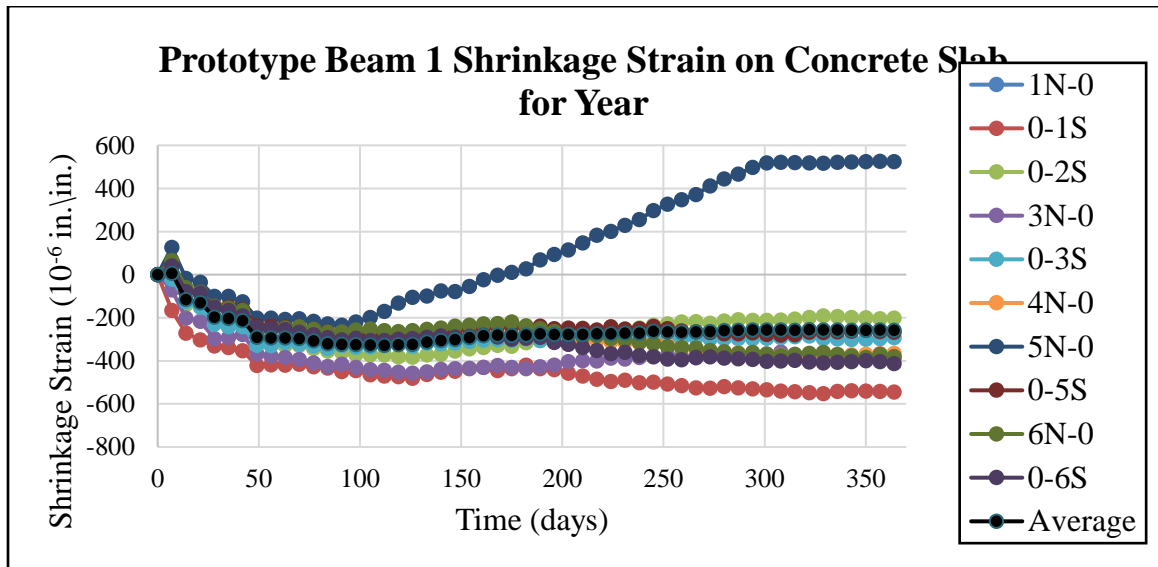


Figure 43: Prototype Beam 1 Shrinkage Strain on Concrete Slab for Year

Table 25: Prototype Beam 2 Shrinkage Strain on Concrete Slab for Year

Prototype Beam 2 Shrinkage Strain on Concrete Slab for Year							
Time (days)	Shrinkage Strain (10^{-6} in./in.)						Average
	3N-2N	2N-1N	1N-0	0-1S	1S-2S	2S-3S	
0	0	0	0	0	0	0	0
7	-357	-365	-487	-383	-469	-349	-402
14	-392	-314	-417	-303	-486	-231	-357
21	-425	-352	-432	-298	-524	-279	-385
28	-430	-367	-422	-323	-499	-291	-389
35	-448	-412	-472	-373	-554	-332	-432
42	-496	-445	-505	-404	-610	-344	-467
49	-498	-465	-525	-420	-620	-359	-481
56	-502	-482	-520	-435	-630	-371	-490
63	-506	-493	-533	-449	-635	-382	-500
70	-510	-507	-545	-457	-640	-401	-510
77	-513	-523	-558	-461	-645	-417	-520
84	-522	-527	-568	-467	-650	-423	-526
91	-512	-532	-572	-470	-666	-409	-527
98	-507	-538	-579	-480	-645	-420	-528
105	-512	-540	-565	-477	-655	-408	-526
112	-509	-530	-560	-475	-660	-413	-525
119	-504	-520	-549	-491	-671	-407	-524
126	-507	-529	-530	-487	-659	-409	-520
133	-500	-520	-539	-466	-650	-419	-516
140	-497	-512	-535	-477	-632	-404	-510
147	-486	-515	-520	-469	-625	-399	-502
154	-476	-500	-512	-460	-617	-405	-495
161	-483	-491	-501	-445	-610	-407	-490
168	-490	-486	-505	-440	-620	-412	-492
175	-485	-484	-496	-435	-630	-408	-490
182	-470	-490	-507	-450	-605	-400	-487
189	-475	-499	-503	-445	-590	-413	-488
196	-480	-507	-500	-435	-595	-404	-487
203	-492	-515	-505	-448	-600	-410	-495
210	-504	-522	-499	-467	-603	-420	-503
217	-515	-517	-489	-478	-597	-427	-504
224	-505	-507	-502	-472	-587	-431	-501
231	-499	-497	-520	-468	-597	-433	-502
238	-505	-486	-507	-483	-579	-422	-497
245	-522	-504	-515	-490	-586	-417	-506
252	-515	-500	-534	-495	-599	-414	-510
259	-503	-512	-516	-500	-600	-406	-506
266	-487	-499	-527	-486	-612	-390	-500
273	-485	-486	-524	-477	-627	-387	-498
280	-496	-479	-539	-475	-635	-398	-504
287	-511	-489	-529	-480	-629	-386	-504
294	-504	-497	-537	-491	-617	-381	-505
301	-498	-493	-548	-489	-610	-370	-501
308	-505	-474	-557	-503	-599	-383	-504
315	-512	-485	-565	-497	-617	-376	-509
322	-495	-498	-543	-509	-605	-365	-503
329	-480	-502	-527	-499	-622	-360	-498
336	-473	-500	-515	-485	-618	-379	-495
343	-465	-499	-509	-462	-640	-388	-494
350	-482	-487	-513	-452	-647	-375	-493
357	-475	-490	-524	-446	-650	-365	-492
364	-470	-493	-528	-439	-653	-370	-492

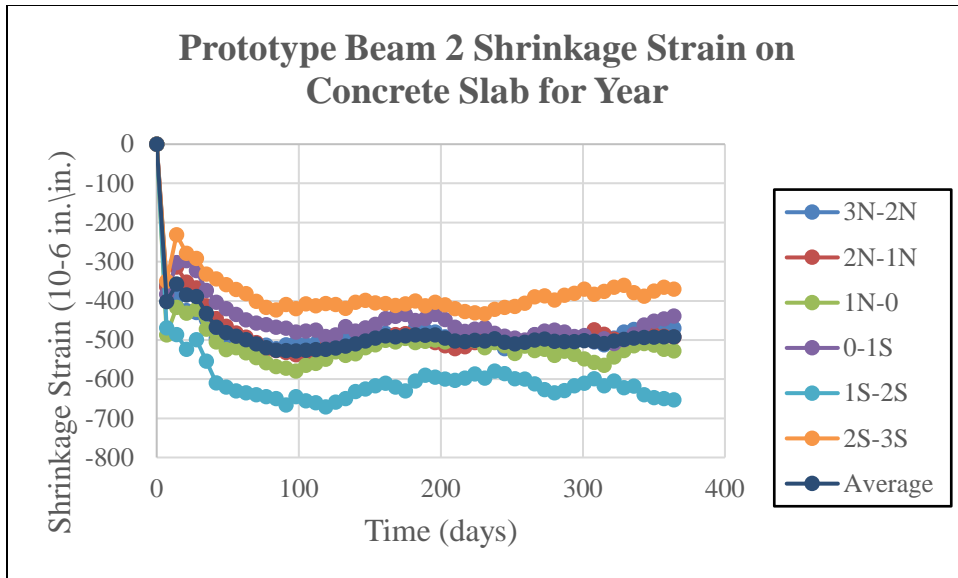


Figure 44: Prototype Beam 2 Shrinkage Strain on Concrete Slab for Year

For both Prototype Beams, the average strain readings from the DEMEC points in the concrete slab are reported in Table 26 and Figure 45 for the 1st week, and Table 27 and Figure 46 for a year.

Table 26: Average Shrinkage Strain on Concrete Slab for 1st Week

Average Strain on Concrete Slab for Week		
Time (hours)	Shrinkage Strain (10^{-6} in./in.)	
	Prototype Beam 1	Prototype Beam 2
0	0	0
1	-10	-18
2	-25	-41

3	-28	-50
4	-40	-66
5	-53	-81
6	-78	-97
9	-91	-123
12	-110	-144
15	-134	-135
18	-151	-129
21	-151	-145
24	-179	-155
48	-87	-294
72	-81	-291
96	-79	-320
120	-52	-274
144	-5	-344
168	6	-402

Figure 45: Average Shrinkage Strain on Concrete Slab 1st Week

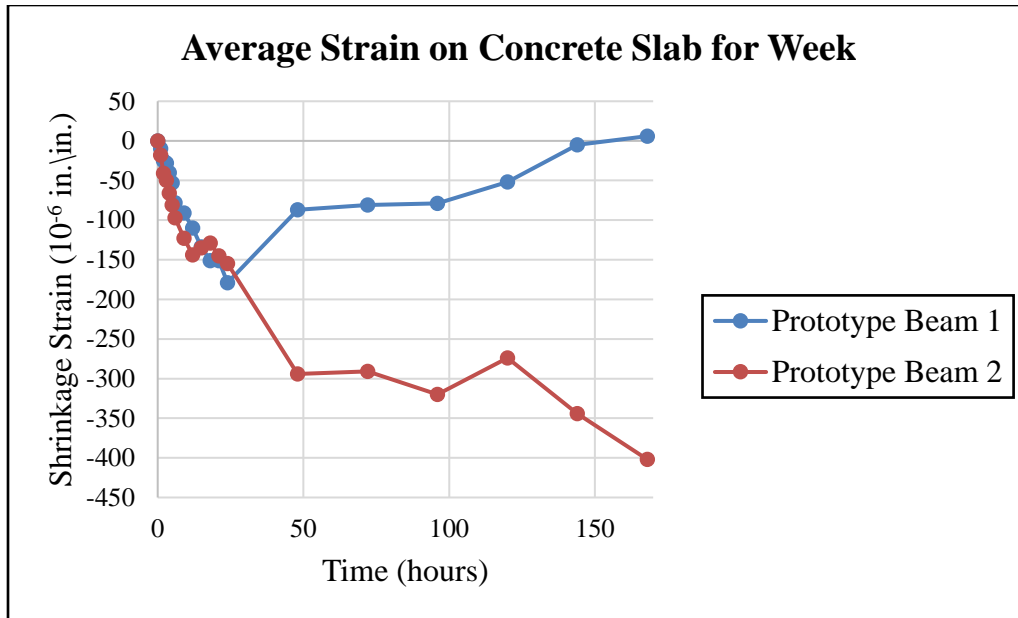


Table 27: Average Shrinkage Strain on Concrete Slab for Year

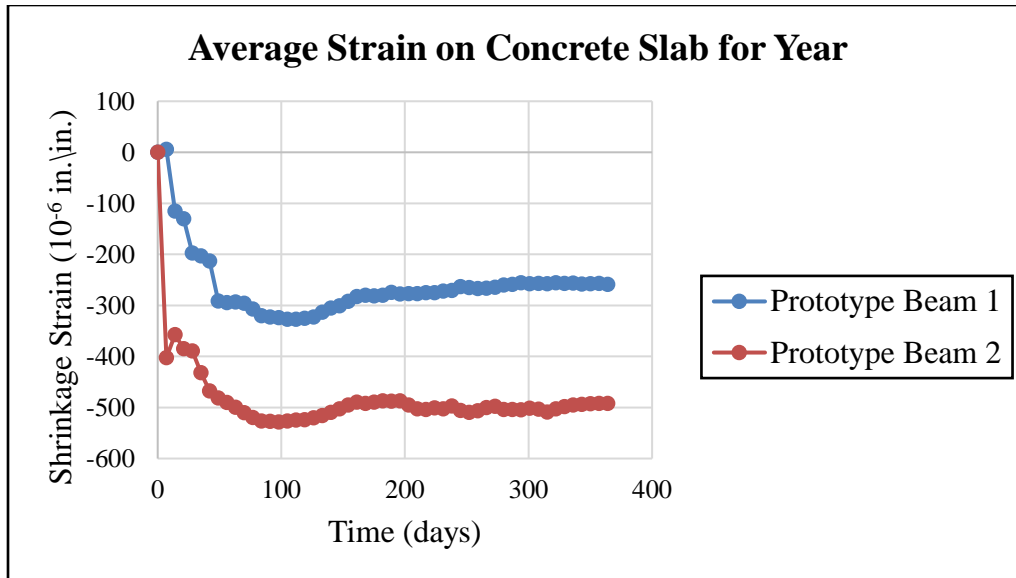
Average Strain on Concrete Slab for Year		
Time (days)	Shrinkage Strain (10 ⁻⁶ in./in.)	
	Prototype Beam 1	Prototype Beam 2
0	0	0
7	6	-402
14	-115	-357
21	-130	-385
28	-197	-389
35	-203	-432

42	-213	-467
49	-291	-481
56	-294	-490
63	-293	-500
70	-296	-510
77	-307	-520
84	-320	-526
91	-323	-527
98	-324	-528
105	-327	-526
112	-327	-525
119	-325	-524
126	-323	-520
133	-313	-516
140	-305	-510
147	-301	-502
154	-292	-495
161	-283	-490

168	-280	-492
175	-282	-490
182	-280	-487
189	-275	-488
196	-277	-487
203	-277	-495
210	-277	-503
217	-275	-504
224	-275	-501
231	-272	-502
238	-271	-497
245	-263	-506
252	-265	-510
259	-267	-506
266	-266	-500
273	-264	-498
280	-260	-504
287	-259	-504

294	-256	-505
301	-257	-501
308	-257	-504
315	-258	-509
322	-256	-503
329	-257	-498
336	-256	-495
343	-258	-494
350	-257	-493
357	-257	-492
364	-259	-492

Figure 46: Average Shrinkage Strain on Concrete Slab for Year



For Prototype Beam 1, the strain readings from the 1st week for the web of the steel beam are depicted in Table 28 and Figure 47. The strains readings for Prototype Beam 2 for the 1st week for the web of the steel beams are depicted in Table 29 and Figure 48.

Table 28: Prototype Beam 1 Strain on Steel Beam for 1st Week

Prototype Beam 1 Strain on Steel Beam for Week									
Time (hours)	Strain (10 ⁻⁶ in./in.)								
	1N-0	0-1S	2N-0	0-2S	3N-0	0-3S	4N-0	0-4S	Average
0	0	0	0	0	0	0	0	0	0
1	15	17							16
2	15	17							16
3	15	17							16

4	20	22							21
5	10	27							18
6	-20	-29							-24
9	-40	-16							-28
12	-58	-24							-41
15	-66	-29							-47
18	-76	-39							-57
21	-111	-49							-80
24	-91	-79							-85
48	-35	-18	0	20	66	-20			2
72	-15	2	10	40	35	20			15
96	-30	-13	0	25	25	15	-55	-50	4
120	-50	-39	-5	15	-5	-10	-101	-81	-16
144	20	27	35	60	55	45	-25	-25	41
168	35	52	66	101	81	76	5	5	68

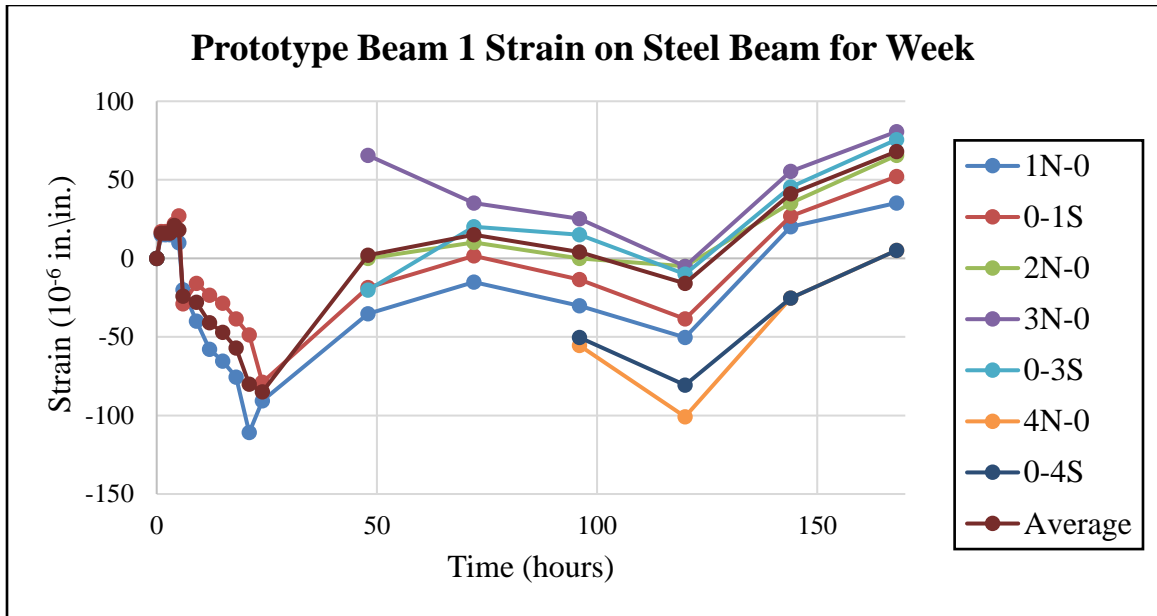


Figure 47: Prototype Beam 1 Strain on Steel Beam for 1st Week

Table 29: Prototype Beam 2 Strain on Steel Beam for 1st Week

Prototype Beam 2 Strain on Steel Beam for Week							
Time (hours)	Strain (10^{-6} in./in.)						
	3N-2N	2N-1N	1N-0	0-1S	1S-2S	2S-3S	Average
0	0	0	0	0	0	0	0
1	0	-5	-12	-10	-20	-9	5
2	-15	-22	-19	-18	-30	-17	-20
3	-28	-42	-32	-30	-30	-24	-31
4	41	-52	-48	-54	-52	-49	-55

5	-63	-67	-67	-71	-78	-72	-70
6	-80	-75	-79	-81	-85	-82	-82
9	-90	-123	-84	-90	-89	-87	-95
12	-96	-133	-100	-96	-93	-97	-102
15	-77	-93	-90	-82	-79	-90	-87
18	-78	-70	-77	-86	-68	-80	-76
21	-63	-57	-77	-93	-68	-70	-71
24	-53	-52	-55	-53	-58	-55	-54
48	-149	-186	-188	-166	-174	-193	-176
72	-181	-196	-183	-192	-174	-191	-186
96	-161	-176	-140	-171	-146	-155	-158
120	-101	-115	-100	-113	-81	-113	-104
144	-108	-125	-115	-126	-101	-123	-116
168	-129	-143	-115	-136	-108	-138	-128

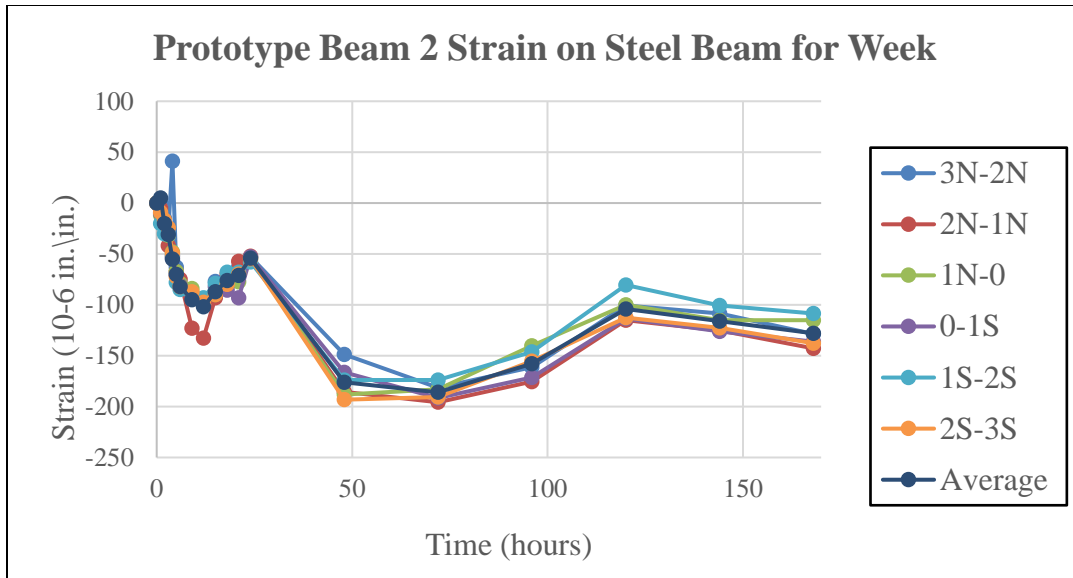


Figure 48: Prototype Beam 2 Strain on Steel Beam for 1st Week

For Prototype Beam 1, the strains in the web of the steel girder after a year are reported in Table 30 and Figure 49. For Prototype Beam 2, the strains in the web of the steel girder after a year are reported in Table 31 and Figure 50.

Table 30: Prototype Beam 1 Strain on Steel Beam for Year

Prototype Beam 1 Strain on Steel Beam for Year									
Time (days)	Strain (10^{-6} in./in.)								Average
	1N-0	0-1S	2N-0	0-2S	3N-0	0-3S	4N-0	0-4S	
0	0	0	0	0	0	0	0	0	0
7	35	52	66	101	81	76	5	5	68
14	-78	-59	-40	-23	-28	-43	-111	-116	-45
21	-76	-59	-45	-15	-20	-40	-91	-111	-43
28	-101	-87	-58	-40	-53	-86	-136	-146	-71
35	-96	-74	-55	-60	-20	-71	-131	-126	-63
42	-96	-69	-50	-30	-45	-60	-121	-131	-59
49	-141	-114	-91	-86	-111	-136	-192	-207	-113
56	-139	-118	-88	-82	-106	-126	-184	-200	-130
63	-145	-111	-93	-78	-100	-118	-179	-190	-127
70	-141	-112	-91	-76	-96	-116	-176	-179	-123
77	-171	-136	-104	-108	-115	-141	-198	-203	-147
84	-186	-147	-123	-116	-131	-161	-212	-222	-162
91	-189	-145	-133	-122	-136	-172	-210	-228	-167
98	-192	-156	-127	-128	-125	-184	-221	-239	-172
105	-202	-162	-139	-133	-138	-179	-237	-246	-180
112	-203	-165	-143	-137	-143	-190	-243	-240	-183
119	-207	-170	-140	-142	-147	-191	-240	-237	-184
126	-203	-165	-135	-135	-140	-186	-234	-235	-179
133	-200	-157	-141	-128	-145	-190	-241	-220	-178
140	-189	-149	-138	-134	-135	-178	-245	-225	-174
147	-193	-142	-129	-122	-137	-182	-247	-215	-171
154	-182	-151	-122	-119	-124	-184	-231	-207	-165
161	-179	-139	-117	-112	-126	-171	-227	-199	-159
168	-167	-127	-112	-105	-118	-169	-218	-202	-152
175	-175	-122	-109	-109	-115	-157	-206	-194	-148
182	-181	-116	-101	-102	-113	-154	-204	-188	-145
189	-175	-109	-90	-99	-107	-144	-188	-183	-137
196	-163	-107	-85	-100	-102	-136	-194	-180	-133
203	-154	-101	-73	-89	-98	-127	-191	-172	-126
210	-156	-96	-88	-92	-95	-117	-183	-174	-125
217	-147	-103	-91	-82	-84	-109	-176	-175	-121
224	-133	-91	-76	-78	-81	-101	-165	-162	-111
231	-119	-85	-67	-73	-80	-99	-170	-165	-107
238	-107	-79	-61	-69	-74	-96	-162	-158	-101
245	-101	-72	-58	-66	-70	-85	-154	-147	-94
252	-98	-77	-54	-67	-66	-91	-161	-150	-96
259	-97	-64	-45	-59	-54	-76	-149	-142	-86
266	-99	-59	-39	-62	-59	-70	-141	-138	-83
273	-101	-52	-41	-57	-47	-74	-138	-142	-82
280	-98	-49	-36	-52	-42	-72	-132	-136	-77
287	-100	-54	-30	-51	-39	-64	-129	-131	-75
294	-96	-60	-34	-55	-33	-61	-128	-134	-75
301	-91	-59	-35	-50	-30	-63	-126	-129	-73
308	-93	-55	-41	-48	-36	-68	-132	-126	-75
315	-95	-53	-36	-45	-29	-66	-135	-118	-72
322	-95	-57	-39	-43	-25	-63	-132	-120	-72
329	-90	-66	-36	-51	-24	-67	-125	-124	-73
336	-87	-58	-38	-52	-29	-76	-122	-130	-74
343	-92	-62	-39	-51	-28	-79	-122	-135	-76
350	-90	-65	-41	-53	-30	-77	-124	-136	-77
357	-95	-67	-44	-52	-31	-75	-126	-133	-78
364	-98	-64	-48	-50	-33	-73	-129	-131	-78

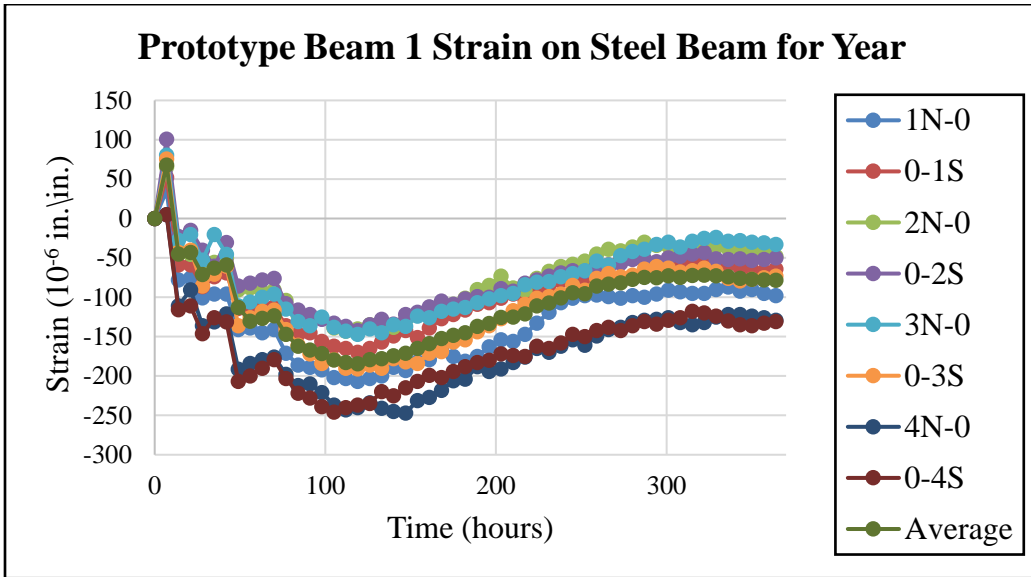


Figure 49: Prototype Beam 1 Strain on Steel Beam for Year

Table 31: Prototype Beam 2 Strain on Steel Beam for Year

Prototype Beam 2 Strain on Steel Beam for Year							
Time (days)	Strain (10^{-6} in./in.)						Average
	3N-2N	2N-1N	1N-0	0-1S	1S-2S	2S-3S	
0	0	0	0	0	0	0	0
7	-129	-143	-115	-136	-108	-138	-128
14	-118	-130	-133	-131	-118	-150	-130
21	-136	-138	-123	-146	-129	-143	-136
28	-151	-135	-150	-154	-179	-153	-154
35	-146	-140	-110	-141	-101	-130	-128
42	-224	-208	-183	-204	-202	-203	-204
49	-204	-200	-185	-195	-178	-192	-192
56	-199	-192	-177	-184	-169	-181	-184
63	-194	-186	-173	-176	-159	-163	-175
70	-212	-214	-197	-201	-186	-192	-200
77	-239	-228	-206	-212	-202	-211	-216
84	-245	-233	-212	-218	-215	-221	-224
91	-252	-237	-209	-222	-212	-226	-226
98	-256	-231	-221	-225	-223	-219	-229
105	-247	-241	-215	-219	-214	-223	-227
112	-252	-245	-212	-217	-212	-227	-228
119	-255	-249	-223	-231	-225	-221	-234
126	-254	-252	-221	-229	-231	-226	-236
133	-252	-249	-212	-217	-224	-220	-229
140	-237	-239	-207	-209	-211	-208	-219
147	-239	-229	-196	-203	-214	-203	-214
154	-241	-233	-189	-199	-203	-197	-210
161	-229	-217	-196	-186	-199	-201	-205
168	-220	-214	-204	-192	-193	-198	-204
175	-207	-207	-199	-190	-188	-184	-196
182	-215	-203	-192	-197	-184	-191	-197
189	-202	-196	-183	-200	-191	-186	-193
196	-191	-194	-175	-204	-193	-175	-189
203	-195	-200	-172	-196	-187	-181	-189
210	-184	-189	-169	-188	-180	-172	-180
217	-179	-185	-157	-183	-173	-169	-174
224	-168	-183	-153	-180	-167	-167	-170
231	-175	-178	-152	-182	-177	-171	-173
238	-180	-165	-146	-186	-174	-180	-172
245	-177	-160	-142	-184	-169	-173	-168
252	-169	-171	-135	-179	-165	-165	-164
259	-154	-165	-141	-175	-158	-167	-160
266	-161	-160	-138	-170	-161	-161	-159
273	-157	-154	-131	-169	-152	-154	-153
280	-148	-142	-127	-160	-146	-143	-144
287	-156	-138	-120	-165	-144	-139	-144
294	-150	-140	-119	-162	-139	-141	-142
301	-146	-133	-113	-166	-134	-133	-138
308	-148	-129	-122	-160	-137	-135	-139
315	-151	-134	-126	-152	-145	-142	-142
322	-149	-125	-122	-145	-151	-133	-138
329	-147	-120	-131	-148	-147	-136	-138
336	-145	-119	-125	-134	-150	-144	-136
343	-146	-115	-128	-130	-144	-147	-135
350	-148	-116	-136	-137	-136	-153	-138
357	-147	-110	-143	-132	-139	-149	-137
364	-149	-105	-148	-139	-149	-155	-141

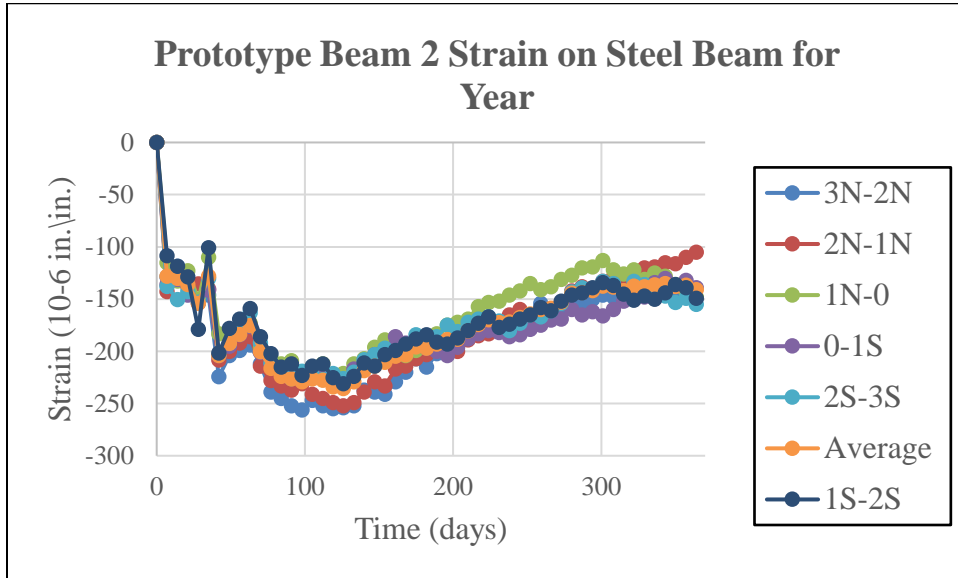


Figure 50: Prototype Beam 2 Strain on Steel Beam for Year

For both Prototype Beams, the average strain readings from the DEMEC points in the web of the steel girder are reported in Table 32 and Figure 51 for the 1st week, and Table 33 and Figure 52 for a year.

Table 32: Average Strain in Steel Beam for 1st Week

Average Strain on Steel Beam for Week		
Time (hours)	Shrinkage Strain (10^{-6} in./in.)	
	Prototype Beam 1	Prototype Beam 2
0	0	0
1	16	5

2	16	-20
3	16	-31
4	21	-55
5	18	-70
6	-24	-82
9	-28	-95
12	-41	-102
15	-47	-87
18	-57	-76
21	-80	-71
24	-85	-54
48	2	-176
72	15	-186
96	4	-158
120	-16	-104
144	41	-116
168	68	-128

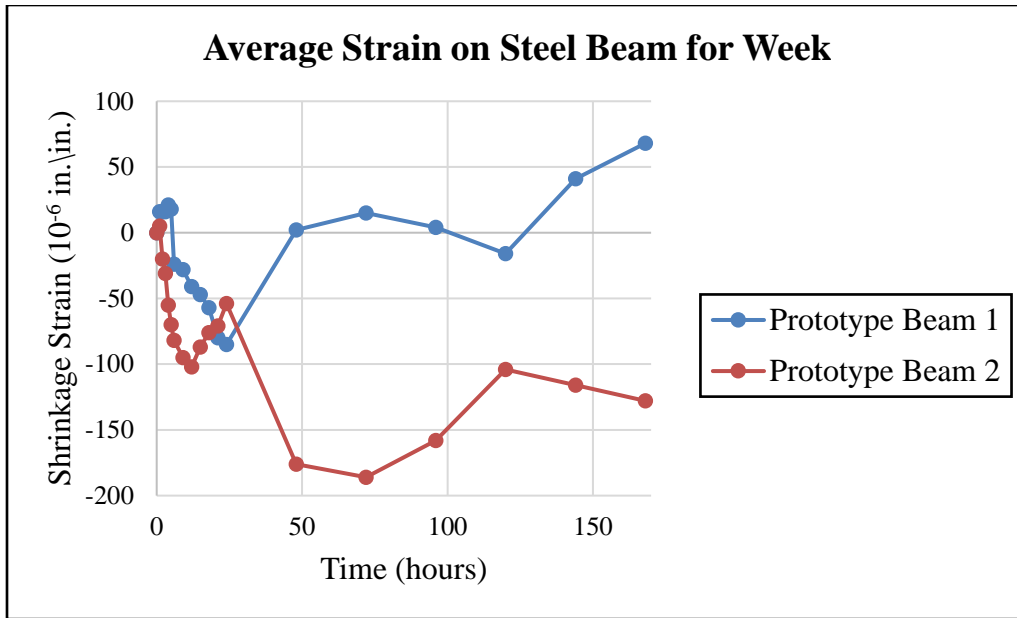


Figure 51: Average Strain in Steel Beam for 1st Week

Table 33: Average Strain in Steel Beam for Year

Average Strain on Steel Beam for Year		
Time (days)	Shrinkage Strain (10 ⁻⁶ in./in.)	
	Prototype Beam 1	Prototype Beam 2
0	0	0
7	68	-128
14	-45	-130
21	-43	-136
28	-71	-154

35	-63	-128
42	-59	-204
49	-113	-192
56	-130	-184
63	-127	-175
70	-123	-200
77	-147	-216
84	-162	-224
91	-167	-226
98	-172	-229
105	-180	-227
112	-183	-228
119	-184	-234
126	-179	-236
133	-178	-229
140	-174	-219
147	-171	-214
154	-165	-210

161	-159	-205
168	-152	-204
175	-148	-196
182	-145	-197
189	-137	-193
196	-133	-189
203	-126	-189
210	-125	-180
217	-121	-174
224	-111	-170
231	-107	-173
238	-101	-172
245	-94	-168
252	-96	-164
259	-86	-160
266	-83	-159
273	-82	-153
280	-77	-144

287	-75	-144
294	-75	-142
301	-73	-138
308	-75	-139
315	-72	-142
322	-72	-138
329	-73	-138
336	-74	-136
343	-76	-135
350	-77	-138
357	-78	-137
364	-78	-141

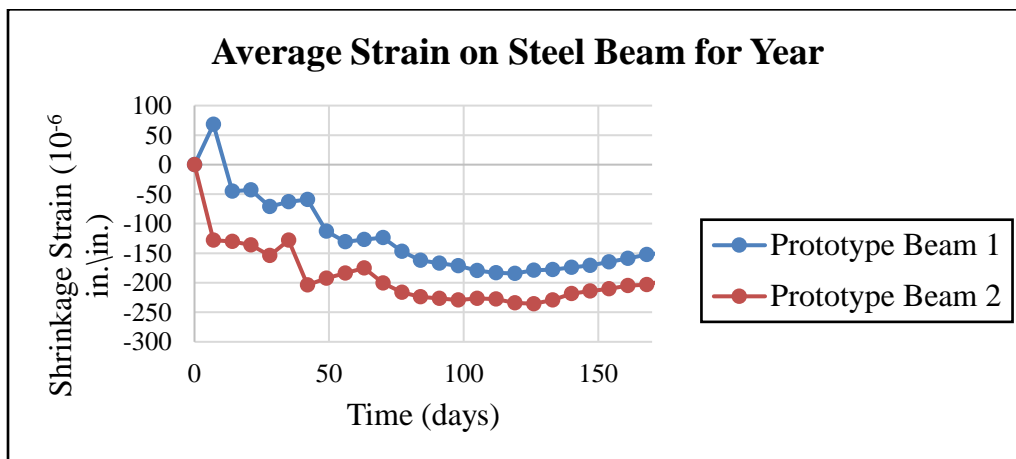


Figure 52: Average Strain in Steel Beam for Year

It is an important factor how temperature fluctuations correlate with shrinkage fluctuations. This is expected because temperature is a contributor to volumetric changes. The strains developing in the steel are consistent with the change in temperature so the shrinkage in the concrete deck is believed to have minimal contribution to the strain that developed in the steel girders. This is observable from Figure 19 shown above.

Figure 52 shows how the shrinkage strains continued to increase over time shortening the concrete, leading to the possible conclusion that shrinkage is a contributor to deflection. The data also shows the amount of variation that can occur in the concrete strain and the measurement technique. This was expected due to different operators and epoxies being used.

Unrestrained Shrinkage Strains from Shrinkage Prisms

The shrinkage prisms were batched to compare the unrestrained shrinkage strains in the prisms to the restrained shrinkage strains in the Prototype Beams. For each batch used to create the prototype beams, four prisms were made with one pair of DEMEC points on each side. These DEMEC readings were averaged and then reported in Table 34 for both Prototype Beams for the 1st week. A visual representation of these values is shown in Figure 53. The values for a year are reported in Table 35 and Figure 54. Initially, readings were conducted hourly before transitioning to a daily period.

Table 34: Unrestrained Shrinkage Strains for 1st Week

Unrestrained Shrinkage Strains for Week	
Time (hours)	Unrestrained Shrinkage Strain (10⁻⁶ in./in.)

	Prototype Beam 1					Prototype Beam 2				
	Specimens				Average	Specimens				Average
	1	2	3	4		1	2	3	4	
0	0	0	0	0	0	0	0	0	0	0
1	-15	-15	-5	15	-5	-16	-26	-21	-25	-22
2	-25	58	-10	-20	1	-12	-34	-16	-20	-21
3	8	-13	8	-171	-42	-10	-41	-9	-17	-19
4	20	0	8	-297	-67	-7	-29	-6	-14	-14
5	86	10	-13	-275	-48	-9	-17	2	-1	-6
6	86	25	-33	-254	-44	-4	-19	8	9	-2
9	68	30	-40	-230	-43	-5	-15	7	14	0
12	25	25	-48	-153	-38	-1	5	16	23	11
15	-13	35	-43	-132	-38	8	6	15	32	15
18	-38	25	-43	-76	-33	-44	-43	-34	-25	-37
21	-3	40	-13	-53	-7	-69	-77	-63	-59	-67
24	-38	35	3	-16	-4	-106	-98	-93	-89	-97
48	-43	35	-35	-8	-13	-121	-113	-88	-112	-109
72	-71	20	-93	-50	-49	-122	-96	-96	-78	-98

96	-126	-68	-141	-108	-111	-111	-95	-74	-131	-103
120	-66	-5	-103	-55	-57	-139	-126	-115	-137	-129
144	-88	-18	-101	-93	-75	-194	-173	-164	-171	-176
168	-222	-40	-121	-98	-120	-223	-212	-202	-218	-214

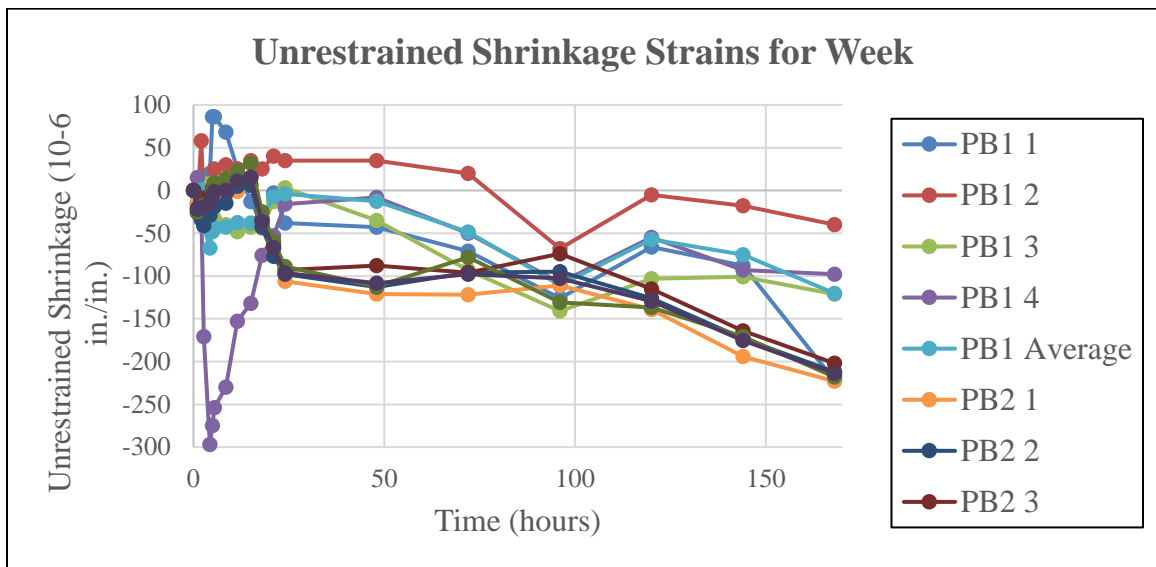


Figure 53: Unrestrained Shrinkage Strains for 1st Week

Table 35: Unrestrained Shrinkage Strains for Year

Unrestrained Shrinkage Strains for Year										
Time (days)	Unrestrained Shrinkage Strain (10^{-6} in./in.)									
	Prototype Beam 1					Prototype Beam 2				
	Specimens				Average	Specimens				Average
	1	2	3	4		1	2	3	4	
0	0	0	0	0	0	0	0	0	0	0
7	-222	-40	-121	-98	-120	-223	-212	-202	-218	-214
14	-353	-270	-348	-330	-325	-295	-265	-255	-285	-275
21	-328	-233	-324	-312	-299	-381	-335	-328	-362	-352
28	-381	-304	-373	-374	-358	-388	-338	-329	-377	-358
35	-392	-314	-367	-373	-362	-449	-389	-372	-440	-413
42	-381	-309	-372	-377	-360	-471	-407	-402	-459	-435
49	-471	-392	-460	-480	-451	-490	-420	-415	-471	-449
56	-475	-390	-462	-475	-451	-505	-434	-432	-487	-465
63	-481	-391	-464	-480	-454	-515	-444	-446	-504	-477
70	-483	-391	-466	-481	-455	-537	-467	-474	-524	-501
77	-503	-400	-496	-502	-475	-558	-488	-480	-547	-518
84	-524	-408	-505	-522	-490	-560	-492	-485	-564	-525
91	-531	-422	-508	-525	-497	-562	-493	-485	-565	-526
98	-522	-417	-498	-515	-488	-558	-490	-482	-561	-523
105	-517	-412	-492	-517	-485	-552	-484	-476	-557	-517
112	-510	-399	-488	-516	-478	-548	-488	-471	-559	-517
119	-505	-402	-491	-509	-477	-555	-476	-467	-553	-513
126	-512	-390	-486	-501	-472	-540	-472	-463	-549	-506
133	-499	-388	-478	-496	-465	-537	-471	-458	-537	-501
140	-490	-385	-485	-494	-464	-533	-475	-455	-541	-501
147	-488	-383	-487	-489	-462	-528	-467	-447	-532	-494
154	-493	-381	-479	-491	-461	-536	-463	-451	-527	-494
161	-487	-379	-489	-492	-462	-529	-465	-452	-525	-493
168	-495	-386	-487	-495	-466	-533	-462	-448	-526	-492
175	-492	-377	-485	-490	-461	-537	-460	-455	-531	-496
182	-487	-381	-478	-492	-460	-543	-457	-449	-528	-494
189	-486	-384	-486	-487	-461	-539	-455	-442	-525	-490
196	-495	-389	-492	-498	-469	-544	-459	-448	-532	-496
203	-502	-401	-501	-500	-476	-551	-461	-455	-538	-501
210	-506	-411	-496	-507	-480	-557	-464	-464	-532	-504
217	-502	-413	-495	-503	-478	-561	-467	-471	-539	-510
224	-511	-416	-502	-509	-485	-567	-473	-469	-548	-514
231	-509	-415	-507	-517	-487	-565	-477	-464	-545	-513
238	-513	-409	-505	-521	-487	-574	-472	-474	-551	-518
245	-515	-407	-503	-526	-488	-581	-481	-476	-556	-524
252	-508	-409	-496	-537	-488	-582	-484	-470	-549	-521
259	-499	-415	-494	-542	-488	-591	-479	-482	-546	-525
266	-495	-419	-492	-538	-486	-587	-469	-487	-548	-523
273	-491	-423	-487	-532	-483	-594	-475	-481	-559	-527
280	-485	-425	-492	-528	-483	-599	-482	-479	-556	-529
287	-489	-421	-497	-523	-483	-604	-485	-476	-549	-529
294	-494	-429	-492	-519	-484	-599	-478	-473	-551	-525
301	-491	-431	-498	-517	-484	-609	-476	-474	-546	-526
308	-496	-427	-506	-509	-485	-605	-466	-470	-529	-518
315	-498	-422	-513	-513	-487	-613	-468	-467	-531	-520
322	-506	-428	-517	-505	-489	-617	-459	-461	-525	-516
329	-514	-432	-515	-499	-490	-622	-461	-465	-517	-516
336	-519	-434	-515	-503	-493	-619	-455	-460	-512	-512
343	-516	-428	-509	-499	-488	-615	-454	-455	-507	-508
350	-511	-423	-501	-502	-484	-607	-457	-458	-510	-508
357	-517	-429	-508	-508	-491	-610	-451	-455	-505	-505
364	-513	-427	-512	-512	-491	-614	-452	-457	-509	-508

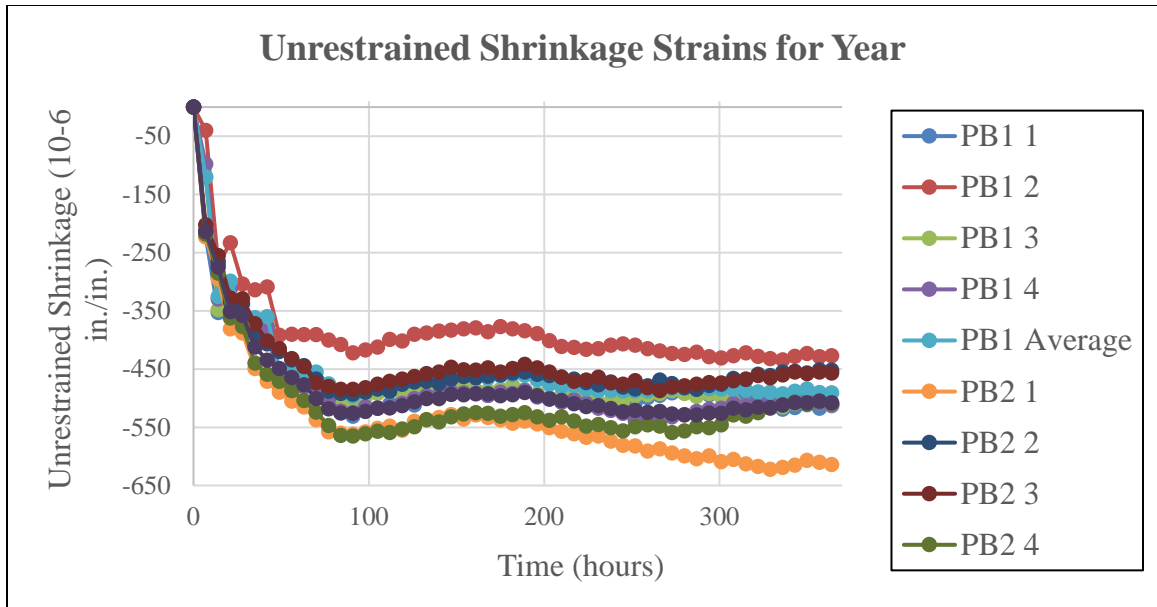


Figure 54: Unrestrained Shrinkage Strains for 1st Year

Figures 53 and 54, and Tables 34 and 35 was compared to the restrained shrinkage strains on the composite beam in to investigate unrestrained shrinkage. Figures 31 to 41 has the restrained shrinkage values for the concrete slab and steel girder for the prototype beams. As expected, the unrestrained shrinkage is greater.

Forensic Investigation

Forensic investigations of three ODOT bridges were performed. Specific information was acquired to assess variations in elevation on the driving surfaces, and other general observations were made about the condition. Phenomena observed and documented were deck cracking, condition of bearings, guardrails, abutments and piers, and surface treatments like diamond grinding. Elevations were measured from both above the bridge deck on the wearing surfaces and below the bridge decks. The information is useful to understand the causes for adverse ride quality and unwanted deflections.

SH 86



Figure 55: SH 86 over Stillwater Creek in Paying County

SH 86 was the first bridge investigated and only has one accessible span due to Lake Carl Blackwell. Figure 55 is a picture of the bridge. SH 86 is a three span bridge with an 8 in. concrete deck and 7 W 33x141 steel girders. From observation and from driving on the bridge, it is apparent that all three spans are sagging as there is a dip occurring at midspan. Through surveying, we determined this dip to be approximately 1.5 in and was compared to the elevations measurements at the abutments and piers on surface. This creates problems for vehicles traveling at high velocities especially if there is heavy traffic. This dip is most likely a result of when the bridge was rehabilitated by placing a new concrete deck causing the beams to sag as was reported shortly after construction. It was also observed that some parts of the slab thickness varied from 8 in. to 10 in. This would affect the time dependent volume changes minimally. The elevations from the study are reported in Table 36 shown below. Span 1 was the only span we had access to from underneath the bridge. Elevation readings were measured at ten ft. intervals for five points

on the roadway's cross section: centerline, two locations just outside the lane markers, and two locations just inside the guardrails.

Table 36: Roadway elevations (ft.) above the north abutment for SH 86.

SH 86 Slab (Roadway) Elevations						
	Distance from North Abutment Joint (ft.)	Elevation (ft.)				
		East Edge (Against Guardrail)	Outside North Bound Lane Marker	Centerline	Outside South Bound Lane Marker	West Edge (Against Guardrail)
Span 1	0	3.90	3.96	4.05	3.96	3.90
	10	3.83	3.88	3.97	3.89	3.83
	20	3.77	3.85	3.95	3.86	3.82
	30	3.76	3.82	3.92	3.86	3.81
	40	3.78	3.85	3.95	3.89	3.83
	50	3.81	3.88	4.00	3.93	3.83
	60	3.90	3.97	4.00	3.97	3.91
Span 2	60	3.88	3.96	4.00	3.96	3.88
	70	3.84	3.91	4.01	3.91	3.81

	80	3.79	3.88	3.98	3.88	3.82
	90	3.78	3.86	3.96	3.88	3.81
	100	3.79	3.88	3.98	3.88	3.81
	110	3.81	3.91	4.01	3.93	3.81
	120	3.91	3.97	4.05	3.98	3.92
Span 3	120	3.90	3.97	4.05	3.97	3.90
	130	3.82	3.92	4.03	3.93	3.83
	140	3.82	3.89	4.01	3.90	3.83
	150	3.82	3.90	3.99	3.89	3.81
	160	3.83	3.91	4.01	3.91	3.82
	170	3.86	3.93	4.03	3.93	3.88
	180	3.95	3.99	4.10	4.00	3.96
South Approach	180	3.96	4.00	4.10	4.00	3.96
	190	3.94	3.99	4.08	3.99	3.95
	200	3.89	3.93	4.05	3.96	3.94
Elevations measured from above north abutment						

This table shows the continued changes in roadway elevations where the driving surface dips 1 in. (0.83 ft.) to 1.75 in. (0.15 ft.) at the midspan of each span. The data in Table 36 shows that the topside elevations show a 1.5 inch dip at the midspan of all three spans compared to the elevation measurements of the bridge deck at the abutments and piers. The measured elevation dip at the centerline in the south span is 1.125 in., center span is 0.75 in., and 1.25 in. in north span. On the outside lane markers, the elevation dips measured range from 0 in. to 1.75 in. These elevation changes are problematic to drivers traveling at high velocities and can create an unpleasant riding surface, but also a potential safety hazard. The drawings by ODOT specify a super elevation of 2% and this is verified through the data. Figure 56 provides a visual representation of Table 36. The northbound and southbound lane strips elevations were measured just inside the guardrail. All measurements were taken in ft. to the top of the concrete deck slab.

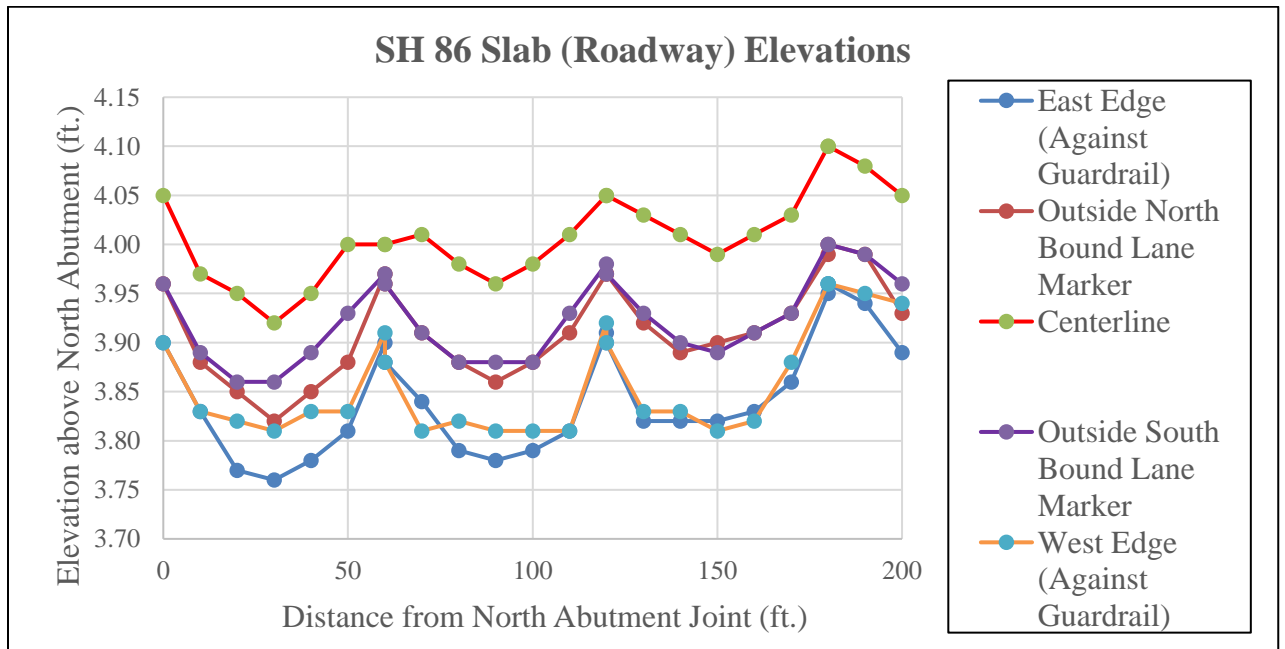


Figure 56: Roadway elevation profile for the SH 86 bridge

The elevations measured to the bottom of the concrete deck. Measurements between girders were taken at approximately midway between the beams. A measurement were taken just outside of the exterior girders and the other measurement was taken at the west or east edge of the concrete deck. SH 86 was the only one of the three bridges that had stay-in-place formwork, a galvanized metal decking. The depth of the metal galvanized deck was measured to be 1.25 inches. To account for this, elevations at the bottom of the concrete deck were measured at the top of the metal decking to get the true profile of concrete slab. The outer elevations were taken directly to the bottom of the concrete. The elevation change at the bottom of the concrete slab was measured directly and those values are reported in Table 37. The readings were taken at ten ft. intervals on the north span.

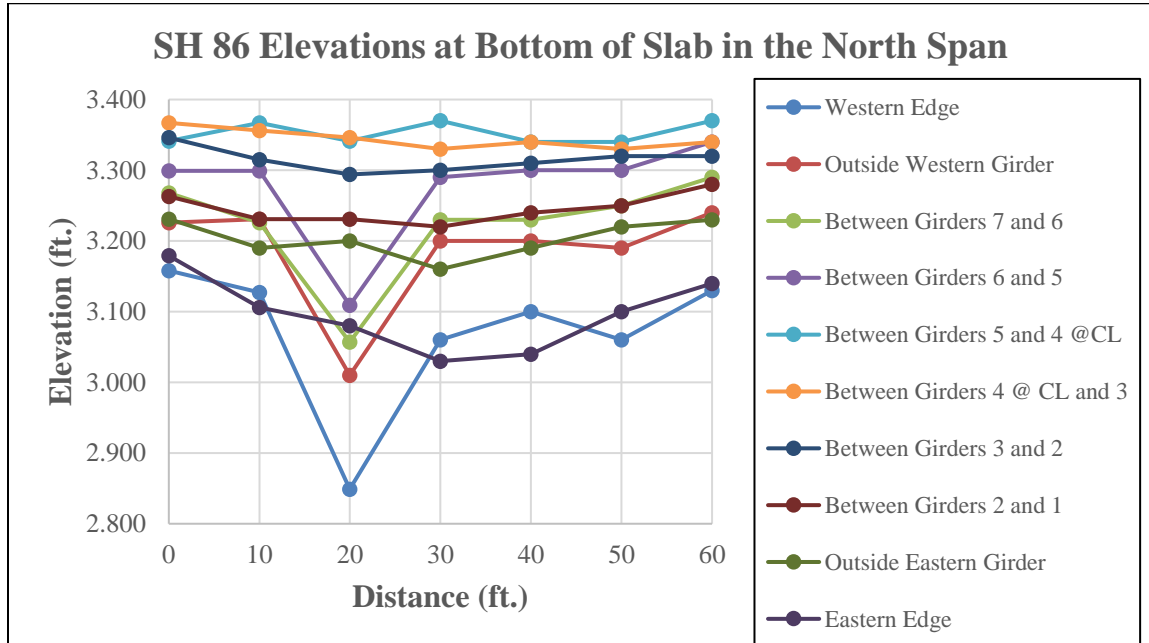
Table 37: Elevations taken at the bottom of the SH 86

SH 86 Elevations at Bottom of Slab in the North Span

	Distance (ft.)	Elevation (ft.)									
		West Edge	Outside Western Girder	Between Girders 7 and 6	Between Girders 6 and 5	Between Girders 5 and 4 @CL	Between Girders 4 @ CL and 3	Between Girders 3 and 2	Between Girders 2 and 1	Outside Eastern Girder	East Edge
North Abutment	0	3.158	3.226	3.268	3.299	3.341	3.367	3.346	3.263	3.231	3.179
	10	3.127	3.231	3.226	3.299	3.367	3.356	3.315	3.231	3.190	3.106
Diaphragm	20	2.849	3.010	3.057	3.109	3.341	3.346	3.294	3.231	3.200	3.080
Midspan	30	3.060	3.200	3.230	3.290	3.370	3.330	3.300	3.220	3.160	3.030
Diaphragm	40	3.100	3.200	3.230	3.300	3.340	3.340	3.310	3.240	3.190	3.040
	50	3.060	3.190	3.250	3.300	3.340	3.330	3.320	3.250	3.220	3.100
South Pier	60	3.130	3.240	3.290	3.340	3.370	3.340	3.320	3.280	3.230	3.140

Elevations measured from above top of the south abutment

Figure 57: Elevations taken at the bottom of north span of SH 86



Excessive slopes were measured and observed at the bottom of the concrete slab from the outsider girder line to the outside edge of the bridge deck. The ODOT drawings specify a super elevation of 2% and this amounts to 0.96 in. or 0.08 ft. elevation change in a 4 ft. area. This 4 ft. area is roughly equivalent to the 4'-8' cantilever from the centerline of the girder to the edge of slab. These values compare fairly well to the values in Table 38. From Table 38, one can see variance in elevations of the bottom of the concrete slab. This indicated that the formwork was perhaps not properly braced before pouring the concrete slab. This would create these unnecessary localized deflection on the driving surface. Elevation control is an important consistent with designing and constructing a bridge as any slight changes could have a significant impact. A difference of 0.96 in. would be expected, but in some cases the variations approached 2 in.

Table 38: Imputed changes in roadway elevations due to localized variance in the formwork

SH 86 Elevation Change in the Cantilevers in the North Span				
	Distance (ft.)	West Side Elevation Difference (in.)	East Side Elevation Difference (in.)	Imputed Change in Elevation Due to Localized Variance (in.)
North Abutment	0.0	-0.82	-0.62	0.00
	10	-1.25	-1.01	0.33
Diaphragm	20	-1.93	-1.44	0.81
Midspan	30	-1.68	-1.04	0.40
Diaphragm	40	-1.25	-1.80	0.49
	50	-1.38	-1.44	0.13
South Pier	60	-1.32	-1.08	0.00
Measured at the bottom of the concrete deck slab				

The cantilever portion was 4' 8" in length and this elevations amounts to 0.08 ft. or 0.96 in., which accounts for the specified 2 % super elevation. But from the table, it is shown that some had values of 1.93 in. on the west side diaphragm at 20 ft.

The slopes at the bottom of the slabs are more severe near the edges of the slab – in the portions of the deck slab formwork that would have been cantilevered from the outside girder to the edge of the slab. The drawings called out 2 % super-elevation which would have resulted in approximately 0.96 in or 0.08 ft. of elevation difference between the readings at 13.33 ft. and the

readings at the edges of the slab at 16.67 ft. Instead, one can see elevation changes that exceed that for a “normal” super-elevation. Tables 39 and 40 have the concrete slab thicknesses calculated from measured elevations on the north span of the SH 86 Bridge over Stillwater Creek, Payne County. Table 39 reports the thickness in ft. and Table 40 reports in in.

Table 39: Concrete slab thickness (ft.) on the north span of SH 86 bridge

SH 86 Slab Thickness						
	Distance from North Abutment Joint (ft.)	Thickness (ft.)				
		East Edge (Against Guardrail)	Outside North Bound Lane Marker	Centerline	Outside South Bound Lane Marker	West Edge (Against Guardrail)
North Span	0	0.72	0.71	0.69	0.71	0.70
	10	0.67	0.65	0.61	0.67	0.70
	20	0.87	0.81	0.61	0.64	0.70
	30	0.65	0.60	0.57	0.67	0.74
	40	0.65	0.63	0.61	0.67	0.74
	50	0.71	0.66	0.66	0.69	0.69
	60	0.73	0.70	0.64	0.71	0.74
1. Slab thickness measured in ft.						

2. Highlighted areas in yellow indicate the thinning of the concrete deck near the centerline

Table 40: Concrete slab thickness (in.) on the north span of SH 86 bridge

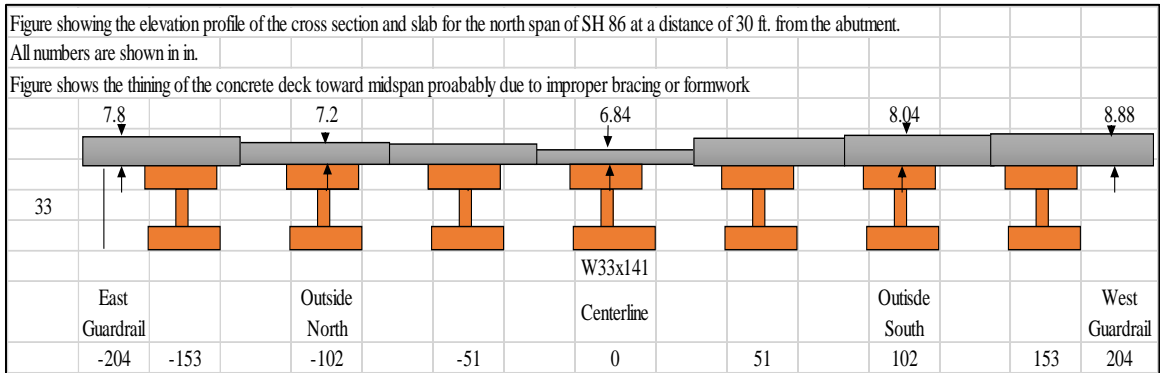
SH 86 Slab Thickness						
	Distance from North Abutment Joint (ft.)	Thickness (in.)				
		East Edge (Against Guardrail)	Outside North Bound Lane Marker	Centerline	Outside South Bound Lane Marker	West Edge (Against Guardrail)
North Span	0	8.64	8.52	8.28	8.52	8.40
	10	8.04	7.80	7.32	8.04	8.40
	20	10.44	9.72	7.32	7.68	8.40
	30	7.80	7.20	6.84	8.04	8.88
	40	7.80	7.56	7.32	8.04	8.88
	50	8.52	7.92	7.92	8.28	8.28
	60	8.76	8.40	7.68	8.52	8.88

1. Slab thickness measured in in.

2. Highlighted areas in yellow indicate the thinning of the concrete deck near the centerline

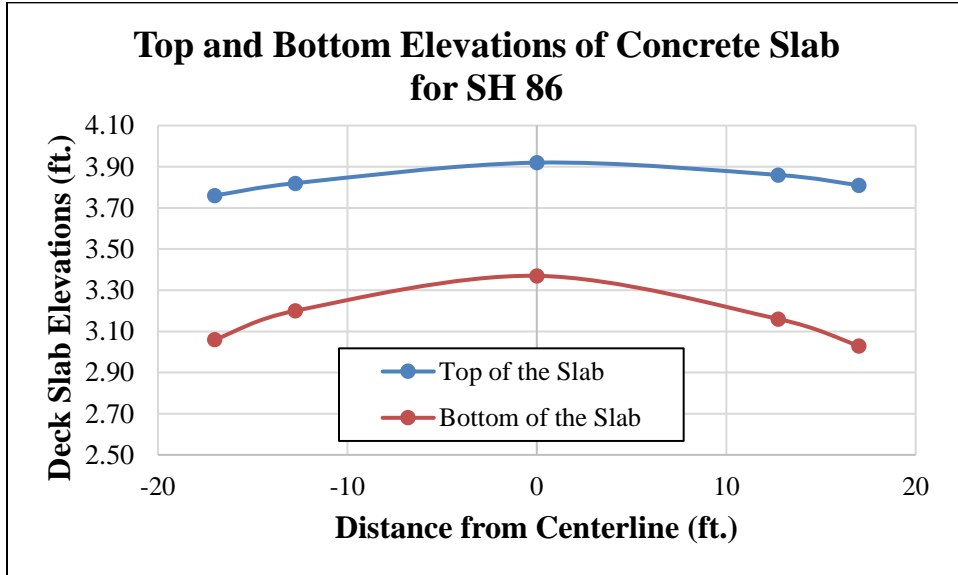
The slab is consistently thinner near the centerlines. This phenomena is consistent with localized, downward deflection of the screed rails, and/or the formwork or bracing that supports the screeds.

Figure 58: Elevation profile of the cross section and slab for SH 86



The figure above shows the elevation profile of the cross section and slab for the north span of SH 86 at a distance of 30 ft. from the abutment. All numbers shown are reported in in. The figure was computed using Table 40. The datum or origin is the CL of the middle interior girder. The figure accurately shows how as you approach the centerline, you can noticeably see the thinning of the concrete deck. The thinning toward the centerline is likely due to poor bracing or formwork. Furthermore, it is worth noting that on the slab area not supported by girders that some of the slab was deflecting downward more than expected. The Figure below provides a visual representation of the elevation change in the top and bottom of the concrete slab at a distance of 30 ft. from the north abutment or midspan of span 1. The values in the figure were obtained with Table 36 and 37. From observation, it is apparent that one side of the concrete slab slopes downward more than the other. This is likely due to localized deflection occurring during construction on the cantilever ends. In addition, in parts of the span the elevation variance every 4 ft. exceeds the 0.08 ft. specified by the 2% super elevation in the specs. Both Figure 58 and 59 show that the riding surface on SH 86 can cause poor ride quality due to variance in elevations.

Figure 59: Top and Bottom Elevations of Concrete Slab for SH 86



SH 14

SH 14 is four span bridge with 5 W 24x94 steel girders and an 8 in. deck. Figure 60 shows the bridge. This was the 2nd bridge investigated for cracks, ride issues, unanticipated deflections, and to perform traditional surveying methods. This was the only bridge that had all spans accessible. In 2010 or 2011, SH 14 was rehabilitated with an 8 in. slab with a super-elevation slope of 1%. The surveying would confirm this elevation with the construction drawings. Elevation readings were taken at the bottom of the concrete deck, at the bottom of the steel girders, and atop of the concrete deck. Elevations were based to T.O. of the south bridge abutment (abutment #1). From observation, it was apparent that the girders sagged at midspan as a result of volume changes, rehabilitation, or long-term use and that some of the webs on the steel girders were out of plane vertically.

The girders sagging at midspan causes the unsmooth rides surface as your will feel a “dip.” Centerline (CL) elevations varied from 3.51 to 3.58 ft. and within the same span, variations were approximately $\frac{3}{4}$ in. or less. Some of these variances were adjusted with diamond grinding in traffic lanes and not in shoulders. This was made visibly apparent and noticeable through our data as there was greater variation in elevations in the shoulders. The crown that is reported in the Table 41 below measures the super elevation from the average elevation of the shoulders to the CL. Table 41 reports the roadway elevations at the top of the concrete deck and Table 42 reports the elevations under the bridge deck. North and south bound shoulders’ elevations were measured on the outside of the lane strips. For underneath the bridge deck, readings were made at approximately mid-way between steel girders, or immediately outside the outside girder. SH 14 is the only bridge where there was access to all the spans from underneath. Table 43 and 44 reports the slab thickness computed from measured elevations comparing the elevation at the bottom of the slab to the elevation of the driving surface. Red numbers indicated concrete slab thicknesses less than the required 8 in. specified in the drawings provided by ODOT. Table 43 reports the thickness in ft. and Table 44 in in.



Figure 60: SH 14 bridge over Eagle Chief Creek in Woods County

Table 41: Roadway elevations for SH 14

SH 14 Slab (Roadway) Elevations					
	Distance from South Abutment Joint (ft.)	Elevation (ft.)			
		North Bound Shoulder	Centerline	South Bound Shoulder	Crown
Span 1	0	3.46	3.51	3.40	0.08
	10	3.42	3.52	3.40	0.11

	20	3.41	3.54	3.42	0.13
	30	3.40	3.53	3.42	0.12
	40	3.47	3.57	3.45	0.11
Span 2	40	3.46	3.55	3.44	0.10
	50	3.38	3.51	3.41	0.12
	60	3.39	3.51	3.41	0.11
	70	3.40	3.53	3.41	0.13
	80	3.47	3.57	3.44	0.12
Span 3	80	3.48	3.57	3.44	0.11
	90	3.47	3.56	3.43	0.11
	100	3.44	3.55	3.43	0.12
	110	3.45	3.56	3.44	0.12
	120	3.49	3.59	3.48	0.11
Span 4	120	3.50	3.58	3.48	0.09
	130	3.46	3.58	3.45	0.13
	140	3.46	3.58	3.45	0.13
	150	3.47	3.58	3.45	0.12

	160	3.52	3.57	3.45	0.08
North Approach	160	3.52	3.57	3.45	0.08
	170	3.43	3.50	3.38	0.09
	180	3.32	3.41	3.27	0.12

1. Roadway elevations reported in ft.
2. Crown is the elevation at the centerline minus the average elevation of the shoulders
3. Elevations in red indicate visible diamond grinding in the traffic lanes between south bound shoulder and centerline

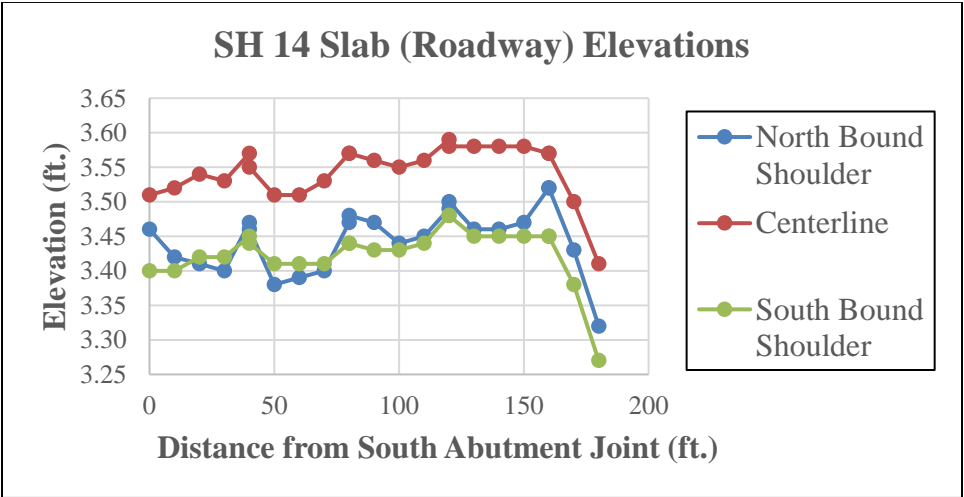


Figure 61: SH 14 Roadway Elevations

Table 42: Elevations at the bottom of the concrete deck of SH 14

SH 14 Elevations at the Bottom of Slab								
	Distance from South Abutment Joint (ft.)	Elevation (ft.)						
		Outside Eastern Girder 1	Between Girders 1 and 2	Between Girders 2 and 3	Average Elevation at Centerline	Between Girders 3 and 4	Between Girders 4 and 5	Outside Western Girder 5
Span 1	2	2.72	2.80	2.85	2.84	2.84	2.79	2.74
	20	2.78	2.78	2.83	2.83	2.82	2.80	2.75
	38	2.79	2.80	2.86	2.86	2.87	2.81	2.80
Span 2	42	2.77	2.80	2.88	2.87	2.87	2.83	2.78
	60	2.79	2.78	2.87	2.86	2.85	2.79	2.74
	78	2.79	2.93	2.93	2.94	2.95	2.91	2.87
Span 3	82	2.80	2.84	2.87	2.87	2.88	2.82	2.80
	100	2.79	2.79	2.84	2.85	2.87	2.82	2.76
	118	2.80	2.82	2.87	2.87	2.88	2.86	2.82
Span 4	122	2.80	2.84	2.87	2.87	2.88	2.82	2.80
	140	2.79	2.79	2.84	2.85	2.87	2.82	2.76
	158	2.80	2.82	2.87	2.87	2.88	2.86	2.82

Elevations reported in ft.

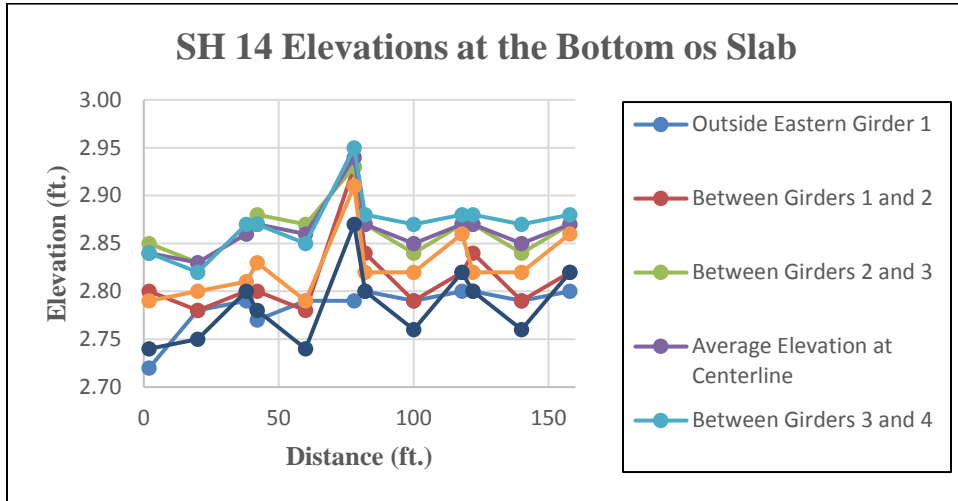


Figure 62: Elevations at the bottom of the concrete deck of SH 14

Span 2 (40 ft. to 80 ft.) had the worst elevation “dip,” about 5/8 in. at CL, but as much as 1.0 in. at the southbound shoulder. Diamond grinding has relieved some of the ride-ability issues since the construction was completed. This bridge had a better driving surface than SH 86.

Table 43: Computed slab thicknesses (ft.) for SH 14

SH 14 Slab Thickness				
	Distance from South Abutment Joint (ft.)	Thickness (ft.)		
		North Bound Shoulder	Centerline	South Bound Shoulder
Span 1	0	0.74	0.67	0.66

	10	0.67	0.69	0.66
	20	0.63	0.71	0.67
	30	0.61	0.69	0.65
	40	0.68	0.71	0.65
Span 2	40	0.69	0.68	0.66
	50	0.60	0.65	0.65
	60	0.60	0.65	0.67
	70	0.61	0.63	0.61
	80	0.68	0.63	0.58
Span 3	80	0.68	0.70	0.65
	90	0.67	0.70	0.66
	100	0.65	0.70	0.68
	110	0.66	0.70	0.66
	120	0.69	0.72	0.67
Span 4	120	0.70	0.70	0.69
	130	0.66	0.72	0.67
	140	0.67	0.74	0.69

	150	0.68	0.73	0.67
	160	0.72	0.70	0.64
<p>1. Slab thickness reported in ft.</p> <p>2. Highlighted areas in yellow indicate the thinning of the concrete deck near the centerline</p> <p>3. Elevations in red indicate visible diamond grinding in the traffic lanes between south bound shoulder and centerline</p>				

Table 44: Computed slab thicknesses (in.) for SH 14

SH 14 Slab Thickness				
	Distance from South Abutment Joint (ft.)	Thickness (in.)		
		North Bound Shoulder	Centerline	South Bound Shoulder
Span 1	0	8.88	8.04	7.92
	10	8.04	8.28	7.92
	20	7.56	8.52	8.04
	30	7.32	8.28	7.80
	40	8.16	8.52	7.80

Span 2	40	8.28	8.16	7.92
	50	7.20	7.80	7.80
	60	7.20	7.80	8.04
	70	7.32	7.56	7.32
	80	8.16	7.56	6.96
Span 3	80	8.16	8.40	7.80
	90	8.04	8.40	7.92
	100	7.80	8.40	8.16
	110	7.92	8.40	7.92
	120	8.28	8.64	8.04
Span 4	120	8.40	8.40	8.28
	130	7.92	8.64	8.04
	140	8.04	8.88	8.28
	150	8.16	8.76	8.04
	160	8.64	8.40	7.68

1. Slab thickness reported in in.

2. Highlighted areas in yellow indicate the thinning of the concrete deck near the centerline

3. Elevations in red indicate visible diamond grinding in the traffic lanes between south bound shoulder and centerline

Diamond grinding visibly reduced the depth of the lines that were likely installed with finishing. The measured slab thicknesses (using the engineering level) are consistent with the depth of the slab measured from pre-existing core holes in the deck in spans 2 and 4. In spans 2 and 4, the pre-existing hole was located between the wheel tracks in the northbound driving lane of SH 14. This core hole was measured at approximately 7.25 in. of thickness, and corresponds with the slab thicknesses shown in Tables 43 and 44. ODOT could not specify the origins of the core and it is obviously unrepaired. These direct measurements are shown in the following photograph in Figures 63 and 64.



Figure 63: A pre-existing core hole discovered in span 2 of SH 14



Figure 64: This pre-existing core hole discovered in span 4 of SH 14

US 281

US 281 over Mule Creek in Northern Woods County was the third and final bridge investigated for cracks, ride issues, unanticipated deflections, and to perform traditional surveying methods. This bridge had only one accessible span due to steep elevation variance from the rocky and high grass walking surfaces underneath the bridge and Mule Creek. Figure 65 is a picture of the bridge.

On US 281, no diamond grinding was performed on the concrete bridge deck and elevations were performed on the top of the bridge deck at the centerline and at the north and south bound shoulders. Span 3 was the only span accessible from underneath the bridge deck. The roadway elevation data is presented in Table 45. For all three spans, variance in the centerline elevations was about 1/8 in. or 0.125 in. US 281 was reported to have had screed rails for the new concrete bridge deck set atop the outside steel girders, and that the slab from the rail to the outside edge of the deck was screeded by hand. This bridge ride ability was ok and not as unpleasant as SH 86.

Tables 46 and 47 shows the slab Thicknesses for the US 281 Bridge. The slab thickness is nearly 9 in. throughout. Tables 45 shows the slab thickness in ft. and Table 46 in in.



Figure 65: US 281 over Mule Creek in Northern Woods County

Table 45: Roadway elevation taken on US 281

US 281 Slab (Roadway) Elevations					
	Distance from North Abutment Joint (ft.)	Elevation (ft.)			
		North Bound Shoulder	Centerline	South Bound Shoulder	Crown
South		3.53	3.68	3.47	0.18
Approach		3.50	3.67	3.48	0.18

		3.51	3.70	3.49	0.20
Span 1	0	3.51	3.69	3.49	0.19
	5	3.47	3.68	3.47	0.21
	10	3.44	3.68	3.46	0.23
	15	3.45	3.68	3.46	0.23
	20	3.48	3.68	3.48	0.20
	25	3.49	3.69	3.51	0.19
	30	3.51	3.69	3.52	0.18
Span 2	30	3.50	3.69	3.51	0.19
	35	3.49	3.69	3.50	0.20
	40	3.49	3.69	3.47	0.21
	45	3.49	3.69	3.48	0.21
	50	3.48	3.69	3.48	0.21
	55	3.48	3.69	3.49	0.21
	60	3.48	3.68	3.48	0.20
Span 3	60	3.49	3.69	3.49	0.20
	65	3.48	3.70	3.50	0.21

	70	3.47	3.69	3.50	0.21
	75	3.47	3.69	3.50	0.21
	80	3.49	3.69	3.49	0.20
	85	3.51	3.70	3.51	0.19
	90	3.55	3.74	3.54	0.20
<p>1. Roadway elevations reported in ft.</p> <p>2. Crown is the elevation at the centerline minus the average elevation of the shoulders</p>					

Table 46: Slab Thicknesses (ft.) for the US 281 Bridge

US 281 Slab Thickness				
	Distance from North Abutment Joint (ft.)	Thickness (ft.)		
		North Bound Shoulder	Centerline	South Bound Shoulder
Span 3	60	0.73	0.76	0.71
	65	0.72	0.77	0.74
	70	0.72	0.76	0.76

	75	0.73	0.75	0.77
	80	0.76	0.76	0.76
	85	0.78	0.78	0.76
	90	0.82	0.82	0.77
Slab thickness reported in ft.				

Table 47: Slab Thicknesses (in.) for the US 281 Bridge

US 281 Slab Thickness				
	Distance from North Abutment Joint (ft.)	Thickness (in.)		
		North Bound Shoulder	Centerline	South Bound Shoulder
Span 3	60	8.76	9.12	8.52
	65	8.64	9.24	8.88
	70	8.64	9.12	9.12
	75	8.76	9.00	9.24
	80	9.12	9.12	9.12
	85	9.36	9.36	9.12

	90	9.84	9.84	9.24
Slab thickness reported in in.				

DISCUSSION

Our laboratory testing on the two prototype beams with a W 8x15 steel girder and an ODOT AA concrete mixture in the deck indicates ultimate shrinkage values approaching the range of 500 microstrains. This validates our assumptions made in the computational analysis and these value are over a year. With additional time and measurements, the rate of increase in shrinkage begins to decline. The shrinkage strains have the potential to cause downward deflections in bridge decks. The graphs and figures reflect that. Deflections past the initial set are caused by a combination of temperature changes, concrete shrinkage or other time dependent volumetric changes. The models do assume elastic behavior not plastic meaning that the concrete has not cracked. Cracking was observed on SH 86, SH 14, and US 281, but no cracking occurred or was visible on the Prototype Beams. Shrinkage will be a contributor to cracking as it causes the concrete to expand and contract periodically.

From the forensic investigation, cracking was observed in semi-regular intervals throughout the bridge, indicating that the cracking was a result of innate material properties of the concrete and steel instead of localized loads or geometry. Cracks in the prototype beams were important to see the effects of cracks on the curvature from shrinkage. The questions that must be asked are as follows: (1) Do the cracks act as a relief for the restrained shrinkage and other time dependent volumetric changes? and (2) what is shrinkage true impact on downward deflections on concrete and steel composite beams?

There are a few reasons why the prototype beams did not crack: the concrete is relatively young, the amount of longitudinal and transverse steel reinforcement in the slab, the beams were not imposed to any applied loads to model trucks and other vehicles, and the beams did not experience a temperature gradient like bridges in the field. Comparing the restrained shrinkage stresses to the unrestrained shrinkage stresses, it is observed the different rates of shrinkage, the fluctuations, effects of temperature, and the effects of composite action. This is useful when determining the behavior of shrinkage when designing concrete and steel composite structures.

The evidence from the forensic investigation indicates that ride quality problems are partially a result of construction practices and guidelines. Ride quality problems mean that traveling at high speeds is un-safe and that the bridge serviceability will continually worsen with time. From SH 86 and SH 14 bridge, it is observable that both bridges had thinner decks at the centerline. The thinner concrete deck at the centerline could be a result of unanticipated deflections of the screed rails or screed boards that are used to allow for finished elevations when casting a concrete deck. This evidence is not sufficient enough alone but together with other evidence conclusions can be derived. On SH 86, it was observed that the formwork supporting the screed rails were not adequately supported and this helps explain some of the scatteredness of the data collected from the forensic investigation. If the cantilevered loads had imposed twisting or torsional deformations on the exterior steel girders, then a more discernable deformation pattern in the bridge beams and bridge elevations should have been discovered. The elevation profile of SH 86 further reveals the variance in the data collected.

On SH 86 over Stillwater Creek, a pattern of elevation change on the bottom of the concrete deck was observed. In the 4' 8" cantilever portion of the concrete deck under the bridge, the outward slopes varied and were as large as 1.93 in. lower at the slab edge than the elevation at the next adjacent steel girder. Leading to a conclusion that this problem resulted from bracing the formwork to the steel beam. Non-adequately supported formwork caused the bridge elevations to

be lower at midspan of the spans than at the abutment and piers, where it seemed that the formwork was more adequately braced. It is possible that the screed rails were not placed at elevations that anticipated downward deflections from the casting and curing of the concrete bridge deck. This would have created localized deflections and contributed to unanticipated bridge performance and serviceability issues. At the abutment and the pier, the elevation variance is not as significant and explains why the elevation at the midspans of the driving surfaces are much lower. The specified super elevation on SH 86 is 2% about 0.96 in.

Diamond grinding can aid with ride ability issues as made apparent by SH 14. But, the 1.5 in. dip occurring at midspan of each span of SH 86 cannot be corrected with diamond grinding alone and is a huge safety hazard at high speeds. Surveying methods were used to get elevations of the driving surface for all three spans and to get elevations underneath the northernmost span. From SH 86, the evidence strongly suggests that large and localized deflections occurred within formwork that supported the cantilevered portions of the bridge deck slab. Furthermore, these localized deflections also produced larger than expected deflections of the screeds that set elevation controls for the deck slabs, and in turn resulted in finished concrete slabs with elevations at midspans that are lower than the elevations at the piers and abutments. This can be corrected by properly bracing the formwork and surveying the elevations right before pouring of the concrete deck. Furthermore, this is made apparent by the bridge decks thinning as you approach midspans and centerlines.

Construction practices in the field need to have appropriate quality control measures to ensure the contractor is meeting the requirements of the project to minimize any issues. Quality control is important to make sure that all elevations are being maintained, formwork is being properly braced, and that the designs specifications are being adhered too. Research needs to be performed to further understand the effects of shrinkage and other time-dependent volume changes on deflections, serviceability, and sustainability of steel and concrete composite bridges.

Then, this research needs to be implemented in the codes so the designers have better methods of controlling and mitigating shrinkage and other volumetric effects. Collectively, these three entities can help improve bridge performance and design of the 21st century. But from the forensic investigations performed on the three bridges in Oklahoma, construction errors are likely the culprit of poor ride performance and elevation control.

Altogether the forensic evidence indicates that problems with ride-ability resulted principally from construction related incidences. The evidence strongly suggests that large and localized deflections occurred within formwork that supported the cantilevered portions of the bridge deck slab. This was accomplished by inspecting and surveying the top and bottom of the concrete bridge deck through observation and figures. Furthermore, these localized deflections also produced larger than expected deflections of the screeds that set elevation controls for the concrete deck. Resulting in finished concrete slabs with elevations at midspans that are lower than the elevations at the piers and abutments.

CHAPTER V

CONCLUSIONS AND RECOMMENDATIONS

Conclusions

This research addresses specific phenomenon relating concrete shrinkage to deflections in concrete slab and steel girder composite bridges. The data collected was used to determine if shrinkage is a contributor to unanticipated deflections and poor ride quality. Forensic investigations, on three recently rehabilitated bridges, provided a valuable understanding of the possible causes of adverse ride quality and unexpected deflections. The laboratory data indicates that concrete shrinkage can contribute to downward deflections of concrete bridge decks due to the continuous shrinkage and deflection correlation with time. But, the most likely source of adverse ride quality was the inadequate support on cantilevered formwork and bracing, and insufficient support of screed rails.

The following are the conclusions that were derived from analysis of the laboratory experiments and forensic investigations:

- Concrete shrinkage and measured deflections of the prototype beams indicate that shrinkage of concrete can contribute to downward deflections of composite bridge girders.
- Temperature correlates to strains and deflections. Temperature has a significant effect on shrinkage as higher temperatures decrease strains and lower temperatures increase

strains. As a result, a rise (decrease) in temperature causes the beams to camber up (deflect downward) even if slightly.

- The w/c ratio can create additional shrinkage as more water volume makes the concrete more prone to consistently shrink due to evaporation and absorption in the early states. This can cause cracking and the temperature fluctuations from early stage curing.
- The additional ten gallons (eighty three lbs.) of water in Prototype Beam 2 caused the beam to behave differently as the w/c ratio was increased by 0.6 or 12%. It behaved differently by shrinking at a faster rate, but through time the shrinkage rate of both would decelerate and approach some finite value.
- The computational analysis revealed that the effects of shrinkage can be analyzed or estimated, but these estimates are assuming the concrete did not crack and remained elastic.
- Using time dependent numerical models recommended by ACI and other entities could be useful in determining and limiting shrinkage designs. Suggestions for limiting shrinkage strains are high grade coarse, intermediate, and fine aggregates, addressing effects of high or low temperatures, and optimizing the w/c ratio.
- More research is needed about the effects of concrete once it cracks and transitions to plastic behavior then a plastic state then ultimately failure. It is possible that the effect of drying shrinkage can help mitigate cracks. This could have potentially been addressed more if the Prototype Beams had cracked.
- More research needs to be conducted on the effect of shrinkage on deflection and serviceability.

- From the forensic investigations of the three ODOT bridges, cracks were observed on the surface and underneath the bridge deck. However, no cracks were observed on the prototype beams after two years.
- Particularly near the center line, concrete bridge decks are thinner because the bracings were not adequately supported during the pouring of the concrete slab.
- The elevation data indicates that the formwork and bracing for the concrete deck and cantilevered deck portions were inadequately supported. This led to deflection of the screed rails that supported the concrete finishing machines, which in turn led to problems in ride quality.
- Diamond grinding can be used to help alleviate some ride problems, but this is not sufficient enough with severely unpleasant riding surfaces.
- US 281 had three overlays poured which would have also contributed to deflections and ride quality. Each overlay would have had to be properly accounted for in the design and construction.
- Before starting the rehabilitation process, inspection for the conditions of the supports, pier caps, girders, etc. needs to be conducted to see if they are adequate. Some of the supports observed were in undesirable conditions.
- The field investigations provide evidence that construction errors are likely the main cause of poor elevation control of finished bridge deck surfaces. This was observed when some of the visual changes in elevations or unpleasant riding surfaces were a result of construction practices or calculations.

These findings aim to increase the understanding of how to mitigate the effects of shrinkage and other time-dependent volume changes on bridge performance. Helping reduce the rehabilitation costs over a bridge's lifespan, resulting in a decreased amount of Oklahoma's bridges being rated as structurally deficient. These findings were submitted to ODOT on October 31st, 2014. The findings will be further disseminated through presentations at ACI and PCI conferences, publications in peer reviewed journals, and a YouTube page. This research will help refine bridge design methodologies, leading to improved infrastructure sustainability, rehabilitation methods, and public safety across America. Overall, this research has provided insight into some of the effects and nature of shrinkage and its possible contribution to deflections and riding performance. Further study through forensic investigations, laboratory experiments, and theoretical modeling is needed.

Recommendations

Laboratory testing and forensic investigation revealed that one or more preventions methods could have been done to mitigate the adverse ride quality issues on some of the rehabilitated bridges in Oklahoma.

1. Shrinkage should be included in the design of steel and concrete composite bridges. Shrinkage can be accounted for by using an assumed shrinkage strain and designing the structure to account for the stresses, strains, and deflections that shrinkage will cause. The approach would be similar to the computational analysis. But, further research is needed on an acceptable shrinkage range for Oklahoma. In addition, time dependent numerical models can be used in the design process.
2. Time dependent volume changes such as shrinkage can be a contributor to downward deflection. Currently, ODOT does not have any specifications limiting restrained shrinkage stresses, but they should consider adding it to their design specifications. Addressing shrinkage

in design will help reduce the amount of deflection and ride issues that occur as a result of shrinkage. Limiting shrinkage strains would result in ODOT using high grade coarse, intermediate, and fine aggregates and optimizing the w/c ratio.

3. Before the rehabilitation process begins, forensic investigations need to be done on the existing bridge to observe conditions of the supports, abutments, pier caps, columns, approach slab and girders. Generally during the rehabilitation process, the existing steel girders are left in place and only the concrete slab is removed. The abutment and other parts of the bridge are reconstructed not rehabilitated. This will aid in ODOT knowing if there are other measures that need to be taken on the rehabilitation process besides just the bridge deck.

4. ODOT should specify that before a concrete slab is poured that a third party surveyor is mandatory to ensure proper elevation control before the bridge deck is poured. This will help minimize additional unanticipated deflections as elevations specified in the design will be double checked. This method could ensure quality control by minimizing elevations error before construction.

5. Elevations records should be maintained from the start of the project until the project is finished. This will help to be able address where a problem could have originated and preventive measures could be implemented in the future. In addition, this would help the contractor have to be more responsible for the serviceability and ride ability of the finished bridge.

6. Quality control is one of the most important parameters that could be used to save ODOT money on rehabilitation cost. Quality control ensures that the concrete is meeting all of the provisions specified in ODOT's 701.01 Mix Design and Proportioning guidelines. If concrete is used in a bridge deck that does not meet ODOT AA requirements such as strength, w/c, minimum cement content, slump, or air content then this could create unforeseeable problems down the road on bridge performance and serviceability. If concrete that is delivered onsite is not suitable

for any of the reasons listed above or others then it should not be used in bridge deck. This quality control should also extend to elevations as well such as formwork, bracing, and screeds.

REFERENCES

1. Al-deen, S., Ranzi, G., & Vrcelj, Z. (2011). Shrinkage Effects on the Flexural Stiffness of Composite Beams with Solid Concrete Slabs: An Experimental Study. *Engineering Structures*.
2. Alexander, S. (2003). How Concrete Shrinkage Affects Composite Steel Beams. *New Steel Construction*.
3. Amadio, C., & Fragiaco, M. (1997). Simplified Approach to Evaluate Creep and Shrinkage Effects in Steel-Concrete Composite Beams. *Journal of Structural Engineering*.
4. Bradford, M. (1991). Deflections of Composite Steel-Concrete Beams Subject to Creep and Shrinkage. *ACI Structural Journal*.
5. Bradford, M. (1997). Shrinkage Behavior of Steel-Concrete Composite Beams. *ACI Structural Journal*.
6. Chaudhary, S., Nagpal, A., & Pendharkar, U. (2009). Control of Creep and Shrinkage Effects in Steel Concrete Composite Bridges with Precast Decks. *Journal of Bridge Engineering*.
7. Csagoly, P. & Long, A.E. (1975). A Note on Shrinkage Stresses in Continuous Steel-Concrete Composite Bridges. *The Structural Engineer*.
8. Holloway, R. (1972). Precast Composite Sections in Structures. *ACI Journal*.
9. Jung, C., Kwak, H., & Seo, Y. (2000). Effects of the Slab Casting Sequences and the Drying Shrinkage of Concrete Slabs on the Short-Term and Long-Term Behavior of Composite Steel Box Girder Bridges Part 1. *Engineering Structures* 23(500).
10. Kosmatka, S., & Wilson, M. *Design and Control of Concrete Mixtures*. Portland Cement Association, 2011. Print.
11. Kyaw, M., & Ong, K. (2006). Monitoring of Early Age Shrinkage Using Image Analysis and its Use in the Repair of Bridges. *Bridge Maintenance, Safety, Management, Life-Cycle Performance and Cost*.
12. LePatner, B. <http://www.saveourbridges.com>. 2012.
<http://www.saveourbridges.com/basics.html>.
13. Neuwald, A. "Water-to-Cement Ratio and Aggregate Moisture Corrections." www.precast.org. May 2010. <http://www.precast.org/2010/05/water-to-cement-ratio-and-aggregate-moisture-corrections/>
14. Russell, B.W., & Bowen, C. (2005). The State of the State's Bridges, Research Report.
15. [AASHTO - Bridging the Gap](http://www.transportation1.org). Transportation1.org. 2008-03-17. Retrieved 2012-06-02.
16. ["Enhancing Disaster Resilience of Highway Bridges to Multiple Hazards."](http://www.rita.dot.gov) www.rita.dot.gov. April 2014.
http://www.rita.dot.gov/utc/publications/spotlight/spotlight_2014_04. April 2013.
17. "Status of the Nation's Highways, Bridges, and Transit." www.fhwa.dot.gov. October 2013. <http://www.fhwa.dot.gov/policy/2004cpr/chap3c.htm>. April 2011.

18. "Update on Oklahoma Bridges and Highways." [www.okladot.state.ok.us](http://www.okladot.state.ok.us/cwp-8-year-plan/pdfs/BridgeHighwayUpdate_2012.pdf). October 2012.
http://www.okladot.state.ok.us/cwp-8-year-plan/pdfs/BridgeHighwayUpdate_2012.pdf.
[October 2012.](http://www.okladot.state.ok.us/cwp-8-year-plan/pdfs/BridgeHighwayUpdate_2012.pdf)

APPENDICES

Concrete Cracking Strains (10 ⁻⁶ x in/in) Computed from Tensile Strengths and Elastic Modulus Data				
Batch Date	Cracking Strain Day 1	Cracking Strain Day 3	Cracking Strain Day 7	Cracking Strain Day 28
6-Aug	72	90	104	79
7-Aug	92	101	90	78
13-Aug	92	95	103	97
13-Aug	82	101	107	82
15-Aug	83	78	96	89
19-Aug	67	93	105	83
20-Aug	61	78	79	78

VITA

Kendall Ke'Vonn Belcher

Candidate for the Degree of

Master of Science

Thesis: LABORATORY AND FIELD INVESTIGATIONS FOR CAUSES OF
UNWANTED DEFORMATIONS IN EXISTING STEEL GIRDER BRIDGES
REHABILITATED WITH CONCRETE DECKS

Major Field: Civil Engineering

Biographical:

Education:

Completed the requirements for the Master of Science in your Civil
Engineering at Oklahoma State University, Stillwater, Oklahoma in May 2017.

Completed the requirements for the Bachelor of Science in Civil Engineering at
Louisiana Tech University, Ruston, Louisiana/Lincoln Parish in May 2013.

Experience: Teacher's Assistant for Structural Analysis, Strength of Materials,
Structures, and Dynamics.

Professional Memberships: Chi Epsilon the Civil Engineering Honor Society
and the National Society of Black Engineers